AN ANALYSIS OF THE METHYL ROTATION DYNAMICS IN THE S_0 ($\tilde{X}^1A_1$) AND T_1 ($\tilde{a}^3A_2$) STATES OF THIOACETALDEHYDE FROM PYROLYSIS JET SPECTRA.

BY

Hafed Ashur Bascal ,B.Sc.

A Thesis
submitted to
the Department of Chemistry
Brock University

In partial fulfillment
of the requirements for the degree
Master of Science

Brock University
St. Catharines , Ontario
September 1991

IN THE NAME OF GOD,
MOST GRACIOUS, MOST MERCIFUL

ABSTRACT

Jet-cooled, laser-induced phosphorescence excitation spectra (LIP) of thioacetaldehyde CH_3CHS, CH_3CDS, CD_3CHS and CD_3CDS have been observed over the region 15800 - 17300 cm^{-1} in a continuous pyrolysis jet. The vibronic band structure of the singlet-triplet $n \rightarrow \pi^*$ transition were attributed to the strong coupling of the methyl torsion and aldehydic hydrogen wagging modes . The vibronic peaks have been assigned in terms of two upper electronic state (T_1) vibrations; the methyl torsion mode ν_{15}, and the aldehydic hydrogen wagging mode ν_{14}. The electronic origin $0_0^0 a_1$ is unequivocally assigned as follows: CH_3CHS (16294.9 cm^{-1}), CH_3CDS (16360.9 cm^{-1}), CD_3CHS (16299.7 cm^{-1}), and CD_3CDS (16367.2 cm^{-1}).

To obtain structural and dynamical information about the two electronic states, potential surfaces $V(\theta,\alpha)$ for the θ (methyl torsion) and α (hydrogen wagging) motions were generated by ab initio quantum mechanical calculations with a 6-31G* basis in which the structural parameters were fully relaxed. The kinetic energy coefficients $B_\theta(\alpha,\theta)$, $B_\alpha(\alpha,\theta)$, and the cross coupling term $B_{\alpha\theta}(\alpha,\theta)$, were accurately represented as functions of the two active coordinates, α and θ. The calculations reveal that the molecule adopts an eclipsed conformation for the lower S_0 electronic state (α=0°,θ=0°) with a barrier height to internal rotation of 541.5 cm^{-1} which is to be compared to 549.8 cm^{-1} obtained from the microwave experiment. The conformation of the upper T_1 electronic state was found to be staggered (α=24.68°,θ=-45.66°). The saddle point in the path traced out by the aldehyde wagging motion was calculated to be 175 cm^{-1} above the equilibrium configuration. The corresponding maxima in the path taken by methyl torsion was found to be 322 cm^{-1}. The small amplitude

normal vibrational modes were also calculated to aid in the assignment of the spectra. Torsional-wagging energy manifolds for the two states were derived from the Hamiltonian $H(\alpha,\theta)$ which was solved variationally using an extended two dimensional Fourier expansion as a basis set. A torsional-inversion band spectrum was derived from the calculated energy levels and Franck-Condon factors, and was compared with the experimental supersonic-jet spectra. Most of the anomalies which were associated with the interpretation of the observed spectrum could be accounted for by the band profiles derived from ab initio SCF calculations.

A model describing the jet spectra was derived by scaling the ab initio potential functions. The global least squares fitting generates a triplet state potential which has a minimum at (α=22.38°,θ=-41.08°). The flatter potential in the scaled model yielded excellent agreement between the observed and calculated frequency intervals.

ACKNOWLEDGMENTS

The author would like to express his gratitude to Professor D.C.Moule for the continuous guidance, encouragement and cooperation throughout this project.

I would also like to thank Dr.D.J.Clouthier and J.Karolczak, of the University of Kentucky, for providing us with the experimental spectra.

Thanks are also due to the members of my committee Professors E.A.Cherniak, S.M.Rothstein, K.Gough, and R.H.Hiatt.

To my wife and son, thank you for your inspiration.

TABLE OF CONTENTS

LIST OF TABLES

LIST OF FIGURES

CHAPTER ONE

INTRODUCTION

1.1) AN OVERVIEW

The ground state spectroscopy of the simple aliphatic carbonyl compounds CH_3CHO, and $(CH_3)_2CO$ has recently been the subject of several studies[1,2]. The spectral simplification afforded by supersonic-jet spectroscopy coupled with powerful computer methods, has enabled the spectroscopist to elucidate the nature of the excited states for such molecules. The vibrational and rotational dynamics of the higher electronic states have been investigated in some detail in several studies[3,4,5].

On the other hand, less is known about the aliphatic thiocarbonyl species CH_3CHS, and $(CH_3)_2CS$. The effect of replacing the oxygen in the carbonyl group with a heavy sulphur atom is evidenced by the relative instability of the aliphatic thiocarbonyl compounds. The thiocarbonyl species CH_3CHS, and $(CH_3)_2CS$ polymerize readily, usually forming cyclic trimers, whereas their oxygen analogues are stable at room temperature. Photoelectron and microwave techniques have demonstrated that under low pressure conditions the lifetime of thioacetaldehyde with respect to polymerization is about 10 seconds, and that of thioacetone is much longer, of the order of several minutes[6]. Moreover, these compounds possess a vile smell. These two problems have delayed the study of the aliphatic thiocarbonyl species.

Thioacetaldehyde, CH_3CHS, was first characterized by microwave and photoelectron spectroscopies among the pyrolysis products of 1,3,5-trimethyl-s-trithiane, $(CH_3CHS)_3$ [7]. Kroto *et al* have determined the ground state structure, the dipole moment, and the internal rotation barrier.

The infrared and Raman spectra have not been measured due to the instability of the compound.

The low lying electronic states of thioacetaldehyde have been studied by Moule and others[8]. The spectrum of thioacetaldehyde was found to have similarities to spectra of other aliphatic thiocarbonyl compounds. The spectrum shows six transitions in the 190-700nm region. The absorptions were assigned to the intervalence singlet and triplet $n \rightarrow \pi^*$ and singlet $\pi \rightarrow \pi^*$ transitions, and to the three Rydberg singlet transitions $n \rightarrow 4s$, $n \rightarrow 4p_y$, $n \rightarrow 4p_z$.
The phosphorescence-excitation, and resolved emission spectra of thioacetaldehyde were investigated by Judge et al [9]. The torsional fine structure in the spectrum provided the information to determine the rotational barriers of the methyl group for both the singlet ground state $\tilde{X}^1A_1$ and the triplet excited electronic state $\tilde{a}^3A_2$. The system $\tilde{a}^3A_2 \rightarrow \tilde{X}^1A_1$ of CH_3CHS and its isotopomers was assigned. The analyses indicated that the torsional motion in the triplet state was coupled to the large amplitude wagging of the aldehyde hydrogen. The observed phase shift in the torsional angle was attributed to the effects of hyperconjugation between methyl hydrogens and the π(CS) orbitals.

The ab initio SCF study, of the methyl internal rotation and aldehyde hydrogen wagging of thioacetaldhyde in the T_1 and S_0 states, has been performed by Smeyers et al [10]. The preferred conformations for the ground and lowest triplet electronic states were found to be the eclipsed and anti-eclipsed forms respectively (Figure 3.7). The calculated barrier heights to methyl rotation were also reported.
The decay dynamics of the lowest triplet and lowest singlet states of CH_3CHS were studied by Steer et al [11]. The lifetime of the radiative T_1 state under collision-free conditions was observed to be 10 μs . Weak emission was reported following

excitation to the S_1 state. Intersystem crossing to the T_1 is the likely path of the radiationless decay of the S_1 state .

In a recent study of thioacetaldehyde, the potential energy surfaces for both the ground and first excited triplet states were calculated by ab initio restricted Hartree Fock and unrestricted Hartree Fock methods. This study confirmed that the structure of thioacetaldehyde in the excited state differs from that of the ground state. The two-dimensional Schrodinger equations for the torsion and wagging motions were solved for both singlet and first triplet states. The relative band positions and strengths were determined from the eigenvalues and eigenvectors. The study also proposed new assignments for the higher bands in the visible spectrum of thioacetaldehyde.

1.2) PURPOSE OF THIS WORK

In spite of the relative success of previous experimental studies, the vibronic fine structure in the electronic spectrum of thioacetaldehyde is still by and large not assigned. This in part is due to the background congestion and to the overlap of adjacent bands. The origin band, for example, could not be observed directly in the absorption spectrum due to overlap with the adjacent strong hot bands.

On the other hand, the theoretical ab initio self consistent field ,SCF, calculations were carried out with a short basis set 4-31G+d(S).
In Smyers' [10] study, the ground and excited state potential energy surfaces were calculated using the experimental geometry without full optimization. The employment of a partially optimized geometry could lead to erroneous energy calculations[13].

In this work, the kinetic energy was also improperly handled. Laane[14,15,16] has examined the errors associated with fixed reduced masses in the calculation of the kinetic energy, and has introduced the concept of a kinetic energy expansion as the proper solution to this problem.

The technique of laser induced phosphorescence has been used to record the electronic spectra of the supersonic-jet-cooled thioacetaldehyde[17]. In this work the spectra are reported and assigned. The reduction in the translational, rotational, and to a lesser extent, the vibrational temperature is expected to remove much of the torsional hot band structure and the background congestion, and to give a better view of the higher vibronic bands in the spectrum. Hence, this work is intended to circumvent many of the experimental difficulties encountered in the previous studies.

It is the intention of this work to assign and analyze the new supersonic-jet spectra and to correct the previous theoretical studies. Geometry optimization at all of the selected grid points will lead to proper potential energy surfaces. The kinetic energy is to be modeled as an expansion function of both torsion and wagging. This, then, will yield the complete Hamiltonian. The two-dimensional Schrodinger equations for torsion and wagging motions will be solved for both the ground and first triplet electronic states. The relative peak locations and intensities will be determined using the eigenvalues and eigenvectors. The theoretical spectrum will be calculated and fitted to the observed supersonic-jet spectrum. Hence, "experimental" potential energy surfaces will be generated, and will yield invaluable information about the properties of the ground and excited triplet electronic states.

The analysis of the thioacetaldehyde spectra, in this way, can be used as a bench mark to test the validity of the UHF procedure in describing the properties of triplet excited electronic states.

CHAPTER TWO
SUPERSONIC JET SPECTRA

2.1) SUPERSONIC JET

Supersonic-jet-cooled expansion has become a powerful tool for investigating unstable molecules[18,19,20,21] . In this section a brief overview of the properties of the supersonic-jet is provided.

The supersonic-jet consists of a gas reservoir at high pressure p_0, an orifice or nozzle of diameter D, and a low pressure region P_1 which is maintained by giant vacuum pumps. Figures (2.1), and (2.2) give the top and side view of the jet-apparatus. The diameter of the nozzle ,D, is greater than the mean free path for collisions between the atoms or molecules passing through it. This is necessary, in order that the collisions occur during and after the gas exits from the nozzle. These collisions will steer the random motions of the molecules in the expansion into a mass flow in the direction of the resulting beam. In addition to initiating the highly directional motions, the free jet narrows the gas velocities (i.e the range of velocities is reduced). This is important since the translational temperature is measured from the width of the velocity distribution, and consequently the narrowing of the velocity distribution means a lower translational temperature.

The coldest temperatures are attained when the conditions of free collisions and supersonic speeds are met. The word supersonic is used here to mean high Mach numbers.

$$Mach\ Number\ (M) = \frac{u}{a}$$

where u is the mass flow velocity and a is the speed of sound in the gas.

$$\textit{Local Speed Of Sound} \quad (a) \; = \; \left(\frac{\gamma K T_{tr}}{m}\right)^{\frac{1}{2}}$$

where: γ is the heat capacity ratio C_p/C_v at constant pressure and volume, K is the Boltzmann constant, m is the molecular mass, and T_{tr} is the translational temperature. The Mach number is increased by reducing the local speed of sound rather than increasing the mass flow velocity.

The carrier gas used is an atomic gas such as helium or argon. Such gases have no rotational or vibrational degrees of freedom and hence a low heat capacity. The molecules of interest collide with the carrier gas and experience a marked lowering of their translational and rotational temperature and to a lesser extent their vibrational temperature.

It has been shown that for a continuous jet at a distance greater than a few orifice diameters, the Mach number can be written as [18]

$$M \; = \; 3.26 \left(\frac{X}{D}\right)^{\gamma-1}$$

where x is the downstream distance, and D is the nozzle diameter (γ =5/3 for a monoatomic gas). This equation describes the Mach number in the region where two body collisions take place. But, at some point in the expansion the velocity reaches a terminal value, and the system enters the collision free region. In this region, due to the equilibration of the internal degrees of freedom with the translational bath, the temperature reaches its coldest value. The Mach number also attains a terminal value ,M_T, that is

approximated by[18]

$$M_T = 133\ (P_0 D)^{0.4}$$

The above equation was found to describe the Mach number freezing for several carrier gases reasonably well. The terminal temperature ,T_T, is given by [18]

$$T_T = T_0\ [\ 1 + 5896\ (P_0 D)^{0.8}\ ]^{-1}$$

where T_0 is the ambient temperature. This equation implies that lower temperatures could be achieved by increasing P_0 and therefore the number of binary collisions, and/or the diameter of the nozzle. The limiting conditions compete with the speed of the pump and the rate of condensation.

Should the pump speed become inadequate for evacuation of the chamber, shock waves from the ambient temperature background gas would increase the translational temperature. Hence, high pumping speeds are required to eliminate the shock waves from advancing to the collision free region in the jet. In this experiment an Edwards mechanical booster pump/rotary pump combination was used.

The condensation of the expansion gas through dimerization and trimerization will hinder the cooling process by releasing the heat of condensation. This problem could be avoided by choosing proper ratios for (P_0/D), since this controls the number of binary and ternary collisions.

FIGURE (2.1)

Topview of the laser-jet apparatus

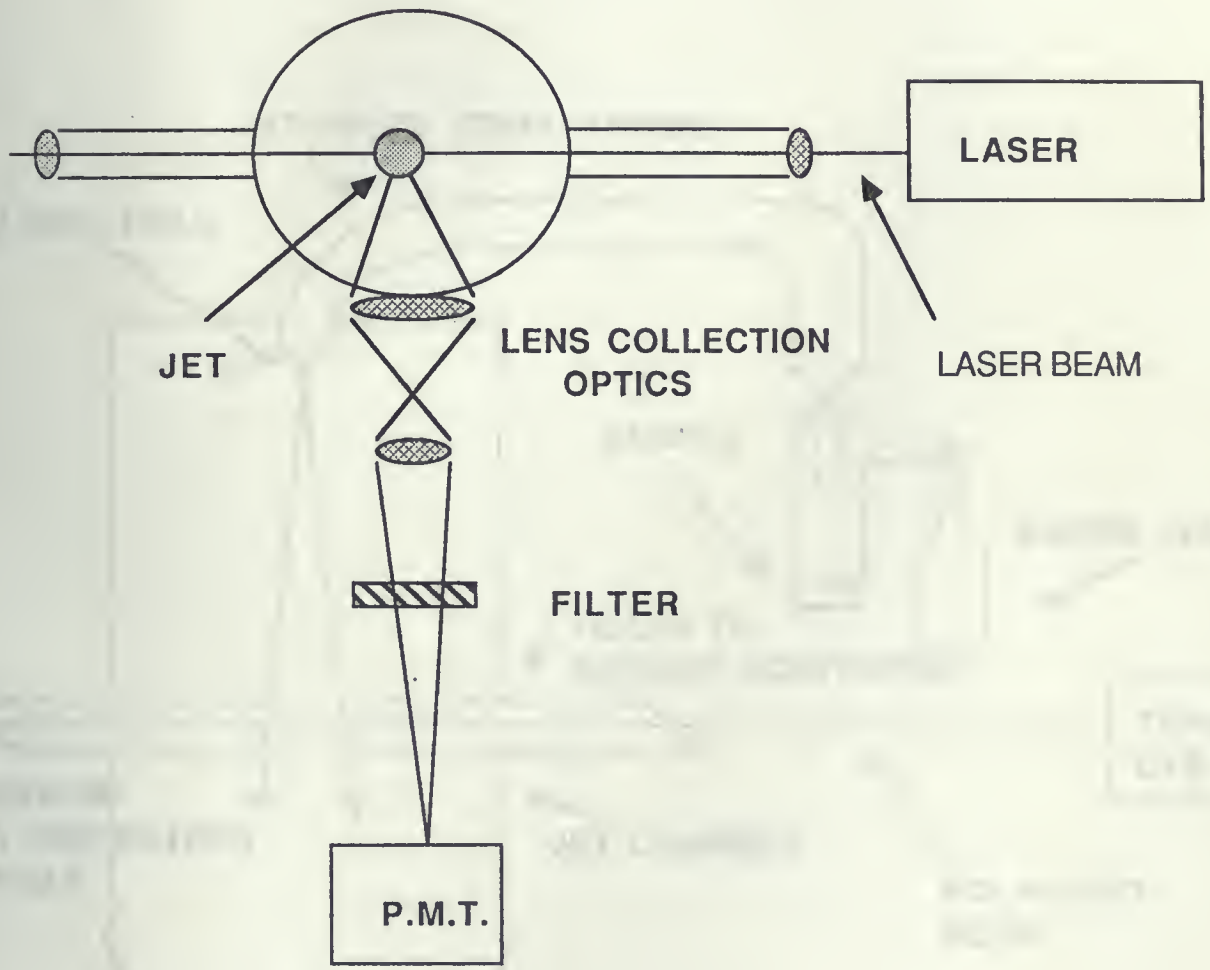

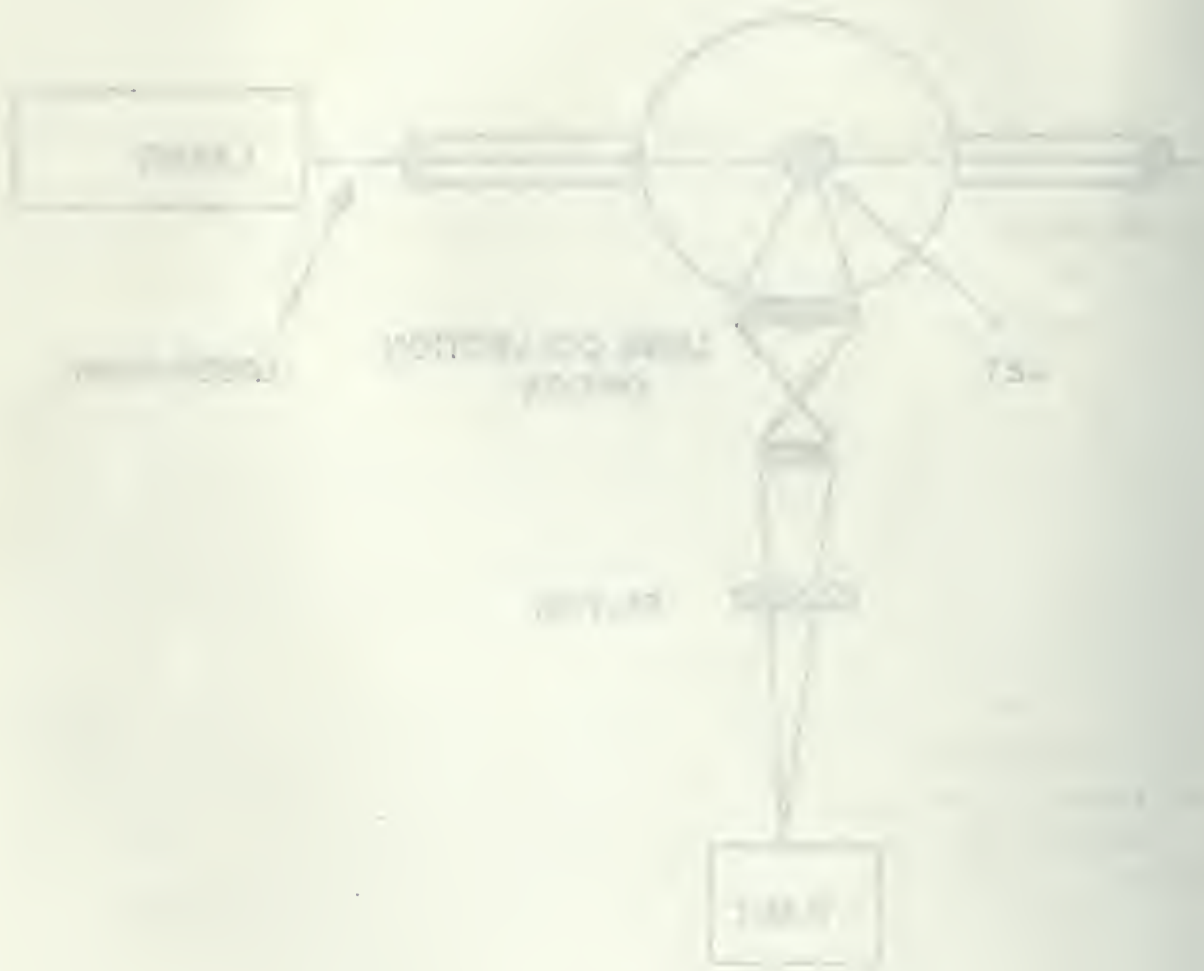

FIGURE (2.2)

Side view of the laser-jet apparatus

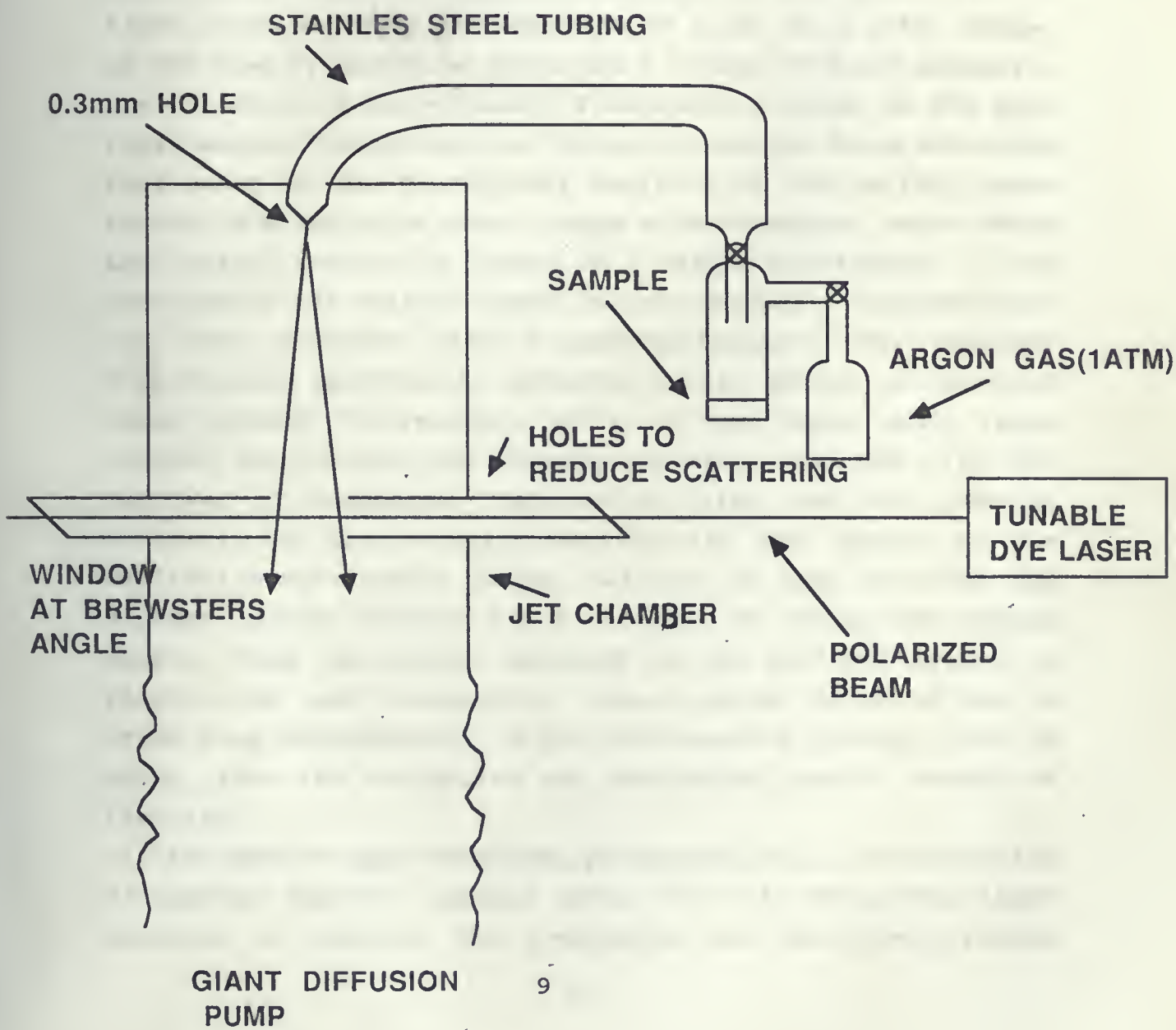

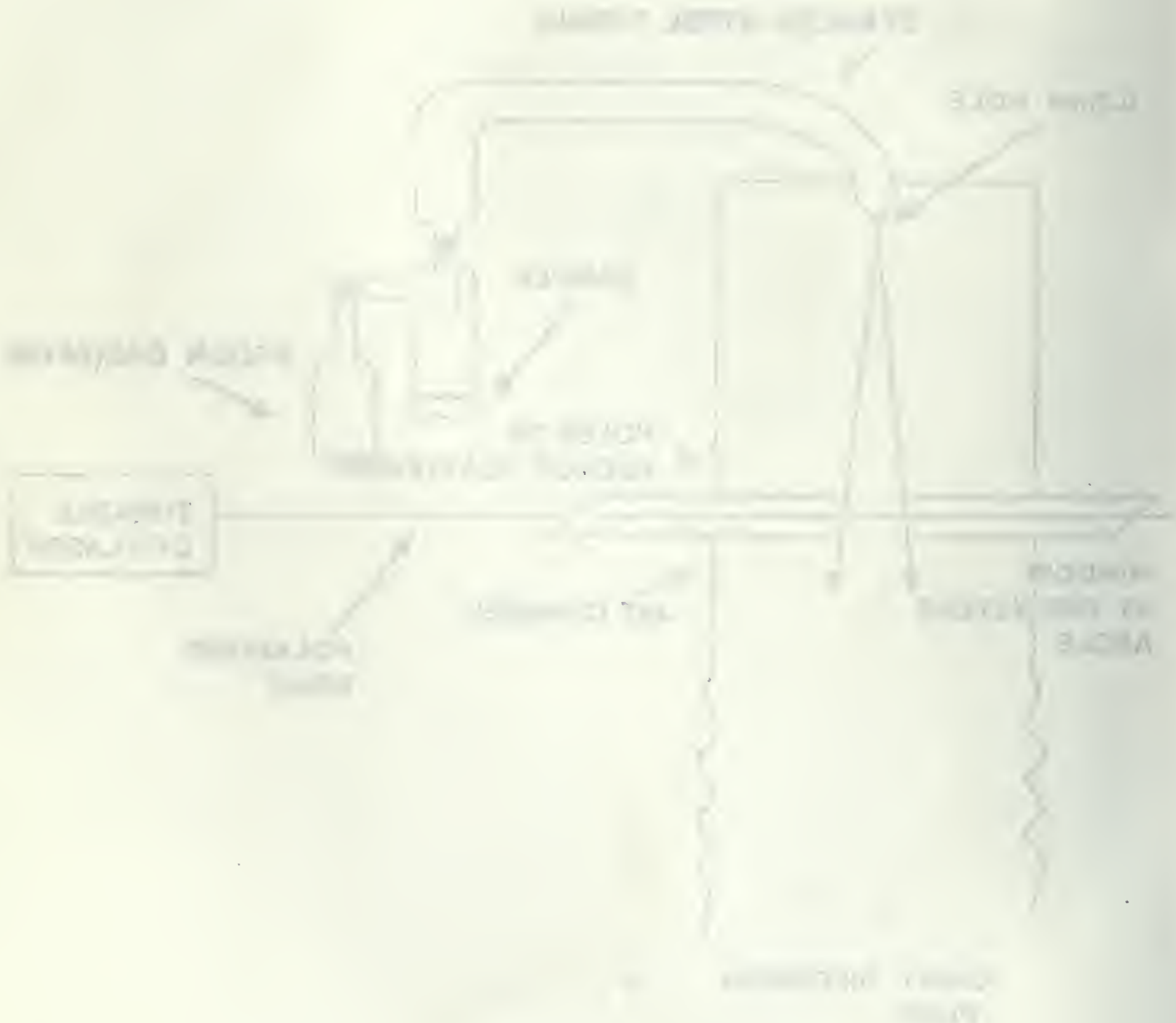

2.2) LASER INDUCED EXCITATION PHOSPHORESCENCE [23,28]

As a consequence of the substantial cooling created in the supersonic jet, the electronic spectra of thioacetaldehyde and its isotopomers exhibit excellent vibrational resolution. The detection of the molecule in the jet chamber without any perturbation from the medium is accomplished by using photons from a laser beam. The method of laser induced excitation fluorescence has been used to study the electronic spectra. The deactivation of molecules excited by the absorption of light often involves the emission of light at a later stage. In the case of molecules there are a number of decay pathways, one of which is spin-allowed fluorescence which is the most rapid means of deactivation. The radiationless decay processes that occur in the vibrational manifold of the excited state result in an emission over a range of wavelengths, even though the initial excitation occurs at a single wavelength. If the spectrum of the emitted light is sent through a monochrometer and then detected with a photomultiplier, the resolved fluorescence spectrum is obtained ; this method is known as Laser Induced Fluorescence (LIF). On the other hand, laser induced excitation spectroscopy is not concerned with the resolved fluorescence, but rather with how the overall intensity of the emission varies with the change of the excitation wavelength. Hence, L.I.E.F. is used to study the excited states whereas L.I.F. is used to study the ground state. Since the signal detected by the photomultiplier is relative to zero background, every photon detected has to arise from fluorescence. If the fluorescence quantum yield is unity, then the absorption and excitation spectra should be identical.

In the case of spin forbidden phosphorescence, the foregoing discussion applies equally well. In this case the light emission is delayed. The techniques for observing triplet

electronic states would then be called L.I.E.P. ,laser induced excitation phosphorescence.

2.3) EXPERIMENTAL

The experimental work was carried out at the University of Kentucky by D.C.Moule, J.Karolczak and D.J.Clouthier[17]. The author of this work received the spectra for assignment, and did not perform any of the actual experimental investigations. A summary of the synthesis and the jet experiments is provided below.

The synthesis of the solid trimer 1,3,5-trimethyl-s-trithiane is as described by Kroto et al [6]. The trimer was synthesized by passing H_2S gas through an ice cold mixture of HCl and acetaldehyde. The deuterated species were produced from the equivalent acetaldehydes. Samples of CH_3CDO, CD_3CHO, and CD_3CDO were supplied by MSD isotopes. The trimer was contained in a bulb which was heated to 50-60°C to increase the vapour pressure. The vapour was entrained in a stream of 1-atmosphere argon, and the mixture pyrolyzed at 700°C (see Fig.(2.3)) just prior to expansion through a 150 micron nozzle into the vacuum chamber. From past experience, it was estimated that rotational temperatures of 5-10 K were obtained under these conditions. In order to accentuate the weak hot bands, warm jet spectra were also recorded by altering the expansion conditions to prevent complete cooling of the molecules in higher vibrational levels which are populated in the high temperature pyrolysis zone.

The pyrolysis jet is illustrated in figure (2.4)[24]. One of the notable features of the pyrolysis jet assembly is that the pyrolysis tube extends 1 cm beyond the heated area so that the nozzle is cooler than the pyrolysis tube. The pyrolysis

assembly is mounted on an XYZ translation stage so that the distance from the apparatus to the intersecting laser beam can be varied with no alignment errors.

The phosphorescence of thioacetaldehyde was initiated with a Nd:YAG pumped dye laser system (Lumonics HY 750 + HyperDye 300) using Rhodamine 6G, Rhodamine 610 and Coumarin 540A laser dyes (Exciton). Laser powers of 1-5 mJ per pulse and line widths of approximately 0.1 cm^{-1} were employed. The emission was detected by imaging the cold portion of the supersonic expansion through a suitable cutoff filter to reject scattered light and onto a high gain, red sensitive photomultiplier (EMI 9816 QB). The excitation spectra were wavelength calibrated by simultaneously observing the optogalvanic effect from a neon filled hollow cathode U/Ar lamp.

Wavelength calibrated and laser power corrected spectra were obtained by simultaneously recording the phosphorescence excitation spectrum, optogalvanic spectrum and laser power on a computerized data acquisition system[25]. The pulsed signals were processed by gated integrators prior to digital acquisition.

FIGURE (2.3)

The synthesis of Thioacetaldehyde

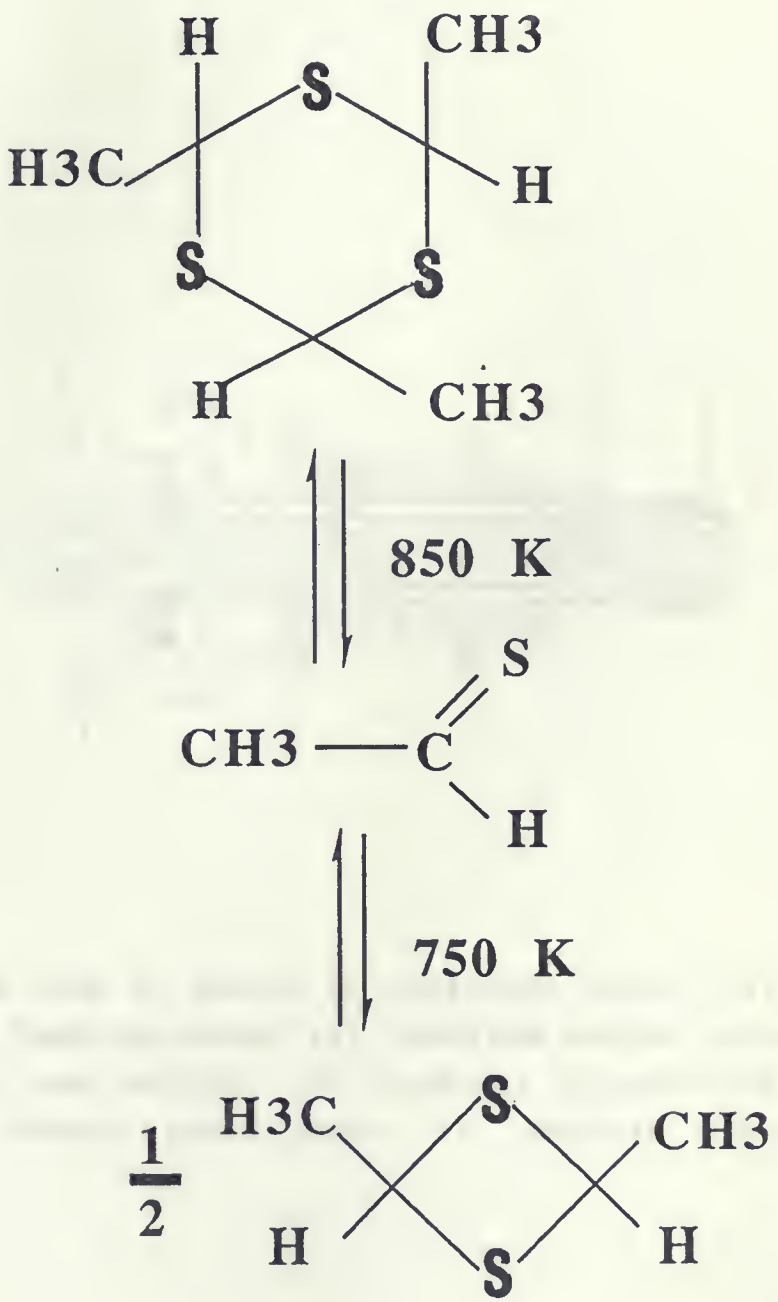

FIGURE (2.4)

Schematic drawing of the pyrolysis jet assembly

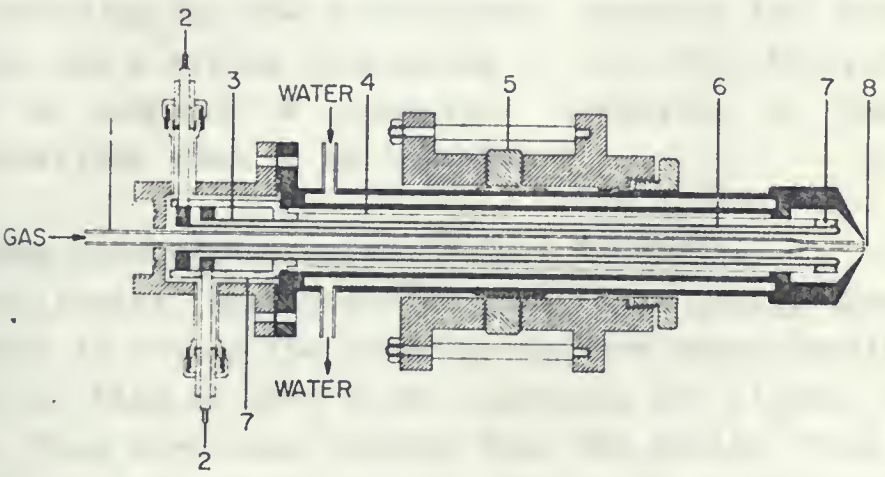

(1)pyrolysis tube of quartz or stainless steel; (2) O-ring sealed vacum feed-throughs; (3) tantalum heater outer tube; (4) tantalum heat shield; (5) vertical translation stage; (6)tantalum heater inner tube; (7) ceramic insulators; (8)nozzle

CHAPTER THREE
THEORY : PART ONE
ab initio METHODS

Computational ab initio quantum chemistry is aimed at evaluating the properties of atoms, molecules, radicals, ions, solids, and all other chemical species. The words ab initio hint at an attempt to solve the Schrodinger equation from first principles. The model considers the chemical species as a group of positive nuclei and negative electrons which move under the influence of electrostatic coulombic potential. The exact solution to the Schrodinger equation has never been attained for a system consisting of more than two particles. Hence to achieve a practical solution, a number of approximations need to be introduced.

3.1) BORN-OPPENHEIMER APPROXIMATION [26,27,28,29]

The initial approximation made in ab initio quantum chemistry is called the Born-Oppenheimer approximation. The essence of this is that since electrons are lighter than the nuclei, they move more rapidly than the nuclei. Thus one may consider the electrons to be moving in a fixed field of nuclei. The total Hamiltonian for N electrons and M nuclei is given by;

$$H = -\sum_{i=1}^{N} \frac{1}{2}\nabla_i^2 - \sum_{A=1}^{M} \frac{1}{2M_A}\nabla_A^2 - \sum_{i=1}^{N}\sum_{A=1}^{M} \frac{Z_A}{r_{iA}} + \sum_{i=1}^{N}\sum_{j>i}^{N} \frac{1}{r_{ij}} + \sum_{i=1}^{M}\sum_{B>A}^{M} \frac{Z_A Z_B}{R_{AB}}$$

The first term is the kinetic energy of the electrons, the second term is the kinetic energy of the nuclei, the third term is the coulomb attraction between electrons and nuclei,

the fourth term is the repulsion of electrons, and the fifth term is the repulsion between nuclei. Within the Born Oppenheimer approximation, the second term is neglected and the fifth term is treated as a constant. The remaining terms define the electronic Hamiltonian.

3.2) SELF-CONSISTENT FIELD (HF) METHODS[26,28,29,30]

The general idea of SCF methods is that each electron moves in an average field due to the nuclei and remaining electrons. The Schrodinger equation involving the electronic Hamiltonian is

$$H_{elec.} \Psi_{elec.} = E_{elec.} \Psi_{elec.}$$

The electronic Hamiltonian operator ,$H_{elec.}$, describes the kinetic and the potential energy operators of the system. The electronic wavefunction is described by the spatial and spin orbitals. The eigenvalue ,$E_{elec.}$, is the sum of the orbital energies of each of the spin orbitals appearing in the wavefunction.

The N-electron wavefunction ,Ψ, is a linear combination of one-electron wavefunctions ,Φ, ;

$$\Psi = \sum_{i=1}^{N} C_{ji} \Phi_i$$

where the coefficents C_{ji} are determined such that the total electronic energy is minimized.

The Hartree-Fock (HF) method is based on the Variational theorem. For an antisymmetric normalized function Φ, the

expectation value of the energy corresponding to this function is

$$\langle E \rangle = \frac{\langle \Phi^* | H_{elec.} | \Phi \rangle}{\langle \Phi^* | \Phi \rangle}$$

If the chosen wavefunction Φ is the exact wavefunction Ψ then the exact lowest possible energy is obtained. If on the other hand Φ is not Ψ then the calculated energy will be higher than the exact energy. This energy value is subject to the single-determinant condition imposed by the (HF) method, and the choice of the basis set.

The variational principle is used to obtain optimum orbitals in the single determinant wavefunction. This is done by selecting a basis set and minimizing E with respect to the coefficients C_{ji}. This leads to the variational condition;

$$\frac{\partial E}{\partial C_{ji}} = 0$$

A) Closed Shell[26,31,32,33]

In restricted Hartree Fock (RHF) procedures electrons doubly occupy the molecular orbitals. Thus the problem of electron spin does not arise because all electrons are paired.

B) Open Shell[26,31,32,33]

In open shell systems, electrons are not completely distributed in pairs among the orbitals. In the unrestricted Hartree Fock (UHF) theory, the two sets of molecular orbitals are defined by two sets of coefficents;

$$\psi_i^{\alpha} = \sum_{j=1}^{N} C_{ji}^{\alpha} \phi_j$$

$$\psi_i^{\beta} = \sum_{j=1}^{N} C_{ji}^{\beta} \phi_j$$

These two orbitals are similar but not identical and this gives flexiblity to UHF over RHF. This is both an advantage and disadvantage of the UHF method. The advantage is in that it allows for spin polarization (the means by which an unpaired electron perturbs paired spins) giving it a true estimate of spin densities. The disadvantage is that UHF gives a higher energy than RHF. Another problem with UHF is the spin contamination by mixing with states of higher spins. The degree of spin contamination can be checked from the $< S^2 >$ parameter given in the output. The expectation value for $<S^2>$ is S(S+1) where S is the total spin.

3) Basis Sets[30,31,32]

In the HF method the N-electron wavefunction is constructed from the molecular orbitals in a single determinant. There are two major types of basis functions. The Slater Type atomic Orbital (STO), and the Gaussian Type atomic Orbital. The STO's are labeled hydrogen-like atomic orbitals 1s, 2s, $2p_x$,..., and they are of the form;

$$\phi_{1s} = \left(\frac{\zeta_1^3}{\pi}\right)^{\frac{1}{2}} \exp(-\zeta_1 r)$$

$$\phi_{2p_x} = \left(\frac{\zeta_2^5}{32\pi}\right)^{\frac{1}{2}} X \exp\left(\frac{-\zeta_2 r}{2}\right)$$

where ζ_1 and ζ_2 are constants determining the size of the orbitals. The integral evaluation using STO basis functions is time consuming, even on a large computer. This has led to the development of another basis function namely the Gaussian type. The GTO's include an exponential term of the form $\exp(-\alpha r^2)$, the radial dependence of such functions is similar to those of a hydrogen like 1s function (1s-STO). The form of GTO functions is;

$$g_s(\alpha, r) = \left(\frac{2\alpha}{\pi}\right)^{\frac{3}{4}} \exp(-\alpha r^2)$$

$$g_x(\alpha, r) = \left(\frac{128\alpha^5}{\pi^3}\right)^{\frac{1}{4}} X \exp(-\alpha r^2)$$

The two obvious disadvantages of using Gaussian functions as basis sets are;

a) Unlike s-type hydrogen like atomic orbitals, Gaussians do not have cusps at r = 0.

b) Their exponential term dies faster at large values of r, than those of hydrogen like atomic orbitals.

The advantage of using Gaussian functions is of great importance, since they made it extremely easy to calculate the integrals involved. In fact, the most widely used computational package for <u>ab initio</u> calculations is the Gaussian series of programs, dealing as the name implies exclusively with GTO's. There are several GTO basis sets; the discussion below explains some of the symbols used to denote them.

STO-nG implies that Slater Type Orbitals simulated by n Gaussian functions are being used as a basis set. The STO-3G

is the minimal basis set in this series. The inability of a minimal basis set to expand or contract its orbitals to fit the moleculer environment led to the use of split-valence or double zeta basis sets. In such basis sets the atomic orbitals consist of an inner compact orbital and an outer diffuse orbital. The size of the atomic orbital that contributes can be varied by the coefficients associated with the compact and diffuse parts. An example of a double-zeta function is the 4-31G basis set. 4-31G means that four Gaussians for the core orbitals, three inner Gaussian valence-orbitals, and one outer valence orbital are used. The heavy (non-hydrogen like) atoms require d-orbitals. For example, this may allow a shift of the center of a p-orbital away from the nucleus. This adjustment is important for molecules containing small rings and for molecules with atoms from the second row. A commonly used polarization basis set, and one we used in this work, is the 6-31G*. The symbol 6-31G* means that six Gaussians for the core, and 3 : 1 split for s and p valence orbitals are used, and the * means that six d-functions are added.

3.4) GEOMETRY OPTIMIZATION[31,32,34,35]

Geometry optimization is used to find stationary points on the potential energy surface. The consequence of using no geometry optimization or partial optimization could be the calculation of an energy value which is far too high. Thus it may be necessary to use complete optimization of the molecular geometry to give points on the potential surface. Also, in the vibrational frequency calculations the geometry used must correspond to the minimum on the potential surface.

The sequence of execution of program modules resulting in the optimization of molecular geometry for a given basis set is illustrated in figure (3.1). The program first requires a

specification of the molecular geometry. The input format used for RHF and UHF are shown in Figure(3.2) and Figure(3.3) respectively. The input of the molecular geometry in the Gamess programs can be specified by either cartesian or internal coordinates. For convenience we used the internal coordinates (bond distances, bond angles, dihedral angles). Four dummy atoms help locate the atoms of the molecule. The dummy atom O is located at the origin and the other three atoms (I,J,K) are located such that each one is at one unit distance along each of the three axes X,Y,Z. A special connectivity notation is used to help relate the atoms of the molecule to one another. This is illustrated in figure (3.4). The dummy atoms are merely used to define the coordinates. The program then converts the internal coordinates to cartesian coordinates. The program requires the definition of other molecular data such as the point group symmetry and basis set type. The point group used is dependent on the geometry, and is either C_s or C_1. The basis set employed is the commonly used 6-31G*. Then, the next step requires the calculation of the integrals from which guess wavefunctions are produced. The SCF equations are solved for the total energy and wavefunctions. With this wavefunction the energy gradient (the first derivatives of the energy with respect to the displacements in nuclear coordinates), is evaluated. The calculation of the energy gradient ends when the calculated geometry has reached a preset degree of convergence. The number of passes through the optimization loop depends on several factors. Such factors are the number of geometrical variables, the convergence requirement, and the choice of initial structure. Generally for a system with n variables between n and 2n cycles are needed to ensure that the bond lengths and angles have converged to within 0.001 Å and 0.1° respectively.

Figure(3.1) Program sequence for molecular geometry optimization.[31]

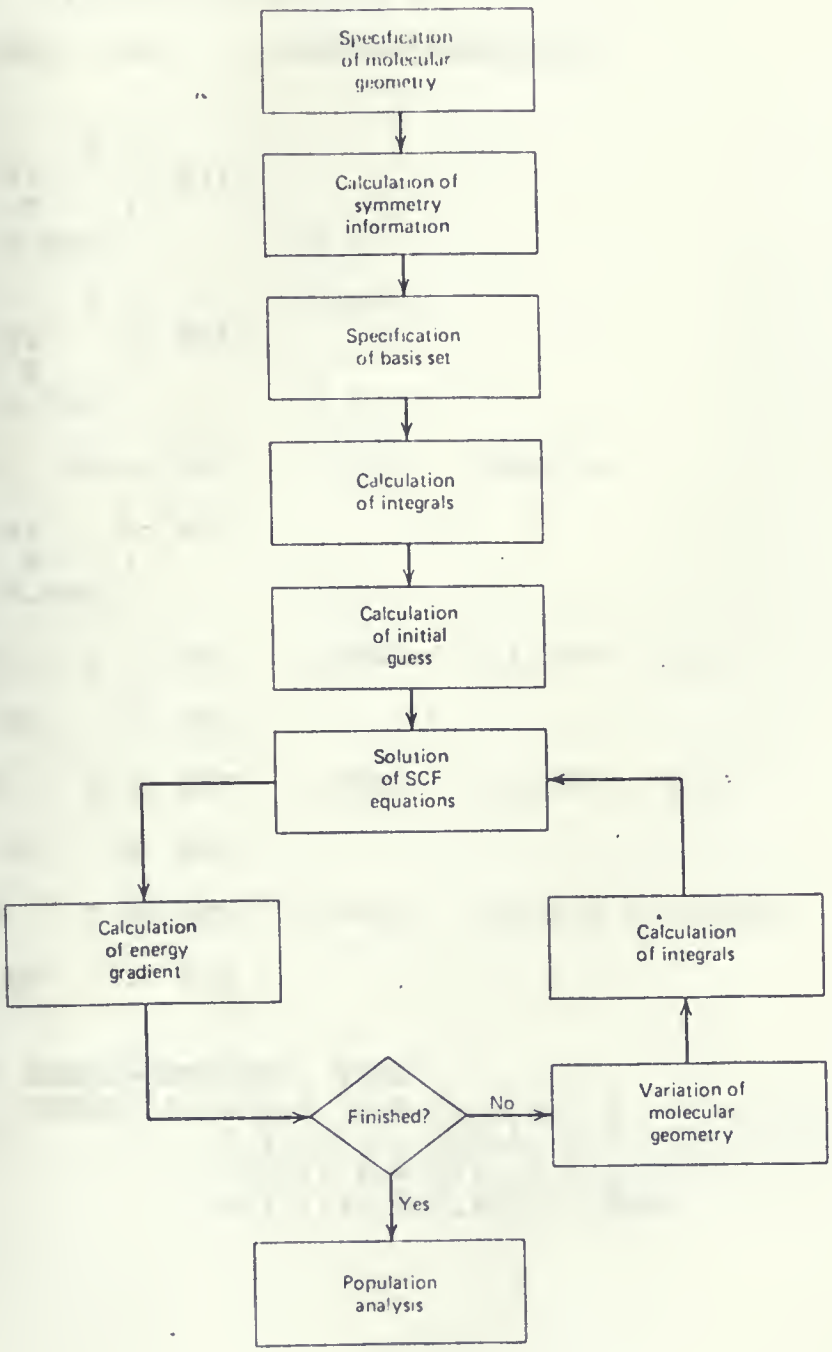

FIGURE (3.2)
Input of Gamess data for RHF methods

```
 $CONTRL SCFTYP=RHF RUNTYP=OPTIMIZE UNITS=HINT NZVAR=15 EXETYP=RUN
 $END
 $STATPT  IFREEZ(1)=6,9 $END
 $DATA
.....  RHF/6-31G*.....thioacetaldhyde...
CS

CARBON       6.0
    1   SV     6  N31
    3    D     1
    1   0.800              1.0

CARBON       6.0          1.4964                              -
    1   SV     6  N31
    3    D     1
    1   0.800              1.0

SULPHUR     16.0  PCC    1.6063    126.6162                   +     2     1
  J
    1   SV     6  N31
    3    D     1
    1   0.650              1.0

HYDROGEN     1.0  PCC    1.0804    111.6403   0.0             -     2     1
  J
    1   SV     6  N31

HYDROGEN     1.0  TCT    1.0910    114.4506   0.0             +     1     2
  J
    1   SV     6  N31

HYDROGEN     1.0  TCT    1.098     109.531 121.5326           +     1     2
  5
    1   SV     6  N31

 $END
 $GUESS  GUESS=EXTGUESS  $END
 $ZMAT   IZMAT(1)= 1,1,2, 1,2,3, 2,1,2,3, 1,2,4, 2,1,2,4,
                   4,4,2,3,1, 1,5,1, 2,5,1,2, 3,5,1,2,3,
                   1,6,1, 2,6,1,2, 3,6,1,2,5, 1,7,1,
                   2,7,1,2, 3,7,1,2,5  $END
```

FIGURE (3.3)
Input of Gamess data for UHF methods

```
 $CONTRL SCFTYP=UHF  MULT=3 RUNTYP=OPTIMIZE UNITS=HINT NZVAR=15
  EXETYP=RUN $END
 $
 $DATA
.....  RHF/6-31G*.....thioacetaldehyde...
CS

CARBON       6.0
    1   SV     6  N31
    3    D     1
    1   0.800              1.0

CARBON       6.0          1.506                              -
    1   SV     6  N31
    3    D     1
    1   0.800              1.0

SULPHUR     16.0  PCC    1.610       125.28                  +     2     1
  J
    1   SV     6  N31
    3    D     1
    1   0.650              1.0

HYDROGEN     1.0  PCC    1.089       119.40      0.0         -     2     1
  J
    1   SV     6  N31

HYDROGEN     1.0  TCT    1.098       110.12      0.0         +     1     2
  J
    1   SV     6  N31

HYDROGEN     1.0  TCT    1.098       110.12    120.0         +     1     2
  5
    1   SV     6  N31

 $END
 $GUESS  GUESS=EXTGUESS  $END
 $ZMAT   IZMAT(1)= 1,1,2, 1,2,3, 2,1,2,3, 1,2,4, 2,1,2,4,
                   4,4,2,3,1, 1,5,1, 2,5,1,2, 3,5,1,2,3,
                   1,6,1, 2,6,1,2, 3,6,1,2,5, 1,7,1,
                   2,7,1,2, 3,7,1,2,5  $END
```

Figure(3.4) Programmed standard connections used in calculating coordinates.[34]

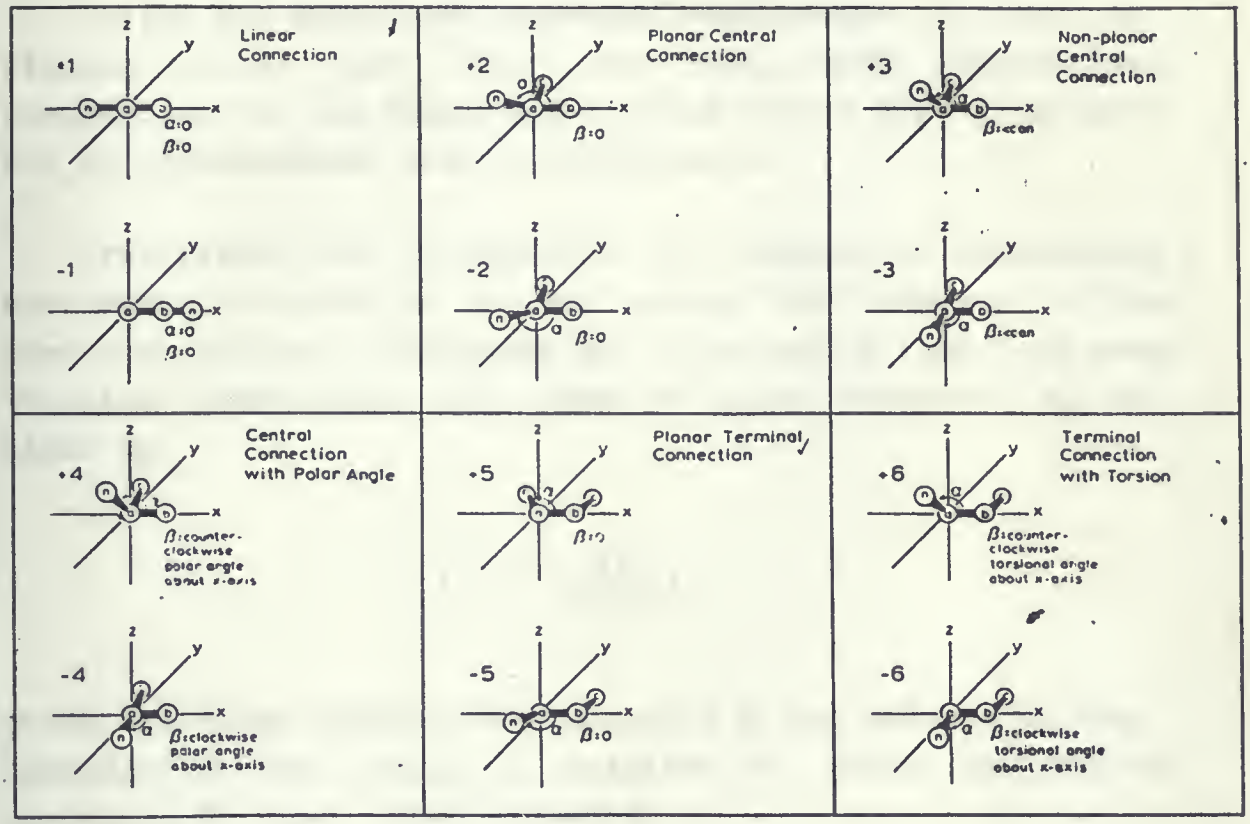

3.5) VIBRATIONAL FREQUENCY CALCULATION[31]

The calculated normal-mode vibrational frequencies provide several important benefits. First they can be used to distinguish between local minima and saddle points. Secondly they provide a means of characterizing the molecule. Thirdly they provide us with thermodynamic properties of the molecule.

Using the optimized cartesian coordinates, as shown in figures (3.5), and (3.6) the normal-mode vibrational frequencies for the ground and excited states were calculated for thioacetaldehyde and its isotopomers.

The vibrational frequencies are computed by determining the second derivatives of the energy with respect to the cartesian nuclear coordinates and transforming them into mass weighted coordinates. The quadratic force constants f_{ij} are given by

$$f_{ij} = \left(\frac{\partial^2 V}{\partial q_i \partial q_j}\right)_{eq}.$$

where the mass-weighted displacements q_i are defined by the location of the nuclei X_i relative to their equilibrium positions $X_{i,eq}$ and their masses M_i.

$$q_i = M_i^{\frac{1}{2}} (X_i - X_{i,eq.})$$

V is the potential energy at the equilibrium nuclear configuration. The f_{ij} may be computed by numerical second differentiation;

$$\frac{\partial^2 V}{\partial q_i \partial q_j} \approx \frac{\Delta(\Delta V)}{\Delta q_i \Delta q_j}$$

or by numerical first differentiation of the analytical first derivatives

$$\frac{\partial^2 V}{\partial q_i \partial q_j} \approx \frac{\Delta\left(\frac{\partial V}{\partial q_i}\right)}{\Delta q_j}$$

The calculation yielded 3N normal-mode vibrational frequencies. Six of these are zero due to the translational and rotational degrees of freedom. The frequencies were scaled by 0.9 to correct for anharmonicity and the overestimation of force constants resulting from neglect of the correlation energy.

FIGURE (3.5)
Input format for the S_0 normal mode calculation

```
 $CONTRL SCFTYP=RHF  RUNTYP=HESSIAN UNITS=BOHR  NZVAR=15
  TIMLIM=6000.0 $END
 $FORCE METHOD=NUMERIC NVIB=2 $END
 $DATA
 RHF/6-31G*/Calc of vib. freq. d-6 S0, E,E
CS

CARBON       6.0      -0.0044257723     -0.000298383      0.0000000000
       1   SV     6  N31
    3     D     1
    1   0.800            1.0

CARBON       6.0       2.8240961693    -0.0013502716     0.0000000000
    1   SV     6  N31
    3     D     1
    1   0.800            1.0

SULPHUR     16.0       4.6354832924     2.4346518811     0.0000000000
    1   SV     6  N31
    3     D     1
    1     0.650          1.0

HYDROGEN     1.0       3.6681871432    -1.8616057810     0.0000000000
    1   SV     6  N31

HYDROGEN     1.0     -0.7577142899      1.8974623884     0.0000000000
    1   SV     6  N31

HYDROGEN     1.0     -0.6922958437     -1.0133466490    -1.6501035434

    1   SV     6  N31

 $END
 $GUESS GUESS=EXTGUESS $END
 $ZMAT   IZMAT(1)= 1,1,2, 1,2,3, 2,1,2,3, 1,2,4, 2,1,2,4,
                   4,4,2,3,1, 1,5,1, 2,5,1,2, 3,5,1,2,3,
                   1,6,1, 2,6,1,2, 3,6,1,2,5, 1,7,1,
                   2,7,1,2, 3,7,1,2,5  $END
```

FIGURE (3.6)
Input format for the T_1 normal mode calculation

```
 $CONTRL SCFTYP=UHF  RUNTYP=HESSIAN  UNITS=BOHR  NZVAR=15
  TIMLIM=6000.0  MULT=3 $END
 $FORCE METHOD=NUMERIC NVIB=2 VIBSIZ=0.005 $END
 $DATA
 UHF/6-31G*/Calc of vib. freq.
CN       1

CARBON       6.0      0.0035622917   0.0549014555   0.0224065267

    1   SV     6  N31
    3    D     1
    1     0.800          1.0

SULPHUR     16.0     -1.6421346731   2.9124251891   -0.0032778852
    1   SV     6  N31
    3    D     1
    1     0.650          1.0

CARBON       6.0     -1.4164806118  -2.4043612981   -0.0040958699
    1   SV     6  N31
    3    D     1
    1     0.800          1.0

HYDROGEN     1.0      1.8633506915   0.1454527653    -0.7967081357
    1   SV     6  N31

HYDROGEN     1.0     -2.2180528629   -2.8054657622    -1.8562651015
    1   SV     6  N31

HYDROGEN     1.0      -2.9525938111   -2.3971605541    1.3537715414

    1   SV     6  N31

HYDROGEN     1.0      -0.1521313864   -3.9426136368    0.4813195573

    1   SV     6  N31

 $END
 $GUESS GUESS=EXTGUESS $END
 $ZMAT   IZMAT(1)= 1,1,2, 1,1,3, 2,3,1,2, 1,1,4, 2,4,1,3,
          4,4,1,3,2, 1,3,5, 2,5,3,1, 3,5,3,1,2, 1,3,6, 2,6,3,1,
            ,6,3,1,5, 1,3,7, 2,7,3,1, 3,7,3,1,5  $END
```

3.6) CONFIGURATION INTERACTION[26,27,29,31]

The Hartree-Fock approximation is quite reasonable in many cases; however, it has its limitations. The Hartree-Fock method approximates many-electron interactions by the assumption that each electron exists in an average field produced by all the remaining electrons, i.e the single-determinant wavefunction does not consider the correlation between electrons of opposite spin. The energy error resulting from this approximation is called the correlation energy. Hence, the correlation energy is the difference between the exact solution of the non-relativistic Hamiltonian, and the Hartree-Fock limit.

$$E\ (\text{CORRELATION}) = E\ (\text{H-F}) - E\ (\text{EXACT})$$

The neglect of the correlation energy is particularly serious where potential energy surfaces and dissociation processes are considered. The effect of electron correlation on the properties of excited electronic states has not been extensively studied. However, it is known that the energies and physical properties of excited states are very sensitive to the neglect of electron correlation. The electron correlation problem is dealt with by many methods, the most widely used of which is Configuration Interaction.

Configuration Interaction has emerged as one of the most popular techniques for including effects of correlation in many-electron systems. The idea of CI is to ignore the restriction that the electronic wavefunction must be a single determinant. In this model, the wavefunctions are taken to be linear combinations of single determinants. This is also known as Configuration Mixing (CM).

THEORY : PART TWO
THE POTENTIAL AND KINETIC ENERGIES

3.7) THE POTENTIAL ENERGY[12,36-45]

In this work, the torsional motion arising from the methyl group and the out of plane wagging of the aldehyde hydrogen atom will be modeled in the same way, ie, the torsion as a three fold rotation around the C-CH3 bond, and the wagging as a one fold rotation of the hydrogen around an imaginary axis perpendicular to the C-H bond lying in the CCS molecular plane and passing through the aldehyde carbon atom.

The Hamiltonian operator for single hindered rotation in the rigid rotor approximation can be written:

$$H(\theta) = -\frac{\partial}{\partial\theta} B(\theta) \frac{\partial}{\partial\theta} + V(\theta)$$

where B(θ) is the internal rotation constant and V(θ) is the potential energy function. The angle θ, which is defined in fig (3.7), measures the torsional displacement of the rotor relative to the CCS plane of the molecule.

In the following discussion we shall use the formalism of Altmann[36] which has been justified by Woodman[37] to describe the non-rigid symmetry operations, rather than using the Longuet-Higgins[38] theory.

The existence of a symmetry plane in the rotors (-CH3 or -H) and in the frame of the molecule allows the non-rigid group describing these motions to be expressed as[39]:

$$S_a = (C_n^I \wedge U^I) \sim C_{nv}$$

FIGURE (3.7)
The wagging and torsion angles

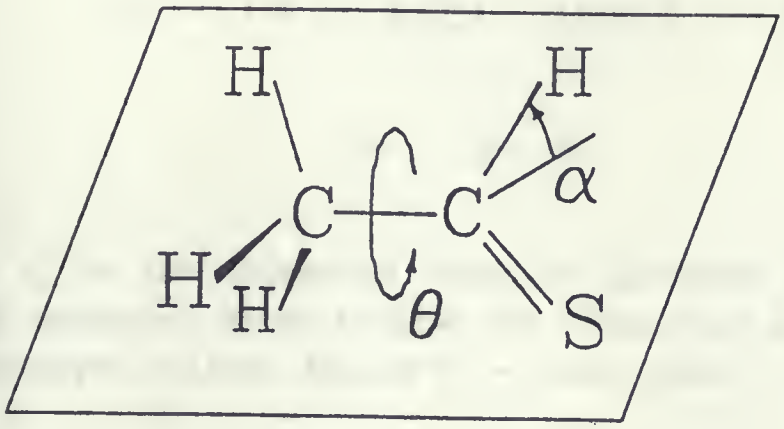

THE α AND θ ANGLES

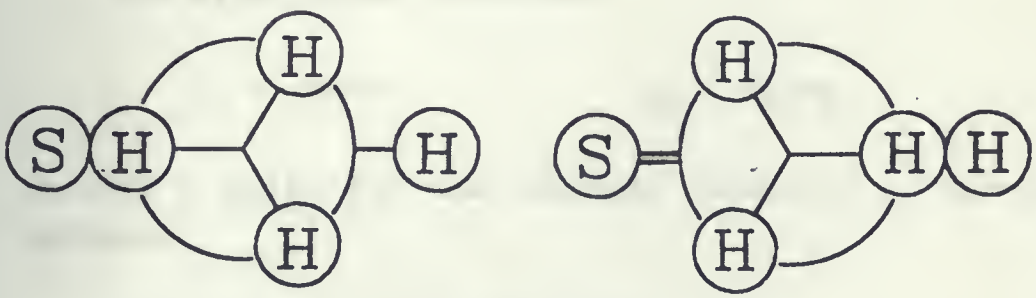

S_0 (ECLIPSED) T_1 (ANTIECLIPSED)

where n is the periodicity of the rotation.
The subgroups C_n^I and U^I are defined as follows:

$$C_3^I = [\hat{E} + \hat{C}_3 + \hat{C}_3^2] \quad also \quad C_1^I = [\hat{E}]$$

$$U^I = [\hat{E} + \hat{U}]$$

where $\hat{C}_3$ is the threefold rotation operator, and $\hat{U}$ is the switch operator, which rotates the rotor (the methyl group or the hydrogen moiety) from θ to $-\theta$ such that

$$\hat{U}f(\theta) = f(-\theta)$$

S_a is a nonrigid group which is isomorphic to the symmetry point group C_{nv}. In the case of thioacetaldehyde n=3, and the corresponding symmetry group is isomorphous to C_{3v}. From the character tables of the symmetry point group C_{3v}, the symmetry eigenvectors corresponding to the irreducible representations of the nonrigid group S_a can be constructed on the free rotor basis.

The sine-cosine functions:

$$\chi_{a1} = \cos K\theta \quad ; \quad \chi_{a2} = \sin K\theta$$

provide a basis for the one-fold rotation of the aldehyde hydrogen.

For the three-fold rotor these are

$$\chi_{a1} = \cos 3K\theta \quad ; \quad \chi_{a2} = \sin 3K\theta$$
$$\chi_e = \cos(3K \pm 1)\theta$$
$$\chi_e = \sin(3K \pm 1)\theta$$

Since the potential energy function must be unchanged under all of the operations of the group, it can be developed in terms of the a_1 symmetry eigenvectors.

$$V(\Theta) = \sum_K A_K^C \cos(nK\Theta)$$

The minimal Fourier expansion will take the simple form of an n-fold minimum potential function:

$$V(\Theta) = A_0^C + A_0^C \cos(n\Theta)$$

The starting point for this analysis was the two dimensional Hamiltonian operator, $H(\alpha,\theta)$, for the combined large amplitude wagging and torsional motions.

$$H(\alpha,\theta) = -\frac{\partial}{\partial\alpha} B_\alpha(\alpha,\theta) \frac{\partial}{\partial\alpha} + 2\frac{\partial}{\partial\alpha} B_{\alpha,\theta}(\alpha,\theta) \frac{\partial}{\partial\theta}$$

$$+\frac{\partial}{\partial\theta} B_\theta(\alpha,\theta) \frac{\partial}{\partial\theta} + V(\alpha,\theta)$$

In this equation $B_\alpha(\alpha,\theta)$, $B_\theta(\alpha,\theta)$ and $B_{\alpha\theta}(\alpha,\theta)$ are the internal rotation constants and the kinetic interaction terms which are dependent on the hydrogen wagging (α) and methyl torsion (θ) large amplitude coordinates which are defined in Fig (3.7). $V(\alpha,\theta)$ is the potential energy.

The existence of symmetry planes in both rotors and in the frame of thioacetaldehyde allows the nonrigid group for these molecules to be expressed as[39-45]:

$$S_b = (C_3^I \times C_1^I) \wedge V^I \sim C_{3v}$$

The subgroups C_3^I and C_1^I are defined as before while the subgroup V^I has the form:

$$V^I = [\hat{E} + \hat{V}]$$

where $\hat{V}$ is the double switch operation which rotates the methyl group from θ to $-\theta$ and simultaneously displaces the aldehyde hydrogen atom from α to $-\alpha$ such that

$$\hat{V}f(\alpha,\theta) \equiv f(-\alpha,-\theta)$$

S_b is a nonrigid group which is isomorphic to S_a as well as to the symmetry point group C_{3v}. From the character tables the symmetry eigenvectors corresponding to the irreducible representations of the nonrigid point group S_b can be be deduced from the free double rotor function basis as

χ_{a1} = cos3Kθ cosLα and sin3Kθ sinLα

χ_{a2} = cos3Kθ sinLα and sin 3Kθ cos Lα

χ_e = cos(3K $\pm$ 1)θ cosLα and sin(3K $\pm$ 1)θ sinLα

χ_e = cos(3K $\pm$ 1)θ sinLα and sin(3K $\pm$ 1)θ cosLα

The potential energy can be developed in terms of the a_1 symmetry eigenvectors

$$V(\alpha,\theta) - \sum_{K}\sum_{L} [A_{KL}^{CC}\cos K\alpha\ \cos 3L\theta + A_{KL}^{SS}\sin K\alpha\ \sin 3L\theta]$$

Because of the conditions on the limits of the sine function, a minimal Fourier expansion of 10 terms for the potential energy can be put forwards.

$$V(\alpha,\theta) - \sum_{K=0}^{2}\sum_{L=0}^{2} A_{KL}^{CC}\cos 3K\theta\ \cos L\alpha + A_{11}^{SS}\sin 3\theta\ \sin\alpha$$

A grid of energy data points for the wagging and torsion coordinates was calculated for both S_0 and T_1 states, by using the GAMESS suite of RHF and UHF ab initio programs with a 6-31G* basis.

3.8) THE KINETIC ENERGY[14,15,16,46]

The kinetic energy terms can also be developed[15] in terms of a function of α and θ. The importance of the influence of non-constant terms, however, has previously been seen to be very small, when compared with that of the potential energy[16]. In recent years the study of large amplitude vibrations has drawn a considerable amount of attention. In the early studies, the Hamiltonian was generally solved using a reduced potential function, and little effort was made to obtain accurate kinetic energy functions.

While the kinetic energy contribution to the Hamiltonian is not as sensitive to the molecular structure as is the potential energy, it does vary enough that it cannot be regarded as a constant. For this reason, the kinetic energy terms $B_\alpha(\alpha,\theta)$, $B_\theta(\alpha,\theta)$ as well as the interaction constant $B_{\alpha\theta}(\alpha,\theta)$ were evaluated at the same α,θ grid points that were used to define the potential surface. Figure(3.8) gives the input format that show the construction of the cartesian coordinates. Since the molecular structure was optimized at each α,θ data point, it is possible to evaluate the kinetic energy by numerical methods.

To obtain the $B_\alpha(\alpha,\theta)$, $B_\theta(\alpha,\theta)$, and $B_{\alpha\theta}(\alpha,\theta)$ kinetic energy terms it is necessary to numerically determine the vibrational-rotational G matrix, which is given by:

$$G = \begin{vmatrix} I & X \\ X^t & Y \end{vmatrix}^{-1}$$

Where I is the 3x3 moment of the inertia tensor, X is a 3x(3N-6) matrix representing the interaction of the vibrations and rotations, and Y is a (3N-6)x(3N-6) matrix which is the vibrational contribution to the G matrix. For two vibrations the G matrix may be written in an expanded form as:

$$G = \begin{bmatrix} I_{xx} & -I_{xy} & -I_{xz} & X_{11} & X_{12} \\ -I_{yx} & I_{yy} & -I_{yz} & X_{21} & X_{22} \\ -I_{zx} & -I_{zy} & I_{zz} & X_{31} & X_{32} \\ X_{11} & X_{12} & X_{13} & Y_{11} & Y_{12} \\ X_{12} & X_{22} & X_{32} & Y_{12} & Y_{22} \end{bmatrix}^{-1}$$

The elements of this matrix are defined by:

$$I_{ii} = \sum_{\alpha=1} m_\alpha (\boldsymbol{r}_\alpha \cdot \boldsymbol{r}_\alpha - r_{\alpha i}^2), \quad i = x, y, z$$

where x, y and z are the molecular fixed axes.

$$I_{ik} = \sum_{\alpha=1} m_\alpha r_{\alpha i} r_{\alpha k}, \quad i \neq k$$

$$X_{ik} = \sum_{\alpha=1}^{N} m_\alpha \left[\boldsymbol{r}_\alpha \times \left(\frac{\partial \boldsymbol{r}_\alpha}{\partial q_k} \right) \right]_i ,$$

and

$$Y_{ik} = \sum_{\alpha=1}^{N} m_\alpha \left(\frac{\partial \boldsymbol{r}_\alpha}{\partial q_i} \right) \cdot \left(\frac{\partial \boldsymbol{r}_\alpha}{\partial q_k} \right).$$

N is the number of atoms in the molecule, m_α is the mass of the αth atom, $\mathbf{r}_\alpha$ is the coordinate vector to the αth atom originating from the centre of mass, and $r_{\alpha i}$ and $r_{\alpha k}$ are the ith and kth components of the αth vector. The derivatives of the equations were numerically determined by calculating the structure of the molecule before and after 0.010 degree increments in the α and θ directions as $\alpha + \Delta\alpha$, $\alpha - \Delta\alpha$, and $\theta + \Delta\theta$, $\theta - \Delta\theta$. After the centre of mass was determined, the elements of the equations were inserted into the G equation which was inverted to give the desired G matrix. The final stage of the calculation is the identification of the elements G_{44}, G_{55} and G_{45} as the B_α , B_θ and $B_{\alpha\theta}$ internal rotation constants of the Hamiltonian equation. A flow chart of the Inertia program is given in Figure(3.9), and a sample input format is given in Figure(3.10). The B_α kinetic energy points evaluated at the α and θ grid points were fitted to the totally symmetric Fourier expansion:

$$B_\alpha(\alpha,\theta) = \sum_K \sum_L [B_{KL}^{CC}\cos K\alpha\cos 3L\theta + B_{KL}^{SS}\sin K\alpha\sin 3L\theta]$$

Similar fits were made to the B_θ and $B_{\alpha\theta}$ data points for both the ground and excited states.

FIGURE (3 .8)
Input of optimized geometry
(to get C-coordinates for KE. evaluation)

```
 $CONTRL    SCFTYP=RHF    RUNTYP=OPTIMIZE    UNITS=HINT    NZVAR=15
EXETYP=CHECK
 $END
 $STATPT  IFREEZ(1)=6,9 $END
 $DATA
.....  RHF/6-31G*.....thioacetaldehyde...
CN        1

CARBON        6.0
    1   SV     6  N31
    3    D     1
    1     0.800              1.0

SULPHUR     16.0  PCC   1.6063     118.9332                +     1     I
  J
    1   SV     6  N31
    3    D     1
    1     0.650              1.0

CARBON        6.0  PCC   1.4965   114.4506      0.0       -     1     I
  J
    1   SV     6  N31
    3    D     1
    1     0.800              1.0

HYDROGEN      1.0 NPCC   1.0810     90.0      0.0000       +     1     J
  I
    1   SV     6  N31

HYDROGEN      1.0  TCT   1.0804  -111.6403 -0.0100        -     3     1
  I
    1   SV     6  N31

HYDROGEN      1.0  TCT   1.0873  109.5318  121.5326      +     3     1
  5
    1   SV     6  N31

HYDROGEN      1.0  TCT   1.0873  109.5318  121.5326      -     3     1
  5
    1   SV     6  N31

 $END
 $GUESS  GUESS=EXTGUESS  $END
 $ZMAT   IZMAT(1)= 1,1,2, 1,1,3, 2,3,1,2, 1,1,4, 2,4,1,3,
          4,4,1,3,2, 1,3,5, 2,5,3,1, 3,5,3,1,2, 1,3,6, 2,6,3,1,
          3,6,3,1,5, 1,3,7, 2,7,3,1, 3,7,3,1,5  $END
```

FIGURE (3.9)

A flow chart of the Inertia program

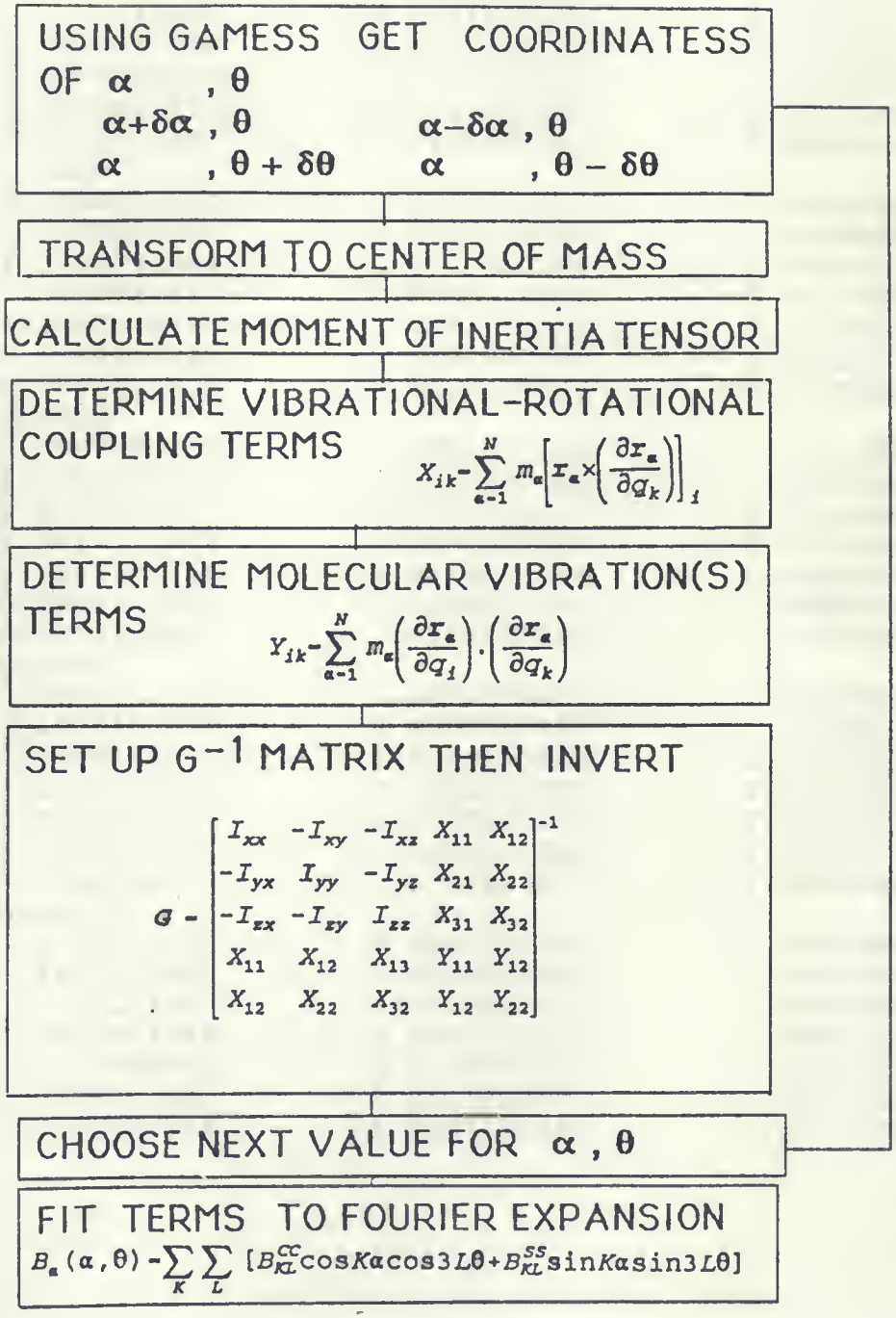

FIGURE (3 .10)
Input for kinetic energy calculations

```
7
0.0000      0.0000
     6.0    0.0000000000        0.0000000000        0.0000000000
    16.0   -1.4685182651        2.6565986869        0.0000000000
     6.0   -1.1705231607       -2.5743583268        0.0000000000
     1.0    2.0427941758        0.0000000000        0.0000000000
     1.0   -3.2097280766       -2.4742571019        0.0000000000
     1.0   -0.5329416835       -3.6188807386        1.6505310140
     1.0   -0.5329416835       -3.6188807386       -1.6505310140
0.0100      0.0000
     6.0    0.0000000000        0.0000000000        0.0000000000
    16.0   -1.4685182651        2.6565986869        0.0000000000
     6.0   -1.1705231607       -2.5743583268        0.0000000000
     1.0    2.0427941447        0.0000000000       -0.0003565348
     1.0   -3.2097280766       -2.4742571019        0.0000000000
     1.0   -0.5329416835       -3.6188807386        1.6505310140
     1.0   -0.5329416835       -3.6188807386       -1.6505310140
 -0.0100    0.0000
     6.0    0.0000000000        0.0000000000        0.0000000000
    16.0   -1.4685182651        2.6565986869        0.0000000000
     6.0   -1.1705231607       -2.5743583268        0.0000000000
     1.0    2.0427941447        0.0000000000        0.0003565348
     1.0   -3.2097280766       -2.4742571019        0.0000000000
     1.0   -0.5329416835       -3.6188807386        1.6505310140
     1.0   -0.5329416835       -3.6188807386       -1.6505310140
0.0000      0.0100
     6.0    0.0000000000        0.0000000000        0.0000000000
    16.0   -1.4685182651        2.6565986869        0.0000000000
     6.0   -1.1705231607       -2.5743583268        0.0000000000
     1.0    2.0427941758        0.0000000000        0.0000000000
     1.0   -3.2097280503       -2.4742571139       -0.0003312214
     1.0   -0.5332039348       -3.6187614968        1.6507077452
     1.0   -0.5326794603       -3.6189999677       -1.6503542326
0.0000     -0.0100
     6.0    0.0000000000        0.0000000000        0.0000000000
    16.0   -1.4685182651        2.6565986869        0.0000000000
     6.0   -1.1705231607       -2.5743583268        0.0000000000
     1.0    2.0427941758        0.0000000000        0.0000000000
     1.0   -3.2097280503       -2.4742571139        0.0003312214
     1.0   -0.5326794603       -3.6189999677        1.6503542326
     1.0   -0.5332039348       -3.6187614968       -1.6507077452
```

THEORY : PART THREE
SPECTROSCOPIC CONSIDERATIONS

3.9) ALLOWED AND FORBIDDEN TRANSITIONS[47,48]

If the oscillating radiation field is not constant over the molecular dimensions, and the magnetic dipole interaction neglected, then the contribution to the Einstein coefficient for absorption and emission is given by;

$$B(e' v' , e'' v'') = \frac{8\pi^3}{3h^2c} (\langle \Psi'_{ev} | \mu | \Psi''_{ev} \rangle)^2$$

where Ψ' and Ψ'' are the excited and ground state wavefunctions.

The treatment of the electric dipole moment starts with:

$$\mu = \mu_{nuclear} + \mu_{electronic}$$

Under the Born-Oppenheimer approximation, the electric transition moment can be written as;

$$M = \langle \Psi'_{es} \Psi'_{v} | \mu_n + \mu_e | \Psi''_{es} \Psi''_{v} \rangle$$

On further simplification (M) becomes:

$$M = \langle \Psi'_{v} | \Psi''_{v} \rangle \langle \Psi'_{e} | \mu_e | \Psi''_{e} \rangle \langle \Psi'_{s} | \Psi''_{s} \rangle$$

If all of the integrals in the above equation are non-zero, the transition is electric dipole allowed. The transition is orbitally and spin allowed and the relative band intensity controlled by the Frank-Condon factor. In order for a transition to be orbitally allowed the integral $< \Psi'_e \, |\mu_e| \, \Psi''_e >$ must be non-zero. If we assume that the ground state and excited state belong to the same point group then we can write:

$$\Gamma(\Psi') \otimes \Gamma(\mu_{x,y,z}) \otimes \Gamma(\Psi'') - \Gamma(\textit{TOTALLY SYMMETRIC})$$

In order for a transition to be spin allowed, the integral $< \Psi'_s \mid \Psi''_s >$ must be non-zero. Because of the orthogonality of the spin functions, the multiplicities of the two states must be identical. For thioacetaldehyde, the S_0 to T_1 transition is spin forbidden as $\Delta S \neq 0$.

The integral $< \Psi'_v \mid \Psi''_v >$ represents overlap of the vibrational wavefunctions of the states involved in the electronic transition and is known as the Franck-Condon factor. Hence the greater the overlap between the two vibrational wavefunctions of the two different states, the stronger the absorption band corresponding to that particular vibrational transition. The practical consequence of the Franck-Condon principle is that the change in geometry upon excitation controls the relative intensity in the band progression.

3.10) THE HAMILTONIAN CALCULATION[12,49,50]

The solutions of the Hamiltonian operator are developed onto the basis of the symmetry eigenvectors, which factorize the Hamiltonian matrix into boxes.

Transition intensities, I_{nm}, between the T_1 upper and S_0 lower torsional states m and n were evaluated by the relationship:

$$I_{nm} \propto g\, \nu\, \langle \psi_n | \psi_m \rangle^2 \exp\left(-\frac{E_m}{KT}\right)$$

where g is the statistical weight, $\nu = E_n - E_m$ the length of the transition (in cm^{-1}), $< \Psi_n \mid \Psi_m >$ the Franck-Condon factor which was calculated from the eigenvectors for the two torsional states, and E_m the torsional energy, relative to the S_0 zero point level.

A modified version of the Etanal[50] program was used to calculate the energies and intensities. A flow chart Fig(3.11) shows the main steps of the Etanal program. A sample input card for the Etanal program is given in Figure (3.12).

FIGURE (3.11)

A flow chart of the Etanal program

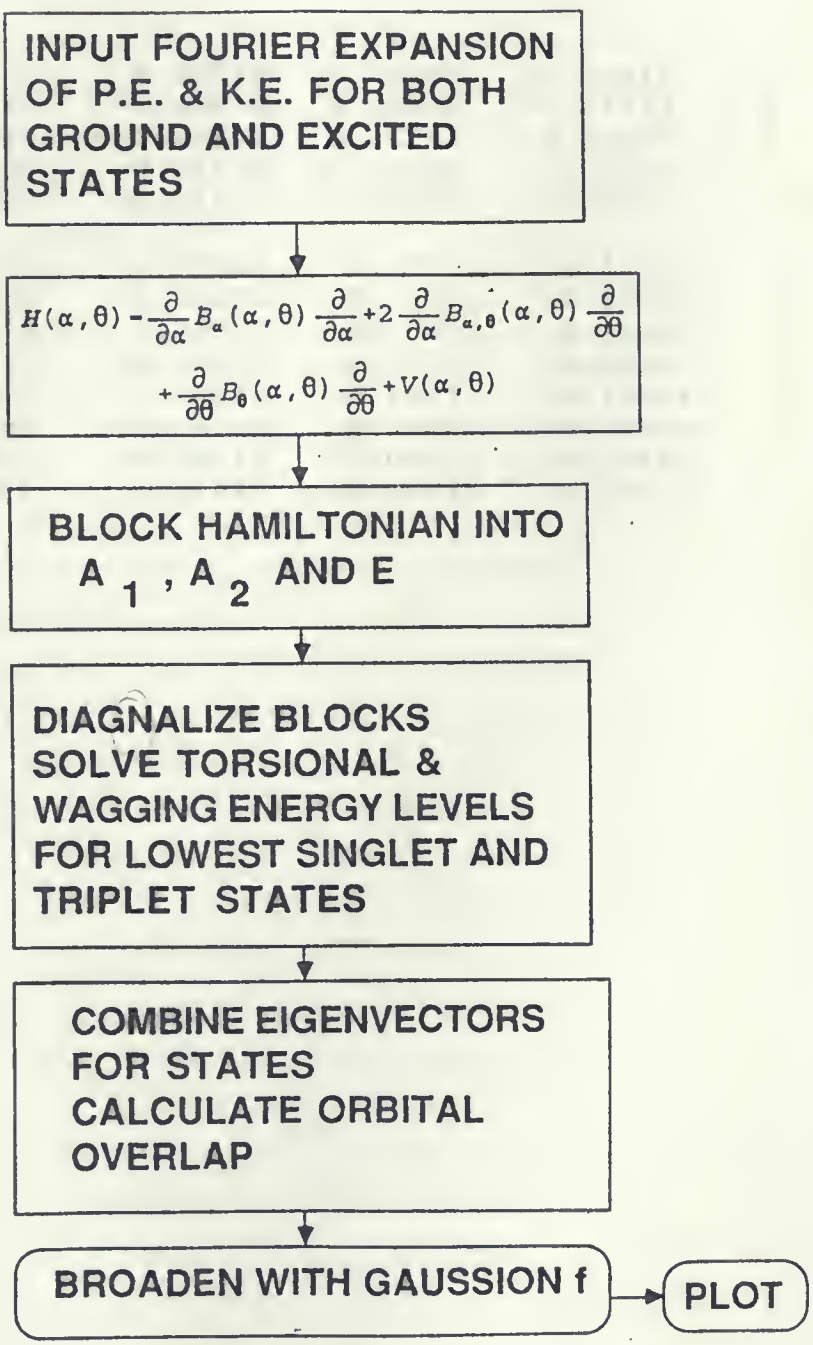

Figure(3.12) A sample input for the Etanal program

```
0 0 1 0 5 100
 12 30 300
5
  19978.15257     8.46545  -3.34552   10.62410    0   0
 -19713.57497    -1.96879   2.10699   -2.01712    0   1
    190.75893    -0.05167   0.04283    0.00281    3   1
   -460.99800     0.04176  -0.05905    0.02424    3   2
    815.29697    -0.01555   0.05802   -0.05433   -3  -1
8
   9021.96216     9.38389  -4.47209   12.13066    0   0
 -10091.42516    -3.48464   3.91084   -4.15156    0   1
   1323.17473     0.38377  -0.40731    0.46283    0   3
    495.77147    -0.02181   0.05264   -0.07084    3   1
   -426.62661     0.06867  -0.10531    0.14424    3   2
      5.99236    -0.02779   0.03607   -0.06205    3   3
     36.42461    -0.02335   0.03552   -0.06464   -3  -1
    135.09182     0.01327  -0.00929    0.02217   -3  -3
```

CHAPTER FOUR

RESULTS AND DISCUSSION

4.1) The Potential Energy

The potential energy function which describes the combined wagging-torsion motion was obtained as a fit of the two-dimensional Fourier expansion, to the calculated total energy points by SPSS, a linear regression program. The ground singlet and excited triplet potential energy data points are given in Tables(4.1) and(4.2) respectively. The expansion coefficients fit for $V(\theta,\alpha)$ in the ground and excited states took the form given in Table(4.3). The two-dimensional plots of the potential energy for both states were done on SURFER, a two-dimensional plotting program. The plots of the singlet and triplet states are given in figures(4.1) and (4.2).

In the ground state, the potential surface shows that the aldehyde wagging mode can be described as a high frequency low amplitude vibration which is localized in a single minimum potential. The wagging-torsion coupling in the ground state is therefore small. Figure(4.3) illustrates selected conformational structures of the S_0 and T_1 states. The top part of the figure shows that the methyl torsion involves movement from point A eclipsed with (α=0,θ=0) to B antieclipsed with (α=0,θ=60) and then onto C eclipsed with (α=0,θ=120). Hence, the torsional motion in the ground state is described by a triple minimum potential. The height of the barrier at point B relative to the equilibrium energy of point A is calculated to be 541.562 cm^{-1}, which is an excellent fit when compared to the microwave value[7] of 549.8 cm^{-1} , and 534.3 cm^{-1} from a hot band analysis of the visible spectrum[9]. This shows that optimization of structure leads to results that are much more accurate than those obtained from partially optimized runs.

The ground state methyl barrier height obtained from a rigid model has been reported[12] to be 458.0 cm^{-1}. Hence, the optimization of the structural parameters and the employment of a larger basis set resulted in overall improvements of the potential energy surface.

The triplet state potential surface proved to be more complex. In the T_1 upper state the CCSH group is no longer planar, due to the out of plane displacement of the aldehyde hydrogen. This causes the aldehyde wagging mode to be a large amplitude low frequency motion. Therefore, the wagging coordinate is described by a double minimum potential, and the energy levels are paired as a result of the inversion doubling.

The potential surface of Figure(4.2) shows that there are four routes by which the minimum energy configuration of the T_1 upper state can be achieved from the ($\alpha=0.0^0,\theta=0.0^0$) configuration of the S_0 state, namely: the clockwise - clockwise ($+74.34^0,+24.68^0$), and counterclockwise - clockwise ($-45.66^0,+24.68^0$) rotations , and the equivalent set defined by the switch operator ($-74.34^0,-24.68^0$) ($+45.66^0,-24.68^0$). potential surface. Thus, it is possible for the structural displacement to occur along either the upward sloping positive diagonal or alternatively along the negative sloping diagonal. As the preference would be for a minimum structural distortion on electronic excitation, the structural changes would take place along the ($-45.66^0,+24.68^0$) ($+45.66^0,-24.68^0$) negative sloping diagonal.

From point D, staggered configuration with ($\alpha=24,\theta=75$), for wagging to occur the molecule must traverse the lowest saddle point on the potential surface at point E, antieclipsed configuration with ($\alpha=0,\theta=60$), and then move on to point F, staggered configuration with ($\alpha=-24,\theta=45$).

With $\alpha=0$ (planar CCSH group), the torsional motion was

displaced by a 60° shift from the ground state triple equilibrium position. The saddle point for the methyl rotation mode is located at point G (α=0,θ=0). The D-G-H line represents a possible path for methyl rotation.

An important fact to note is that while the aldehyde wagging mode involves a 24.60° displacement from the molecular plane it also is associated with a 45.66° rotation of the methyl group. Thus a full cycle of the wagging-torsion coordinates generated six minima in the triplet state potential surface. It was found that while in the ground state the most stable configuration is the eclipsed form, in the excited state the antieclipsed conformation is more stable than the eclipsed conformation by 321.79 - 175.55 =146.24 cm^{-1}. The difference in conformation between the two states is attributed to hyperconjugation which creates a repulsion between the out of plane methyl hydrogens in the lower electronic state and an attractive force between them in the excited state.

It should be noted that UHF method is unable to predict accurate estimates of the excited triplet state potential surface. The methyl barrier height calculated by the UHF procedure is 146.24 cm^{-1}, which is some what higher than the 94.18 cm^{-1} value estimated from the visible spectrum.

Table (4.1) The Potential Energy points[a] of the ground state S_1.

θ	α	E (Hartree)	ΔE (cm^{-1})
0.00000	0.00000	-475.5517476065	0.000
-0.00039	5.00012	-475.5513877417	78.979
-0.00073	10.00020	-475.5503092383	315.684
-0.00096	15.00048	-475.5485094213	710.697
-0.00104	20.00106	-475.5459857791	1264.571
-0.00090	25.00015	-475.5427370818	1977.575
-0.00048	29.99604	-475.5538758951	2850.672
29.99925	-0.00016	-475.5504599177	282.614
29.99685	5.00073	-475.5497863902	430.435
29.99431	10.00121	-475.5484574988	722.093
29.99201	15.00032	-475.5464788576	1156.353
29.99010	19.99673	-475.5438551706	1732.184
29.98876	24.98851	-475.5405912445	2448.531
29.98834	29.97265	-475.5366932499	3304.039
59.06629	0.00000	-475.5492800619	541.561
59.96885	5.00840	-475.5489886030	605.529
59.96171	10.00872	-475.5480775362	805.485
59.95693	15.00744	-475.5465452126	1141.790
59.95532	20.00371	-475.5443879481	1615.253
59.95756	24.99643	-475.5416010430	2226.906
59.96433	29.98411	-475.5381789734	2977.962
89.97880	5.00742	-475.5505284472	267.573
89.98006	10.00665	-475.5498613763	413.978
89.98205	15.00571	-475.5485111835	710.310
89.98416	20.00438	-475.5464654530	1159.295
89.98698	25.00189	-475.5437100182	1764.041
89.99190	29.99687	-475.5402300800	2527.797

a) using 6-31G* basis set.

TABLE (4.2) The Potential energy points[a,b] of the exited state T_1.

θ	α	E (Hartrees)	ΔE (cm^{-1})
0.00000	0.00000	-475.5119274465	321.802
-0.00101	4.99125	-475.5119300040	321.241
-0.00231	9.82624	-475.1192883323	321.498
-0.00420	14.97387	-475.5118964794	328.598
-0.00697	19.96400	-475.5117878354	352.598
-0.01083	24.95071	-475.5115415556	406.495
-0.01589	29.92947	-475.5110832995	507.070
-0.02900	39.82064	-475.5092064357	918.993
-0.04357	49.42417	-475.5056252963	1704.960
-0.05843	58.05350	-475.5005190269	2825.653
29.94000	0.00198	-475.5122652005	247.674
29.93643	4.98964	-475.5121238549	278.780
29.93176	9.97552	-475.5120323437	298.780
29.92559	14.95981	-475.5119684123	312.811
29.91750	19.94189	-475.5118873923	331.354
29.90719	24.91970	-475.5117248061	366.276
29.89466	29.88909	-475.5114015594	437.220
29.86550	39.76623	-475.5099314045	759.881
29.83987	49.40964	-475.5068988608	1425.446
29.82894	58.32163	-475.5022635587	2442.774
60.21593	0.00000	-475.5125938775	175.538
59.91054	4.98653	-475.5126387211	165.696
59.91097	9.97303	-475.5127666708	137.606
59.90929	14.96182	-475.5129396925	99.640
59.90445	19.95288	-475.5130981503	64.863
59.89546	24.94497	-475.5131648863	50.216
59.88182	29.93542	-475.5130509101	75.231
59.84219	39.88890	-475.5119042947	326.883
59.79742	49.70306	-475.5089731501	970.193
59.76796	58.95322	-475.5040143915	2058.512
89.93205	-0.00134	-475.5122759095	245.323
89.93725	4.98662	-475.5124681155	203.139
89.94067	9.97764	-475.5128975548	154.615
89.94128	14.97162	-475.5128975548	108.888
89.93789	19.96773	-475.5130342214	78.894
89.92949	24.96425	-475.5130259021	80.719
89.91543	29.95835	-475.5127884224	132.840
89.87224	39.91359	-475.5112647948	467.237
89.82116	49.68837	-475.5078026645	1227.084
89.78659	58.66840	-475.5023622519	2421.113

a) The increse in energy is with respect to the minima at (α=24.68 , θ=74.34) which is =-475.513393690112 Hartrees.
b) using 6-31G* basis set.

TABLE (4.3) Calculated Expansion Coefficients[a] for the S_0 and T_1 Potential Energy Surfaces of Thioacetaldehyde.

Potential Energy $V(\alpha,\theta)$			
S_0 State[b]		T_1 State[c]	
A_{00}^{CC}	19978.153	A_{00}^{CC}	9021.962
A_{10}^{CC}	-19713.575	A_{10}^{CC}	-10091.425
A_{13}^{CC}	190.759	A_{13}^{CC}	495.771
A_{23}^{CC}	-460.998	A_{23}^{CC}	-426.620
A_{13}^{SS}	815.297	A_{13}^{SS}	36.425
		A_{30}^{CC}	1323.175
		A_{33}^{CC}	5.992
		A_{33}^{SS}	135.092

a) values in cm^{-1}.

b) correlation factor = 0.99992, standard deviation = 13.07422

c) correlation factor = 0.99993, standard deviation = 9.71671

FIGURE (4.1)

The potential energy surface $V(\theta,\alpha)$ for the S_0 ground electronic state .[a]

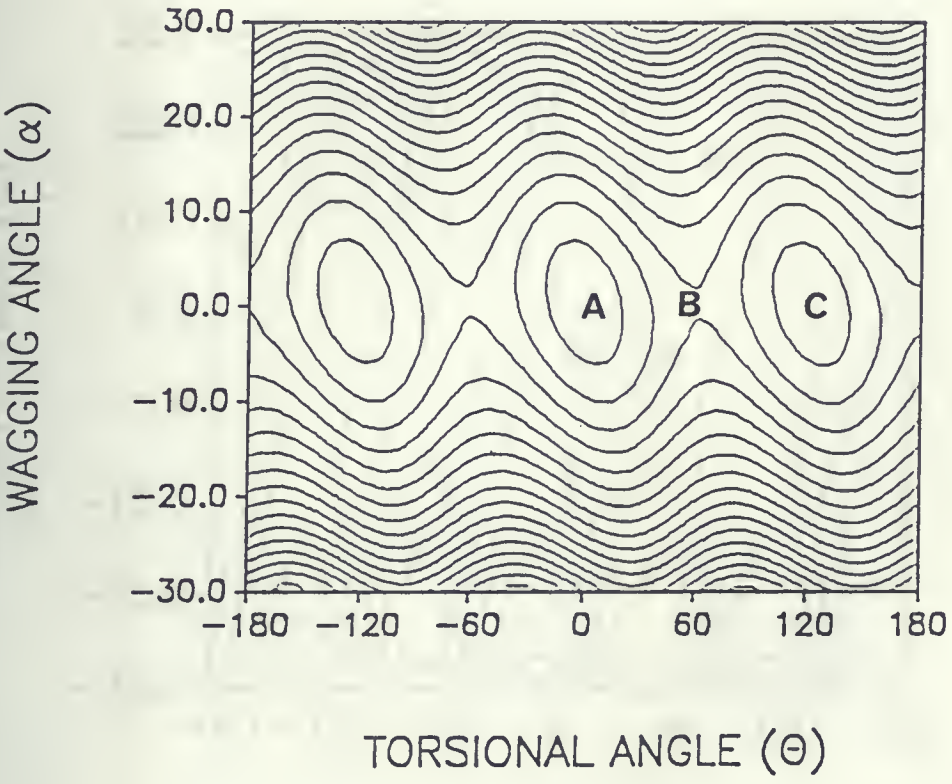

a) The interval between the isopotential lines is $200CM^{-1}$.

FIGURE (4.2)

The potential energy surface $V(\theta,\alpha)$ for the T_1 excited electronic state .[a]

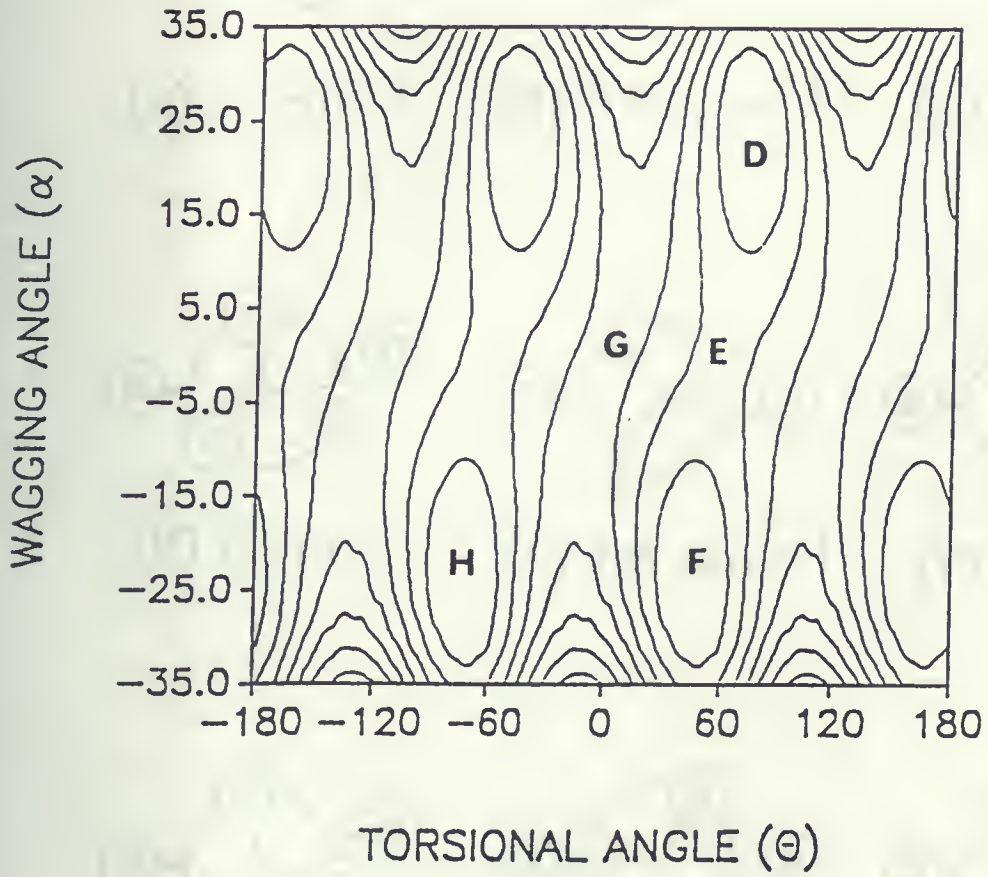

a) The interval between the isopotential lines is $100CM^{-1}$.

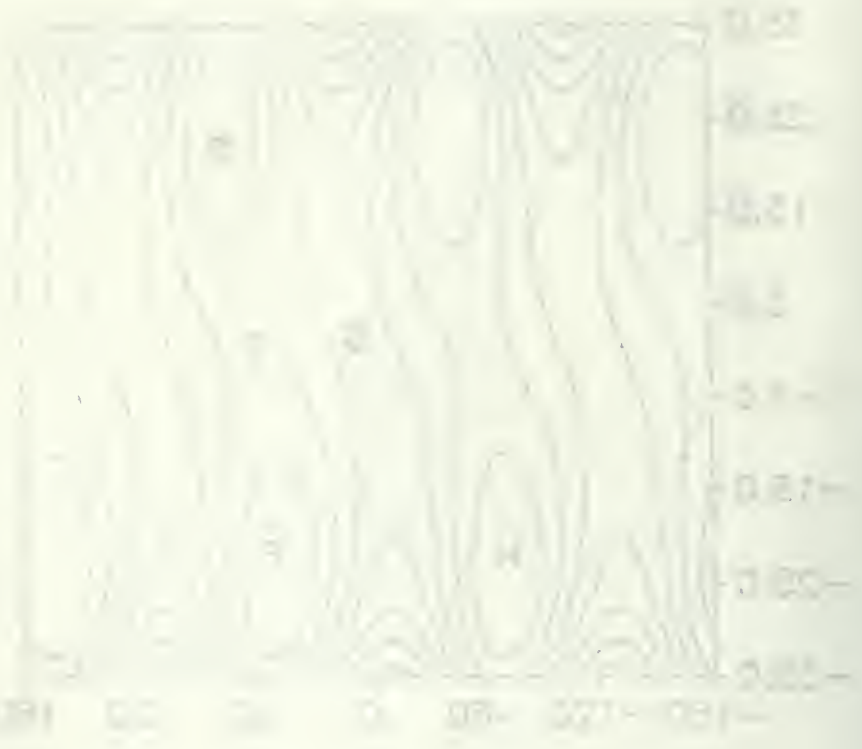

FIGURE(4.3) Selected conformational structures of ground and triplet states.

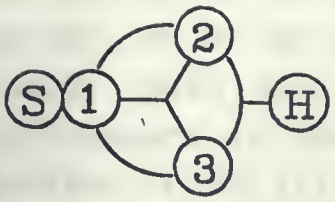

(A) 0 cm^{-1}

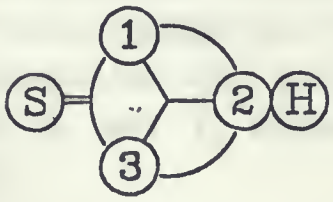

(B) 541 cm^{-1}

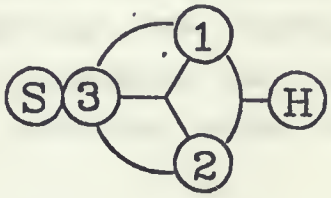

(C) 0 cm^{-1}

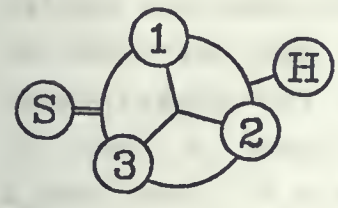

(D) 0 cm^{-1}

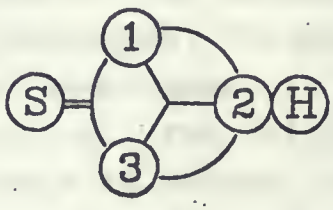

(E) 175 cm^{-1}

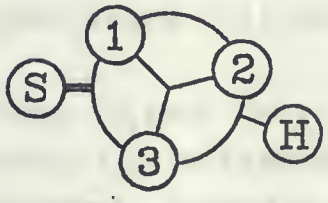

(F) 0 cm^{-1}

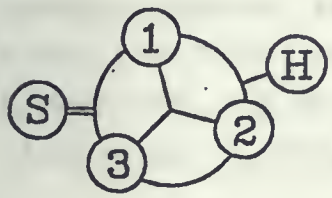

(D) 0 cm^{-1}

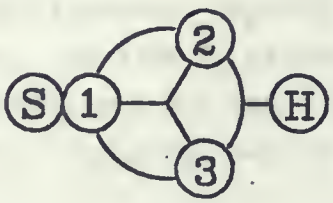

(G) 322 cm^{-1}

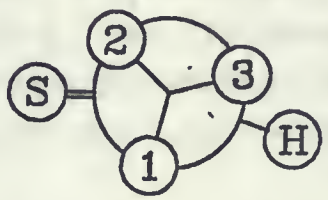

(H) 0 cm^{-1}

4.2) The Kinetic Energy

It has been shown in recent studies[14] that the contribution of the kinetic energy to the Hamiltonian is not as sensitive to the molecular structure as the potential energy and it can not be regarded as a constant. The kinetic energy terms were calculated for thioacetaldehyde and its isotopomers in their S_0 and T_1 states, and are given in tables(4.4) to (4.11).

The data for all four isotopomers in both the S_0 and T_1 state, showed that the variation with respect to the change in α was more pronounced than the variation resulting from the change in θ. A second feature is that the variation of the values was more obvious in the isotopmers CH_3CHS/CH_3CDS than in the other pair CD_3CHS/CD_3CDS. The examples below will show these trends and their magnitudes.
In the S_0 state of d_0, the difference $B_\alpha(\theta=0,\alpha=0) - B_\alpha(\theta=0,\alpha=30) \approx 0.7$ (or 4.4% change) whereas the difference $B_\alpha(\theta=0,\alpha=0) - B_\alpha(\theta=30,\alpha=0) \approx 0.1$ (or 0.5% change). Likewise in the S_0 state of d_1, the difference $B_\alpha(\theta=0,\alpha=0) - B_\alpha(\theta=0,\alpha=30) \approx 0.3$ (or 3.0% change) whereas the difference $B_\alpha(\theta=0,\alpha=0) - B_\alpha(\theta=30,\alpha=0) \approx 0.03$ (or 0.3% change). But in the S_0 state of d_3, the difference $B_\alpha(\theta=0,\alpha=0) - B_\alpha(\theta=0,\alpha=30) \approx 0.1$ (or 0.7% change) whereas the difference $B_\alpha(\theta=0,\alpha=0) - B_\alpha(\theta=30,\alpha=0) \approx 0.001$ (or 0.0% change). In the S_0 state of d_4, the difference $B_\alpha(\theta=0,\alpha=0) - B_\alpha(\theta=0,\alpha=30) \approx 0.07$ (or 0.8% change) whereas the difference $B_\alpha(\theta=0,\alpha=0) - B_\alpha(\theta=30,\alpha=0) \approx 0.003$ (or 0.0% change)

In the T_1 state such observations are more or less still valid. For example in the T_1 state of d_0, the difference $B_\alpha(\theta=0,\alpha=0) - B_\alpha(\theta=0,\alpha=30) \approx 0.2$ (or 1.2% change) whereas the difference $B_\alpha(\theta=0,\alpha=0) - B_\alpha(\theta=30,\alpha=0) \approx 0.03$ (or 0.2% change). Likewise in the T_1 state of d_1, the difference $B_\alpha(\theta=0,\alpha=0) - B_\alpha(\theta=0,\alpha=30) \approx 0.1$ (or 1.2% change) whereas the difference

$B_\alpha(\theta=0,\alpha=0) - B_\alpha(\theta=30,\alpha=0) \approx 0.01$ (or 0.1% change). And in the T_1 state of d_3, the difference $B_\alpha(\theta=0,\alpha=0) - B_\alpha(\theta=0,\alpha=30) \approx 0.01$ (or 0.1% change) whereas the difference $B_\alpha(\theta=0,\alpha=0) - B_\alpha(\theta=30,\alpha=0) \approx 0.003$ (or 0.0% change). In the T_1 state of d_4, the difference $B_\alpha(\theta=0,\alpha=0) - B_\alpha(\theta=0,\alpha=30) \approx 0.1$ (or 0.4% change) whereas the difference $B_\alpha(\theta=0,\alpha=0) - B_\alpha(\theta=30,\alpha=0) \approx 0.001$ (or 0.0% change). This pattern is true for $B_\alpha(\theta,\alpha)$, $B_\theta(\theta,\alpha)$,and $B_{\theta\alpha}(\theta,\alpha)$ in both the S_0 and T_1 states.

The sign of the $B_{\theta\alpha}$ values is dependent on the angle between the θ and α axes. If the axes are at 90° then $B_{\theta\alpha} = 0$, if the axes are greater than 90° then $B_{\theta\alpha}$ is negative, and if the axes are less than 90° then $B_{\theta\alpha}$ is positive.

The kinetic energy data was fitted to a Fourier series expansion, and the expansion coefficients are given in Tables(4.12) to (4.15). The expansion was then plotted as a function of both wagging and torsion. Plots of the h_4 for S_0 and T_1 states are given in Figures (4.4) to (4.9). The plots showed that the two electronic states are insensitive to the change in the torsion and wagging angles. The structures calculated for the most stable S_0 conformation showed that the in-plane and out-of-plane CH bonds have different lengths 1.0805 and 1.0874 Å, respectively, and change to 1.0888 and 1.0848 Å in the most stable conformation in the T_1 state. The variation in the B's as a function of (θ) is due to the unequal bond distances on the CH_3 group which acts hence as an unbalanced three bladed propeller. The variation in the B's as a function of (α) is somewhat greater than the changes with respect to θ. This is because the CH group acts as a single bladed propeller which is not balanced, with the result that the centre of mass vibrates as the CH oscillates, which in turn changes the kinetic energy.

TABLE (4.4) The kinetic energy data for the S_0 state of CH_3CHS.[a]

θ	α	B_α	B_θ	$B_{\theta\alpha}$
0.00000	0.00000	17.21340	7.57067	-2.49905
-0.00040	5.00010	17.21490	7.58111	-2.50952
-0.00070	10.00020	17.27270	7.62765	-2.55680
-0.00100	15.00050	17.35220	7.69622	-2.62923
-0.00100	20.00110	17.48600	7.81164	-2.75726
-0.00090	25.00020	17.66410	7.98152	-2.94125
-0.00050	29.99600	17.97320	8.24600	-3.22725
29.99930	-0.00020	17.12950	7.54525	-2.43331
29.99690	5.00070	17.13570	7.55377	-2.43735
29.99430	10.00120	17.16340	7.58748	-2.46961
29.99200	15.00030	17.23150	7.65330	-2.53807
29.99010	19.99670	17.34380	7.76723	-2.65443
29.98880	24.98850	17.52670	7.93634	-2.83511
29.98840	29.97270	17.81090	8.19968	-3.11700
59.06630	0.00000	17.06500	7.55197	-2.39741
59.96890	5.00840	17.08380	7.57079	-2.41720
59.96170	10.00870	17.12970	7.61678	-2.46780
59.95690	15.00740	17.21520	7.69905	-2.55665
59.95530	20.00370	17.35870	7.82932	-2.69913
59.95760	24.99640	17.56820	8.03128	-2.91779
59.96430	29.98410	17.91340	8.34459	-3.25957
89.97950	0.00790	17.13690	7.57440	-2.45500
89.97880	5.00740	17.16150	7.59029	-2.48022
89.98010	10.00670	17.21970	7.63447	-2.53706
89.98210	15.00570	17.32000	7.72566	-2.63540
89.98420	20.00440	17.47710	7.85537	-2.78528
89.98700	25.00190	17.70810	8.05891	-3.01310
89.99190	29.99690	18.08320	8.37226	-3.36343

a) values in cm^{-1} ,angles in degrees.

TABLE (4.5) The kinetic energy data for the S_0 state of CH_3CDS.[a]

θ	α	B_α	B_θ	$B_{\theta\alpha}$
0.00000	0.00000	8.64219	6.49289	-1.26174
-0.00040	5.00010	8.64164	6.49741	-1.26631
-0.00070	10.00020	8.66682	6.51883	-1.28585
-0.00100	15.00050	8.69615	6.54865	-1.31529
-0.00100	20.00110	8.74441	6.59309	-1.36403
-0.00090	25.00020	8.81021	6.65768	-1.43130
-0.00050	29.99600	8.90567	6.75158	-1.52712
29.99930	-0.00020	8.61252	6.49578	-1.23987
29.99690	5.00070	8.61586	6.50330	-1.24272
29.99430	10.00120	8.62570	6.51876	-1.25701
29.99200	15.00030	8.65505	6.55045	-1.28673
29.99010	19.99670	8.69652	6.59863	-1.33353
29.98880	24.98850	8.76186	6.66286	-1.40167
29.98840	29.97270	8.85744	6.75958	-1.50066
59.06630	0.00000	8.58722	6.51419	-1.22911
59.96890	5.00840	8.59489	6.52155	-1.23771
59.96170	10.00870	8.61306	6.54003	-1.25913
59.95690	15.00740	8.64635	6.57369	-1.29564
59.95530	20.00370	8.69990	6.62404	-1.35130
59.95760	24.99640	8.77304	6.69762	-1.43117
59.96430	29.98410	8.87866	6.80094	-1.54455
89.97950	0.00790	8.61400	6.51061	-1.24975
89.97880	5.00740	8.62287	6.51244	-1.25912
89.98010	10.00670	8.64513	6.52648	-1.28166
89.98210	15.00570	8.68127	6.56254	-1.31957
89.98420	20.00440	8.73892	6.61034	-1.37582
89.98700	25.00190	8.81449	6.67953	-1.45501
89.99190	29.99690	8.92847	6.78017	-1.56589

a) values in cm^{-1} ,angles in degrees.

TABLE (4.6) The kinetic energy data for the S_0 state of CD_3CHS.[a]

θ	α	B_α	B_θ	$B_{\theta\alpha}$
0.00000	0.00000	15.60280	3.72365	-1.13807
-0.00040	5.00010	15.59530	3.72593	-1.13916
-0.00070	10.00020	15.61130	3.73379	-1.14834
-0.00100	15.00050	15.62660	3.74849	-1.16257
-0.00100	20.00110	15.64160	3.77136	-1.18662
-0.00090	25.00020	15.66120	3.80481	-1.22050
-0.00050	29.99600	15.70570	3.85357	-1.27013
29.99930	-0.00020	15.60360	3.73294	-1.13365
29.99690	5.00070	15.60920	3.73703	-1.13530
29.99430	10.00120	15.60980	3.74544	-1.14220
29.99200	15.00030	15.62000	3.76140	-1.15670
29.99010	19.99670	15.62980	3.78529	-1.17946
29.98880	24.98850	15.65810	3.81914	-1.21400
29.98840	29.97270	15.68280	3.87006	-1.26469
59.06630	0.00000	15.60470	3.75744	-1.14028
59.96890	5.00840	15.60860	3.76165	-1.14466
59.96170	10.00870	15.61170	3.77070	-1.15478
59.95690	15.00740	15.62010	3.78680	-1.17179
59.95530	20.00370	15.63860	3.81159	-1.19874
59.95760	24.99640	15.65500	3.84903	-1.23839
59.96430	29.98410	15.69310	3.90305	-1.29673
89.97950	0.00790	15.60740	3.74712	-1.14389
89.97880	5.00740	15.60650	3.74632	-1.14735
89.98010	10.00670	15.61020	3.75173	-1.15666
89.98210	15.00570	15.62020	3.76863	-1.17401
89.98420	20.00440	15.63850	3.79108	-1.20055
89.98700	25.00190	15.65930	3.82590	-1.23956
89.99190	29.99690	15.70590	3.87764	-1.29646

a) values in cm^{-1} ,angles in degrees.

TABLE (4.7) The kinetic energy data for the S_0 state of CD_3CDS.[a]

θ	α	B_α	B_θ	$B_{\theta\alpha}$
0.00000	0.00000	8.01914	3.38304	-0.75397
-0.00040	5.00010	8.01539	3.38375	-0.75508
-0.00070	10.00020	8.02535	3.39014	-0.76116
-0.00100	15.00050	8.03369	3.40050	-0.77098
-0.00100	20.00110	8.04647	3.41522	-0.78647
-0.00090	25.00020	8.07858	3.43685	-0.80786
-0.00050	29.99600	8.08786	3.46770	-0.83830
29.99930	-0.00020	8.01620	3.39062	-0.75033
29.99690	5.00070	8.01881	3.39369	-0.75146
29.99430	10.00120	8.02085	3.39991	-0.75642
29.99200	15.00030	8.02711	3.41115	-0.76637
29.99010	19.99670	8.03677	3.42735	-0.78167
29.98880	24.98850	8.05557	3.44911	-0.80390
29.98840	29.97270	8.07811	3.48076	-0.83531
59.06630	0.00000	8.01309	3.40681	-0.75234
59.96890	5.00840	8.01553	3.40926	-0.75527
59.96170	10.00870	8.01878	3.41498	-0.76220
59.95690	15.00740	8.02718	3.42566	-0.77385
59.95530	20.00370	8.03916	3.44143	-0.79148
59.95760	24.99640	8.05217	3.46456	-0.81646
59.96430	29.98410	8.07677	3.49626	-0.85157
89.97950	0.00790	8.01728	3.39815	-0.75577
89.97880	5.00740	8.01772	3.39736	-0.75823
89.98010	10.00670	8.02167	3.40003	-0.76473
89.98210	15.00570	8.03111	3.41171	-0.77645
89.98420	20.00440	8.04309	3.42557	-0.79362
89.98700	25.00190	8.05830	3.44677	-0.81791
89.99190	29.99690	8.08943	3.47741	-0.85169

a) values in cm^{-1} ,angles in degrees.

TABLE (4.8) The kinetic energy data[a] for the T_1 state of CH_3CHS.

Θ	α	B_α	B_Θ	$B_{\Theta\alpha}$
0.00000	0.00000	16.64840	6.99261	-1.79932
-0.00100	4.99130	16.64100	6.98673	-1.79335
-0.00230	9.82620	16.64150	6.98865	-1.79723
-0.00420	14.97390	16.65030	6.99568	-1.80845
-0.00700	19.96400	16.66650	7.01154	-1.83415
-0.01080	24.95070	16.71150	7.05432	-1.88736
-0.01590	29.92950	16.80480	7.13257	-1.98329
-0.02900	39.82060	17.24830	7.49819	-2.41284
29.94000	0.00200	16.61140	6.94886	-1.75241
29.93640	4.98960	16.61360	6.94977	-1.75364
29.93180	9.97550	16.60940	6.94749	-1.75418
29.92560	14.95980	16.61380	6.95532	-1.76309
29.91750	19.94190	16.62170	6.97510	-1.78822
29.90720	24.91970	16.66130	7.01460	-1.83945
29.89470	29.88910	16.74930	7.09187	-1.93470
29.86550	39.76620	17.18450	7.45725	-2.36632
60.21590	0.00000	16.59000	6.91719	-1.72277
59.91050	4.98650	16.58370	6.91502	-1.72001
59.91100	9.97300	16.58240	6.91641	-1.72610
59.90930	14.96180	16.57870	6.92633	-1.74158
59.90440	19.95290	16.60500	6.94544	-1.77358
59.89550	24.94500	16.65090	6.99407	-1.83531
59.88180	29.93540	16.74890	7.08268	-1.94513
59.84220	39.88890	17.25850	7.49919	-2.44291
89.93200	-0.00130	16.61110	6.94737	-1.75011
89.93720	4.98660	16.61270	6.94375	-1.75373
89.94070	9.97760	16.60870	6.94666	-1.76167
89.94130	14.97160	16.61830	6.95909	-1.77788
89.93790	19.96770	16.63840	6.97343	-1.80972
89.92950	24.96430	16.70060	7.01976	-1.87259
89.91540	29.95840	16.80260	7.10722	-1.98275
89.87220	39.91360	17.35260	7.53431	-2.49151

a) values in cm^{-1} ,angles in degrees.

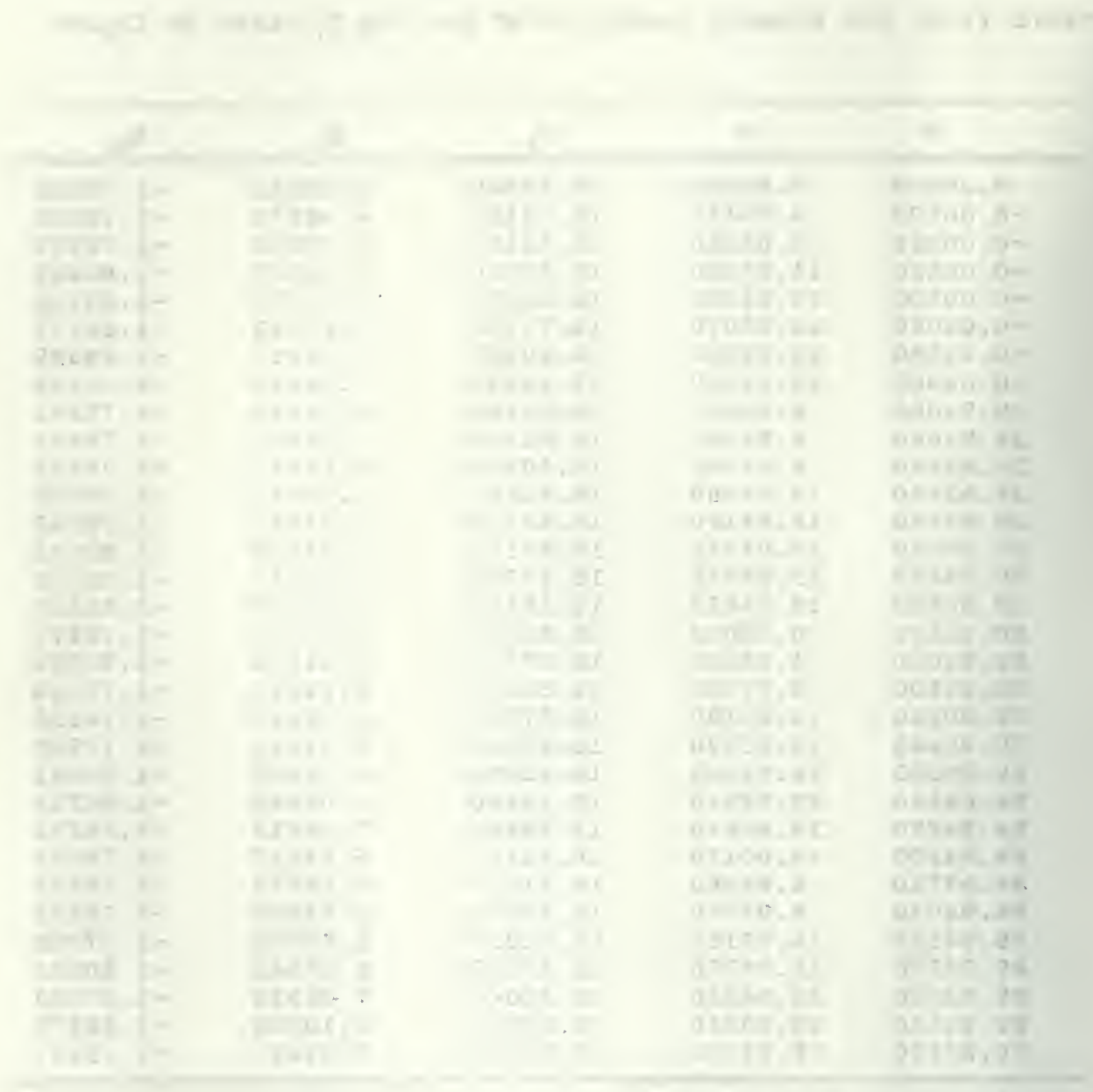

TABLE (4.9) THE kinetic energy data[a] for the T_1 state of CH_3CDS.

θ	α	B_α	B_θ	$B_{\theta\alpha}$
0.00000	0.00000	8.45430	6.30497	-0.98753
-0.00100	4.99130	8.45164	6.30042	-0.98517
-0.00230	9.82620	8.45535	6.30426	-0.99006
-0.00420	14.97390	8.46280	6.31210	-0.99964
-0.00700	19.96400	8.47648	6.32195	-1.01650
-0.01080	24.95070	8.49857	6.34270	-1.04475
-0.01590	29.92950	8.54412	6.38134	-1.09122
-0.02900	39.82060	8.71747	6.52878	-1.26548
29.94000	0.00200	8.43952	6.28186	-0.96647
29.93640	4.98960	8.44053	6.28291	-0.96769
29.93180	9.97550	8.44179	6.28323	-0.97086
29.92560	14.95980	8.44966	6.29058	-0.97946
29.91750	19.94190	8.45824	6.30594	-0.99673
29.90720	24.91970	8.48094	6.32864	-1.02574
29.89470	29.88910	8.52273	6.36260	-1.07213
29.86550	39.76620	8.69075	6.51394	-1.25163
60.21590	0.00000	8.43100	6.26469	-0.95299
59.91050	4.98650	8.42965	6.26490	-0.95286
59.91100	9.97300	8.43164	6.26659	-0.95870
59.90930	14.96180	8.43536	6.27378	-0.97048
59.90440	19.95290	8.45135	6.28486	-0.99054
59.89550	24.94500	8.47598	6.30945	-1.02355
59.88180	29.93540	8.52053	6.34999	-1.07591
59.84220	39.88890	8.71523	6.51175	-1.27492
89.93200	-0.00130	8.43944	6.28026	-0.96482
89.93720	4.98660	8.44176	6.27819	-0.96780
89.94070	9.97760	8.44218	6.28072	-0.97431
89.94130	14.97160	8.45097	6.29081	-0.98603
89.93790	19.96770	8.46451	6.29667	-1.00514
89.92950	24.96430	8.49624	6.31793	-1.03746
89.91540	29.95840	8.53884	6.35949	-1.08869
89.87220	39.91360	8.73995	6.52526	-1.28528

a) values in cm^{-1}, angles in degrees.

TABLE (4.10) The kinetic energy data[a] of the T_1 state of CD_3CHS.

θ	α	B_α	B_θ	$B_{\theta\alpha}$
0.00000	0.00000	15.61150	3.59302	-0.96663
-0.00100	4.99130	15.60660	3.58756	-0.96320
-0.00230	9.82620	15.59810	3.58406	-0.96016
-0.00420	14.97390	15.59070	3.57962	-0.95688
-0.00700	19.96400	15.57060	3.57594	-0.95561
-0.01080	24.95070	15.55750	3.57888	-0.96088
-0.01590	29.92950	15.55500	3.59037	-0.97653
-0.02900	39.82060	15.59370	3.66104	-1.06001
29.94000	0.00200	15.61010	3.57712	-0.95171
29.93640	4.98960	15.61060	3.57742	-0.95206
29.93180	9.97550	15.60330	3.57296	-0.94856
29.92560	14.95980	15.59030	3.56898	-0.94478
29.91750	19.94190	15.56730	3.56773	-0.94427
29.90720	24.91970	15.55600	3.56967	-0.94496
29.89470	29.88910	15.55190	3.58039	-0.96580
29.86550	39.76620	15.58280	3.65481	-1.05326
60.21590	0.00000	15.61190	3.56663	-0.94286
59.91050	4.98650	15.60720	3.56502	-0.94097
59.91100	9.97300	15.59480	3.56089	-0.93865
59.90930	14.96180	15.57300	3.55722	-0.93678
59.90440	19.95290	15.55830	3.55329	-0.93740
59.89550	24.94500	15.53990	3.55756	-0.94511
59.88180	29.93540	15.53160	3.57169	-0.96483
59.84220	39.88890	15.57980	3.65269	-1.06412
89.93200	-0.00130	15.61010	3.57611	-0.95058
89.93720	4.98660	15.50610	3.57236	-0.94962
89.94070	9.97760	15.58780	3.56685	-0.94663
89.94130	14.97160	15.57570	3.56406	-0.94422
89.93790	19.96770	15.55000	3.55731	-0.94369
89.92950	24.96430	15.54560	3.55965	-0.95091
89.91540	29.95840	15.53300	3.57304	-0.96963
89.87220	39.91360	15.59900	3.65536	-1.06801

a) values in cm^{-1} ,angles in degrees.

TABLE (4.11) The kinetic energy data[a] for the T_1 stat of CD_3CDS.

θ	α	B_α	B_θ	$B_{\theta\alpha}$
0.00000	0.00000	8.00416	3.31192	-0.64529
-0.00100	4.99130	8.00195	3.31064	-0.64393
-0.00230	9.82620	7.99892	3.30887	-0.64331
-0.00420	14.97390	7.99746	3.30942	-0.64372
-0.00700	19.96400	7.99011	3.30736	-0.64518
-0.01080	24.95070	7.98502	3.31056	-0.65078
-0.01590	29.92950	7.99039	3.31997	-0.66295
-0.02900	39.82060	8.02076	3.36440	-0.71572
29.94000	0.00200	8.00162	3.30276	-0.63606
29.93640	4.98960	8.00278	3.30328	-0.63668
29.93180	9.97550	7.99809	3.30125	-0.63576
29.92560	14.95980	7.99541	3.30103	-0.63572
29.91750	19.94190	7.98668	3.30272	-0.63805
29.90720	24.91970	7.98478	3.30556	-0.64408
29.89470	29.88910	7.98486	3.31340	-0.65643
29.86550	39.76620	8.01434	3.35917	-0.71203
60.21590	0.00000	8.00155	3.29534	-0.63052
59.91050	4.98650	7.99933	3.29473	-0.62969
59.91100	9.97300	7.99442	3.29280	-0.62967
59.90930	14.96180	7.98430	3.29185	-0.63062
59.90440	19.95290	7.98137	3.29050	-0.63365
59.89550	24.94500	7.97811	3.29483	-0.64114
59.88180	29.93540	7.97654	3.30452	-0.65540
59.84220	39.88890	8.01008	3.35193	-0.71645
89.93200	-0.00130	8.00189	3.30253	-0.63548
89.93720	4.98660	8.00047	3.29981	-0.63544
89.94070	9.97760	7.99267	3.29693	-0.63505
89.94130	14.97160	7.98894	3.29737	-0.63572
89.93790	19.96770	7.98006	3.29364	-0.63781
89.92950	24.96430	7.98066	3.29651	-0.64470
89.91540	29.95840	7.97878	3.30576	-0.65807
89.87220	39.91360	8.02248	3.35505	-0.71757

a) values in cm^{-1} ,angles in degrees.

TABLE(4.12) Calculated expansion coefficients for the S_0 and T_1 kinetic energy surfaces of CH_3CHS .[a]

	$B_\theta(\theta,\alpha)$	$B_{\alpha\theta}(\theta,\alpha)$	$B_\alpha(\theta,\alpha)$
		S_0 STATE	
$B_{C\ C}^{0\ 0}$	12.8579	-8.21671	22.8268
$B_{C\ C}^{1\ 0}$	-5.32388	5.79951	-5.71821
$B_{C\ C}^{1\ 3}$	-0.135450	0.09959	-0.00657
$B_{C\ C}^{2\ 3}$	0.146880	-0.151790	0.08152
$B_{S\ S}^{1\ 3}$	-0.151770	0.217540	-0.179100
		T_1 STATE	
$B_{C\ C}^{0\ 0}$	15.2375	-11.2915	27.0937
$B_{C\ C}^{1\ 0}$	-9.38018	10.7592	-11.8972
$B_{C\ C}^{3\ 0}$	1.09698	-1.22767	1.42329
$B_{C\ C}^{1\ 3}$	-0.13022	0.18133	-0.24178
$B_{C\ C}^{2\ 3}$	0.27329	-0.34847	0.47053
$B_{C\ C}^{3\ 3}$	-0.10667	0.13034	-0.20015
$B_{S\ S}^{1\ 3}$	-0.11019	0.15467	-0.23412
$B_{S\ S}^{3\ 3}$	0.04394	-0.04973	0.08420

a) values in cm-1.

TABLE(4.13) Calculated expansion coefficients for the S_0 and T_1 kinetic energy surfaces of CH_3CDS .[a]

	$B_\theta(\theta,\alpha)$	$B_{\alpha\theta}(\theta,\alpha)$	$B_\alpha(\theta,\alpha)$
		S_0 STATE	
$B_{c\ c}^{0\ 0}$	8.46545	-3.34552	10.62410
$B_{c\ c}^{1\ 0}$	-1.96879	2.10699	-2.01712
$B_{c\ c}^{1\ 3}$	-0.05167	0.04283	0.00281
$B_{c\ c}^{2\ 3}$	0.04176	-0.05905	0.02424
$B_{s\ s}^{1\ 3}$	-0.01555	0.05802	-0.05433
		T_1 STATE	
$B_{c\ c}^{0\ 0}$	9.38389	-4.47209	12.13066
$B_{c\ c}^{1\ 0}$	-3.48464	3.91084	-4.15156
$B_{c\ c}^{3\ 0}$	0.38371	-0.40731	0.46283
$B_{c\ c}^{1\ 3}$	-0.02181	0.05264	-0.07084
$B_{c\ c}^{2\ 3}$	0.06867	-0.10531	0.14424
$B_{c\ c}^{3\ 3}$	-0.02779	0.03607	-0.06205
$B_{s\ s}^{1\ 3}$	-0.02335	0.03552	-0.06464
$B_{s\ s}^{3\ 3}$	0.01327	-0.00929	0.02217

a) values in cm-1.

TABLE(4.14) Calculated expansion coefficients for the S_0 and T_1 kinetic energy surfaces of CD_3CHS .[a]

	$B_\theta(\theta,\alpha)$	$B_{\alpha\theta}(\theta,\alpha)$	$B_\alpha(\theta,\alpha)$
		S_0 STATE	
$B_{c\ c}^{0\ 0}$	4.72657	-2.17344	16.25394
$B_{c\ c}^{1\ 0}$	-0.99067	1.03883	-0.65276
$B_{c\ c}^{1\ 3}$	-0.04308	0.03236	0.02078
$B_{c\ c}^{2\ 3}$	0.02587	-0.03079	-0.02317
$B_{s\ s}^{1\ 3}$	-0.00729	0.02894	-0.00586
		T_1 STATE	
$B_{c\ c}^{0\ 0}$	5.59462	-3.19915	17.38678
$B_{c\ c}^{1\ 0}$	-2.32645	2.57402	-2.12446
$B_{c\ c}^{3\ 0}$	0.30971	-0.32813	0.34109
$B_{c\ c}^{1\ 3}$	-0.01821	0.03421	-0.08077
$B_{c\ c}^{2\ 3}$	0.04990	-0.07026	0.16227
$B_{c\ c}^{3\ 3}$	-0.01971	0.02472	-0.08145
$B_{s\ s}^{1\ 3}$	-0.01314	0.02083	-0.07878
$B_{s\ s}^{3\ 3}$	0.01044	-0.00793	0.04686

a) values in cm-1.

TABLE(4.15) Calculated expansion coefficients for the S_0 and T_1 kinetic energy surfaces of CD_3CDS .[a]

	$B_\theta(\theta,\alpha)$	$B_{\alpha\theta}(\theta,\alpha)$	$B_\alpha(\theta,\alpha)$
		S_0 STATE	
$B_{c\ c}^{0\ 0}$	4.02449	-1.41824	8.50635
$B_{c\ c}^{1\ 0}$	-0.63230	0.66726	-0.49193
$B_{c\ c}^{1\ 3}$	-0.02243	0.01829	0.02213
$B_{c\ c}^{2\ 3}$	0.01026	-0.01879	-0.02026
$B_{s\ s}^{1\ 3}$	0.00303	0.01624	-0.00515
		T_1 STATE	
$B_{c\ c}^{0\ 0}$	4.43876	-1.88599	9.11537
$B_{c\ c}^{1\ 0}$	-1.30171	1.41695	-1.30657
$B_{c\ c}^{3\ 0}$	0.16601	-0.16792	0.19388
$B_{c\ c}^{1\ 3}$	-0.00034	0.01381	-0.01995
$B_{c\ c}^{2\ 3}$	0.01623	-0.03114	0.04690
$B_{c\ c}^{3\ 3}$	-0.00769	0.01009	-0.02517
$B_{s\ s}^{1\ 3}$	-0.00387	0.00758	-0.02293
$B_{s\ s}^{3\ 3}$	0.00589	-0.00307	0.01307

a) values in cm-1.

FIGURE (4.4)

$B_\alpha(\Theta,\alpha)$ kinetic energy surface in S_0 CH_3CHS[a]

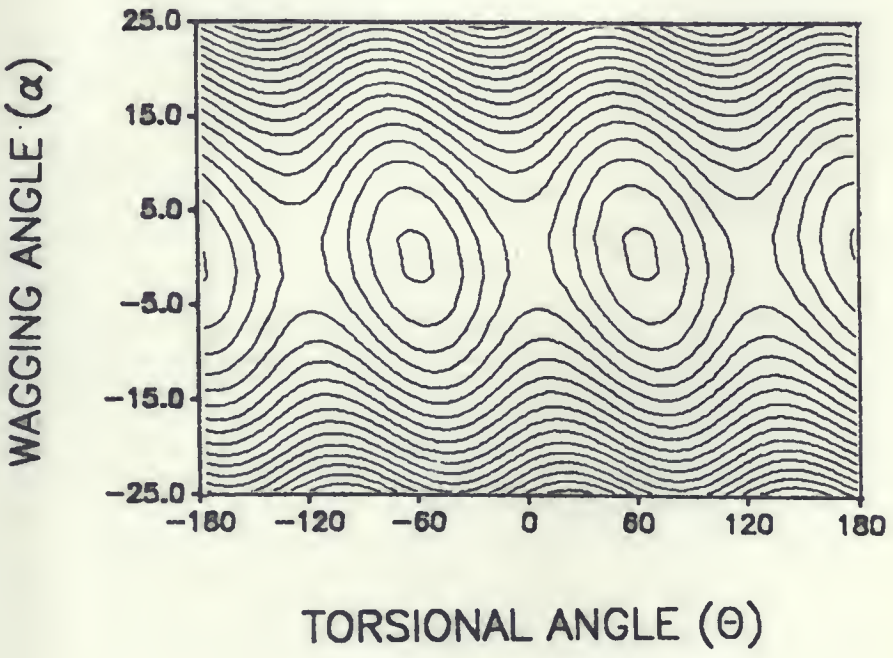

a) contour lines =0.04 cm^{-1}

FIGURE (4.5)

$B_\theta(\theta,\alpha)$ kinetic energy surface in S_0 CH_3CHS[a]

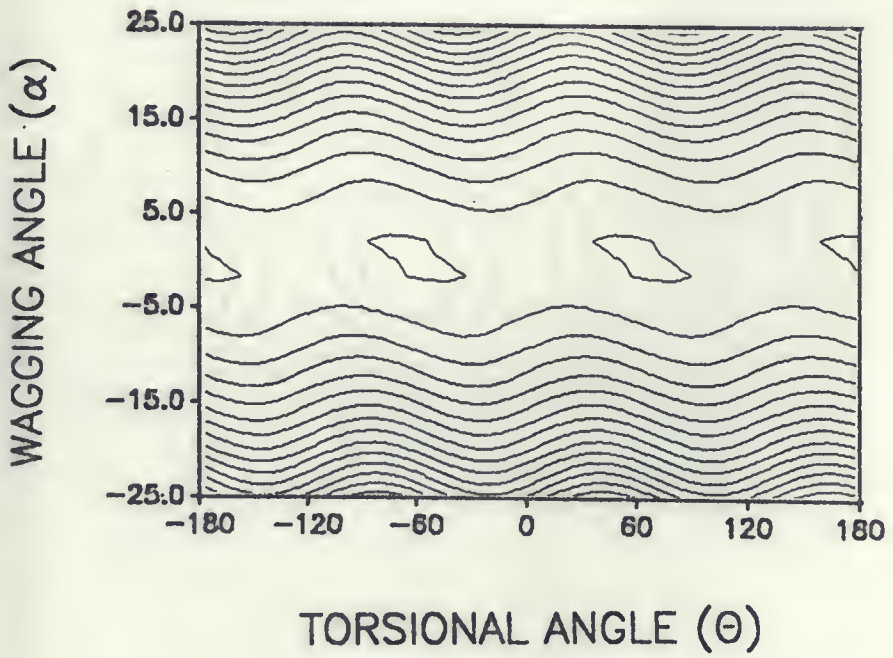

a) contour lines = 0.04 cm^{-1}

FIGURE (4.6)

$B_{\alpha\Theta}(\Theta,\alpha)$ kinetic energy surface in S_0 CH_3CHS[a]

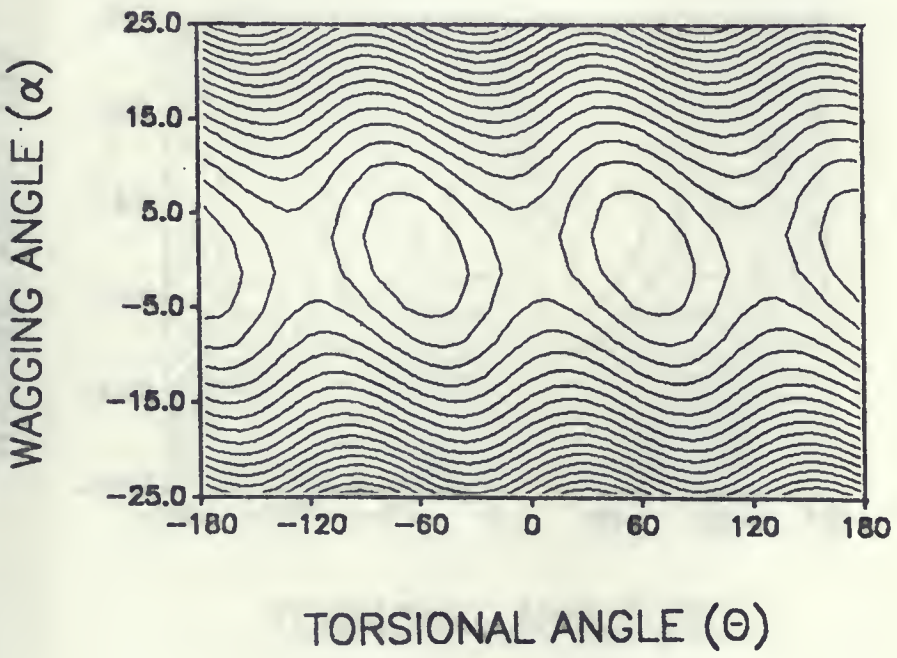

a) contour lines = 0.04 cm^{-1}

FIGURE (4.7)

$B_\alpha(\theta,\alpha)$ kinetic energy surface in T_1 CH_3CHS[a]

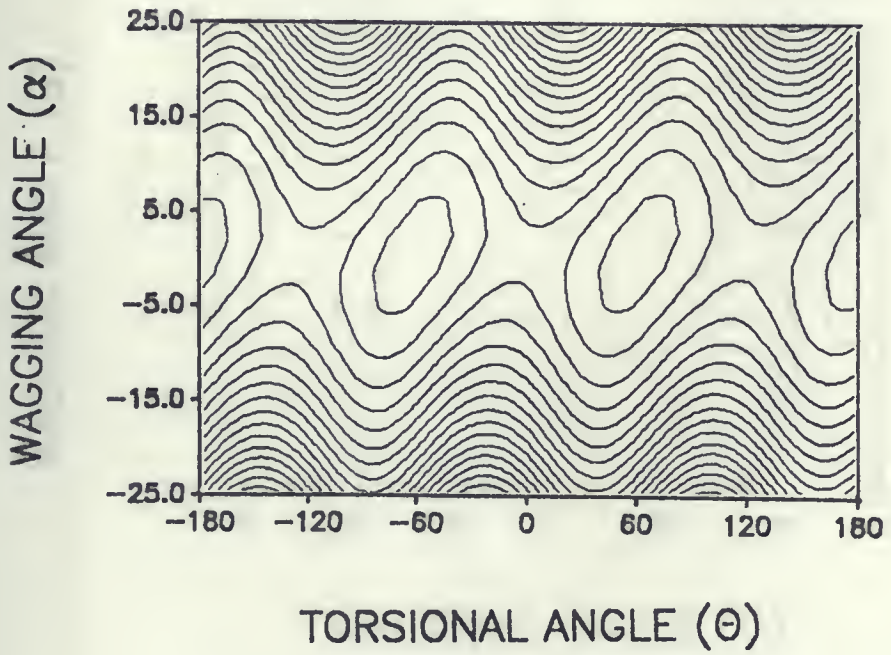

a) contour lines = 0.04 cm^{-1}

FIGURE (4.8)

$B_\theta(\Theta,\alpha)$ kinetic energy surface in T_1 CH_3CHS[a]

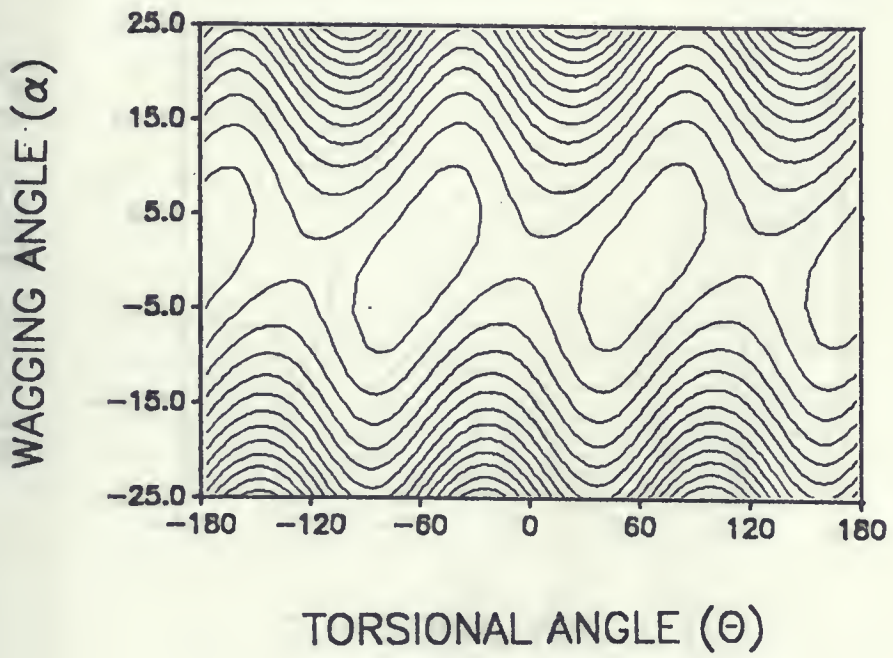

a) contour lines = 0.04 cm^{-1}

FIGURE (4.9)

$B_{\alpha\theta}(\theta,\alpha)$ kinetic energy surface in S_0 CH_3CHS[a]

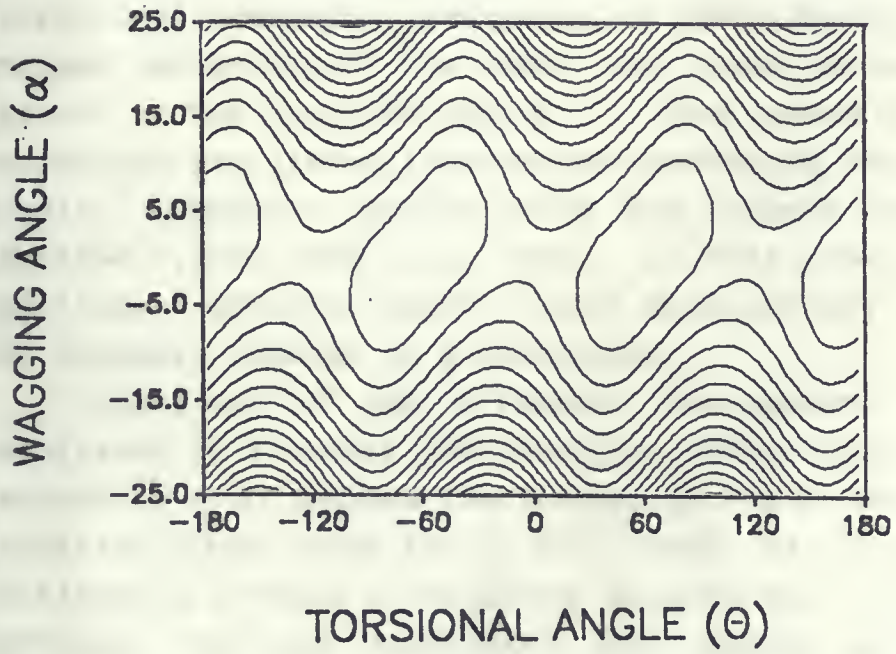

a) contour lines = 0.04 cm^{-1}

4.3) Normal-Coordinate Analysis

The results of the normal-coordinate analysis for the S_0 and T_1 states of h_4, d_1, d_3, and d_4 isotopomers of thioacetaldehyde are listed in Table(4.16). It is found that the calculated harmonic frequencies generally appear to be in constant ratio to the observed anharmonic frequencies. Thus, the data is adjusted by multiplying by the factor 0.89, which corrects for the neglect of the anharmonic terms and electron correlation.

In the S_0 state C_s symmetry is used, while in the T_1 state C_1 is used. The symmetry for the normal modes is assigned by inspecting the output of the calculations. The Mulliken's[22] vibrational numbering convention is used. The vibrations are grouped according to the order that their symmetry species appears in the character table. For each symmetry species the vibrations are listed in order of decreasing wavenumber. The totally symmetric species with the highest wavenumber is labelled ν_1,the next is ν_2, etc.. In this convention (small amplitude vibration model), lower case letters are used for the symmetry species of a vibration.

Comparison of the different isotopomers is of great importance in a normal mode analysis. Substitution of a heavy isotope (D vs H) reduces the frequency of a harmonic vibration involving that atom by $\leq 2^{0.5}$. Thus, it is possible to distinguish between a frequency associated with an aldehyde hydrogen from one associated with methyl hydrogens. The molecular structures, Table(4.17), are utilized as an aid in the assignment of modes. The normal modes ν_1, ν_2, ν_3, ν_4, ν_5, ν_6, and ν_7 are labelled in terms of the internal coordinates as listed. The weak C=S bond and CCS bend appear at their expected frequency range. The assignments of ν_{11}, and ν_{12} are evidenced by the CH_3 vs CD_3 substitution. ν_{13} is assigned to a coupling of the aldehyde and methyl hydrogen motions. ν_{14} is the CH wagging mode, and ν_{15} is the CH_3 torsion mode.

TABLE (4.16) Calculateda Vibrational Frequencies for the S_0 and T_1 States of Thioacetaldehyde[b].

		CH_3CHS	CH_3CDS	CD_3CHS	CD_3CDS
		S_0 State (C_s)			
	$\nu_1(CH_m i.p.)$[c]	2961.72	2958.97	2194.05	2194.38
	$\nu_2(CH_a i.p.)$	2941.81	2170.37	2944.43	2169.92
	$\nu_3(CH_m o.o.p)$	2844.64	2844.88	2047.19	2046.94
	$\nu_4(CCH_m)$	1447.45	1440.72	1152.18	1084.10
	$\nu_5(CCH_m)$	1380.67	1377.96	1048.54	1028.18
a'	$\nu_6(CCH_a)$	1357.33	1250.46	1361.68	1260.80
	$\nu_7(CCH_m)$	1113.91	1074.88	1022.78	909.53
	$\nu_8(CCH_a)$	1054.77	862.69	910.28	859.01
	$\nu_9(C=S)$	796.99	780.93	687.73	677.01
	$\nu_{10}(CCS)$	377.73	373.79	340.87	337.39
	$\nu_{11}(CH_m)$	2889.70	2889.70	2138.36	2138.35
	$\nu_{12}(H_m)$	1438.20	1437.41	1038.65	1037.04
a"	$\nu_{13}(H_m+H_a)$	1034.96	1000.71	944.06	863.71
	$\nu_{14}(CH_a$ wag)	753.02	632.77	634.88	559.53
	ν_{15}(torsion)	149.97	146.97	116.47	112.75
		T_1 State[d] (C_1)			
	$\nu_1(CH_m i.p.)$	2916.31	2916.98	2162.73	2162.18
	$\nu_2(CH_a i.p.)$	2979.63	2191.41	2979.03	2191.89
	$\nu_3(CH_m o.o.p)$	2829.56	2829.57	2037.13	2037.03
	$\nu_4(CCH_m)$	1453.58	1452.59	1109.20	1139.74
	$\nu_5(CCH_m)$	1388.10	1387.50	1047.17	1047.24
	$\nu_6(CCH_a)$	1247.75	1127.74	1226.71	1018.89
	$\nu_7(CCH_m)$	1027.80	1019.54	930.05	885.73
a	$\nu_8(CCH_a)$	959.37	781.13	832.51	781.49
	$\nu_9(C=S)$	673.30	654.85	624.74	619.58
	$\nu_{10}(CCS)$	279.06	275.08	255.00	252.06
	$\nu_{11}(CH_m)$	2888.35	2888.35	2134.68	2134.66
	$\nu_{12}(H_m)$	1447.43	1447.32	1042.53	1043.07
	$\nu_{13}(H_m+H_a)$	993.74	990.42	779.27	723.22
	$\nu_{14}(CH_a$ wag)	444.86	359.92	431.93	347.18
	ν_{15}(torsion)	148.60	145.80	113.58	110.31

a) values in cm-1, scaled by 0.89.
b) 6-31 G* basis, calc. at optimized geom.
c) H_a aldehyde hydrogen, H_m methyl hydrogens.
d) numbering of the modes follows C_s convention of the S_0 state.

TABLE (4.17) Molecular Structures[a] for the S_0 and T_1 States of Thioacetaldehyde. Selected Conformations (α wag, θ torsion).

	S_0 State		T_1 State			
parameter	(0°,0°)	(0°,60°)	(0°,0°)	(0°,60°)	equilib.[b]	b)+60.0
a.u.[d]	.55174758	.54928054	.51192745	.51259379	.51339369	.5113524
cm^{-1}	0.00	541.44	321.79	175.55	0.00	447.9
r(C=S)	1.6064	1.6068	1.7390	1.7404	1.7449	1.744
r(CC)	1.4968	1.5043	1.5018	1.5006	1.5026	1.508
$r(CH_a)$[e]	1.0810	1.0801	1.0744	1.0735	1.0764	1.076
$r(CH_b)$[f]	1.0805	1.0831	1.0838	1.0836	1.0888	1.084
$r(CH_c)$[g]	1.0874	1.0842	1.0871	1.0874	1.0848	1.084
$r(CH_d)$[g]	1.0874	1.0842	1.0871	1.0874	1.0845	1.087
α(CCS)	126.61	125.63	122.41	121.32	120.00	120.7
$\alpha(CCH_a)$	114.43	115.65	121.28	122.38	119.48	119.3
$\alpha(CCH_b)$	111.67	115.57	111.78	109.92	111.85	110.4
$\alpha(CCH_c)$	109.55	109.62	110.99	111.75	111.48	112.1
$\alpha(CCH_d)$	109.55	109.62	110.99	111.75	109.79	111.1
$\delta(H_bCCH_c)$	121.55	121.02	120.20	119.77	120.89	120.2
$\delta(H_bCCH_d)$	121.55	121.02	120.20	119.77	119.61	119.5

a) fully optimized structures with 6-31 G* basis. parameters in Ångstroms and degrees.

b) equilibrium: α(wag)=24.68°, θ(torsion)=-45.66° or α(wag)=-24.68°, θ(torsion)=45.66°.

c) equilibrium +60.0°: α(wag)=24.60°, θ(torsion)=14.34°.

d) energy = -475.00000000 -(a.u.).

e) CH_a aldehyde, in-plane.

f) CH_b methyl: in-plane.

g) CH_c and CH_d methyl: out-of-plane.

4.4) The Calculated Spectra

The Schrodinger equations for the coupled torsion wagging Hamiltonian operator were solved variationally for the S_0 and T_1 electronic states. Fixed and variable kinetic energy terms were used in the Hamiltonian. Solutions were expanded in terms of the symmetry eigenvectors, which factorize the Hamiltonian matrix into boxes. In a recent study[12], it was found that 31 wagging and 37 torsional functions gave a sufficient basis length. This conclusion is confirmed in the present study. This symmetrization reduced the 1147 X 1147 direct product matrix to smaller a_1, a_2, and two e boxes of dimensions 202, 201, and 372+372 respectively.

Table(4.18) gives the calculated energy levels for the CH_3CHS isotopomer derived from variable and fixed kinetic energy terms. A comparison of the data shows that the effect of introducing variable kinetic energy is small for both the S_0 and T_1 electronic states.

Table(4.19) gives the energy levels for the S_0 and T_1 states for the four isotopomers of thioacetaldehyde. When the barrier is high, the levels form a stack with uniform spacing and may be classified by a set of torsional vibrational quantum numbers $v = 0,1,2,\ldots$. The triple minimum of the potential leads to a tripling of the states. In order of increasing energy the 0,1,2,... levels divide into pairs of microstates a_1e, ea_2, $a_1e,\ldots$. Selection rules allow the torsional states to combine as $a_1 \leftrightarrow a_1$, $a_2 \leftrightarrow a_2$, $e \leftrightarrow e$. Consequently, the origin band, which is commonly written 0_0^0, consists of two bands: $0_0^0a_1$ and 0_0^0e. For example, $14_0^1 15_0^1 e$ would be the designation for an $e \leftrightarrow e$ transition between the zero point levels of the two states where one quantum of aldehyde hydrogen wagging ν_{14} and one quantum of methyl torsion ν_{15} are excited. The calculated levels for the S_0 ground electronic

state show that the aldehyde wagging mode, ν_{14} =864.0 cm^{-1}, is a small amplitude out of plane vibration of high frequency and does not couple strongly with the ν_{15} methyl torsion mode. This is evident from the isotope effect. In the S_0 state of CH_3CHS, the ν_{15} mode has a value of 152.01 cm^{-1}, which becomes 145.10 cm^{-1} in CH_3CDS. In addition, the stack of torsional levels in ν_{15} that is built on ν_{14} has an $a_1 \leftrightarrow e$ splitting which is identical to the splitting in the corresponding stack built on the zero point level. For example $(14_0 15_0\ e - 14_0 15_0\ a_1) = 0.203\ cm^{-1}$; $(14_1 15_0\ e - 14_1 15_0\ a_2) = 0.084\ cm^{-1}$.

The excited state shows a completely different pattern because the two modes ν_{14}, and ν_{15} now have large amplitudes. The data illustrates the strength of the coupling. In CH_3CHS the first quantum of torsion $15_0^1 e$ has a value of 82.6 cm^{-1}, which drops to 46.7 cm^{-1} in CH_3CDS. The mixing is so strong that it is difficult to clearly assign the higher torsional levels to quantum numbers. As an example consider the $a_1 \leftrightarrow e$ splitting of the zero level in CH_3CHS which is = 0.213 cm^{-1}, this increases to 59.50 cm^{-1} when it is attached to ν_{14}=1. This would indicate that the methyl group undergoes nearly free rotation when quanta of torsion combine with quanta of wagging mode.

TABLE (4.18) Calculated Torsion - Wagging Energy Levels for the S_0 and T_1 Electronic States of Thioacetaldhyde h_4 with Fixed and Variable Kinetic Energy (in cm^{-1})[a]

υ_{14}	υ_{15}	sym.	S_0(fix.)[b]	S_0(var.)[c]	T_1(fix.)[d]	T_1(var.)[c]
0	0	a_1	0.000	0.000	0.000	0.000
0	0	e	0.018	0.203	0.215	0.213
0	1	e	151.806	152.012	82.398	82.645
0	1	a_2	152.504	152.720	84.328	84.654
0	2	a_1	283.172	283.369	173.092	172.706
0	2	e	290.526	290.922	166.186	167.238
0	3	e	389.101	389.297	190.531	190.243
0	3	a_2	429.315	430.230	171.290	172.500
1	0	a_2	860.861	864.064	313.846	313.361
1	0	e	860.926	864.148	254.337	253.861
1	1	e	994.121	997.205	300.930	302.371
1	1	a_1	995.704	998.976	347.882	347.994

a) Expansion coefficients of $V(\alpha,\theta)$ from Table (4.3)

b) B_α=17.1836; $B_{\alpha,\theta}$=-2.46940; B_θ=7.54545 cm^{-1}.

c) Coefficients B_α, $B_{\alpha,\theta}$ and B_θ from Table (4.12)

d) B_α=16.6484; $B_{\alpha,\theta}$=-1.79673; B_θ=6.99067 cm^{-1}.

TABLE (4.19) Calculated energy levels for the coupled methyl torsion mode , ν_{15} , and the aldehyde wagging mode, ν_{14}, in the S_0 and T_1 electronic states of Thioacetaldehyde isotopmers .[a,b,c,d,e]

			CH_3CHS		CH_3CDS	
ν_{14}	ν_{15}	sym.	S_0	T_1	S_0	T_1
0	0	a_1	0.00	0.00	0.03	0.00
0	0	e	0.02	0.21	0.00	0.14
0	1	e	152.01	82.60	145.10	46.75
0	1	a_2	152.72	84.60	145.42	47.11
0	2	a_1	283.36	172.47	274.81	156.19
0	2	e	290.92	167.23	278.76	129.39
0	3	e	389.29	190.24	381.62	163.38
0	3	a_2	430.23	172.50	407.52	133.25
1	0	a_2	864.00	313.36	625.48	273.17
1	0	e	864.10	253.86	625.52	218.49
1	1	e	997.20	302.37	758.38	245.72
1	1	a_1	998.90	347.99	759.11	329.33
			CD_3CHS		CD_3CDS	
			S_0	T_1	S_0	T_1
0	0	a_1	0.04	0.00	0.07	0.00
0	0	e	0.00	0.01	0.00	0.07
0	1	e	113.21	57.56	109.01	33.72
0	1	a_2	113.22	57.70	109.01	33.75
0	2	a_1	219.43	132.31	211.96	115.76
0	2	e	219.64	134.13	212.06	110.56
0	3	e	315.99	153.78	306.84	116.46
0	3	a_2	318.34	153.77	308.04	110.93
1	0	a_2	817.32	213.79	601.83	196.01
1	0	e	817.32	200.59	601.83	186.05
1	1	e	920.31	241.01	703.34	191.72
1	1	a_1	920.31	269.84	703.35	235.67

a) units in cm^{-1} .
b) data for potential energy from table (4.3).
c) data for kinetic energy from tables (4.12)-(4.15).
d) using 31-wagging and 37-torsion basis length.
e) temperature = 30.0 K.

TABLE(4.20) The calculated transations for the methyl torsion and aldehyde wagging motions in the $T_1 \leftarrow S_0$ system of CH_3CHS.

cold spectrum[a]			warm spectrum[b]		
assg.	cm^{-1}	int.	assg.	cm^{-1}	int.
15_0^3e	253.84	100	$15_2^0a_1$	-283.3	11.7
$15_0^3a_2$	172.47	65.6	15_2^1e	-208.2	15.5
$15_0^2a_1$	167.22	45.7	15_1^0e	-152.2	0.6
15_0^3e	190.22	29.5	$15_1^1a_2$	- 68.0	16.4
15_0^1e	82.62	26.6	$15_1^2a_1$	19.0	29.5
xa_1	277.96	26.5	15_1^2e	38.9	16.2
$14_0^1 15_0^1a_1$	347.99	14.6	15_1^3e	160.6	17.7
$0_0^0a_1$	-0.01	4.1			
0_0^0e	0.19	2.0			
xa_1	453.40	0.6			

a) temp. = 30.0 K
b) temp. = 300.0 K

TABLE(4.21) The calculated transations for the methyl torsion and aldehyde wagging motions in the $T_1 \leftarrow S_0$ system of CH_3CDS.

cold spectrum[a]			warm spectrum[b]		
assg.	cm^{-1}	int.	assg.	cm^{-1}	int.
$14_0^1a_1$	218.47	100.0	15_3^0e	-381.4	20.8
15_0^2e	129.39	59.6	15_2^0e	-274.2	5.2
$15_0^2a_1$	156.19	58.3	$15_1^1a_2$	-98.3	4.3
xa_1	211.43	53.9	15_1^2e	18.2	34.2
$14_0^1 15_0^1 a_1$	329.33	34.2			
15_0^3e	163.33	22.9			
xa_1	271.25	18.4			
15_0^1e	46.75	10.5			
$0_0^0a_1$	-0.01	4.4			
0_0^0e	0.14	2.2			

a) temp. = 30.0 K
b) temp. = 300.0 K

TABLE(4.22) The calculated transations for the methyl torsion and aldehyde wagging motions in the $T_1 \leftarrow S_0$ system of CD_3CHS.

cold spectrum[a]			warm spectrum[b]		
assg.	cm^{-1}	int.	assg.	cm^{-1}	int.
14_0^1e	200.59	100.0	15_3^0e	-315.9	10.5
xa_1	223.47	65.9	15_2^0e	-219.4	4.1
$15_0^2a_1$	132.30	20.5	15_2^1e	-162.0	14.7
$14_0^1 15_0^1 a_1$	269.83	17.3	15_1^0e	-113.2	2.9
15_0^3e	152.78	14.5	$15_1^1a_2$	- 55.5	7.3
xa_0^1	358.54	12.6	15_1^2e	20.9	29.6
15_0^2e	134.13	11.9			
15_0^1e	57.56	5.3			
$0_0^0a_1$	-0.03	0.6			
0_0^0e	0.10	0.3			
xx	100.56	0.2			
$14_0^1a_2$	213.90	0.1			

a) temp. = 30.0 K
b) temp. = 300.0 K

TABLE(4.23) The calculated transations for the methyl torsion and aldehyde wagging motions in the $T_1 \leftarrow S_0$ system of CD_3CDS.

cold spectrum[a]			warm spectrum[b]		
assg.	cm^{-1}	int.	assg.	cm^{-1}	int.
15_0^1e	186.05	100.0	15_3^0e	-306.8	8.5
$14_0^1 15_0^1 a_1$	235.67	58.8	$15_3^1 a_2$	-273.1	2.4
xa_1	184.72	33.4	15_3^2e	-190.3	5.7
$15_0^2 a_1$	115.75	10.8	15_2^0e	-211.9	3.4
15_0^2e	110.56	10.4	15_2^1e	- 95.5	4.0
xa_1	270.29	9.9	$15_2^2 a_1$	- 96.2	9.6
15_0^3e	116.46	4.7	15_1^0e	-109.0	2.5
15_0^1e	33.72	2.2	$15_1^1 a_2$	- 75.2	3.2
$0_0^0 a_1$	-0.06	0.5	15_1^2e	7.4	19.9
0_0^0e	0.07	0.2			
xx	153.18	0.2			
xx	86.99	0.1			

a) temp. = 30.0 K
b) temp. = 300.0 K

Figure(4.10) The ab initio calculated spectrum of CH_3CHS^a.

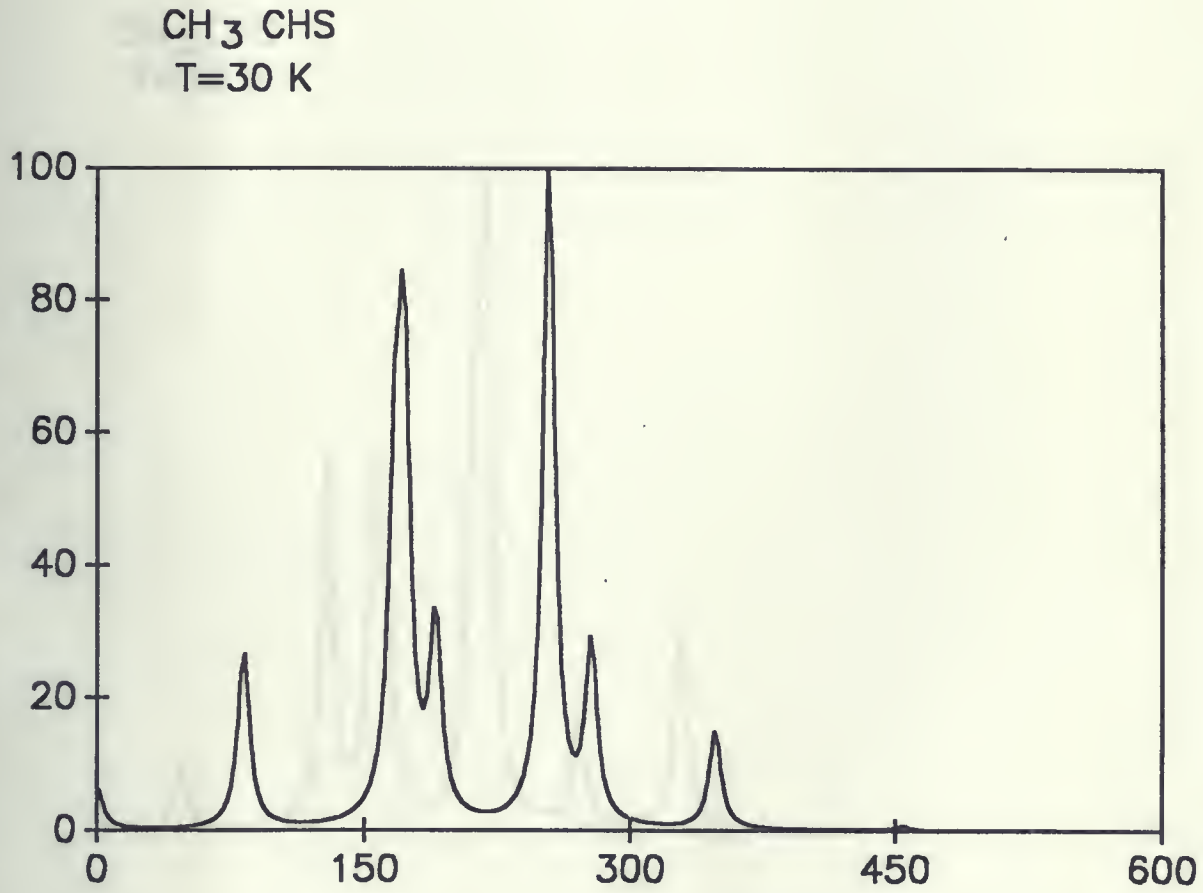

a) T= 30.0 K

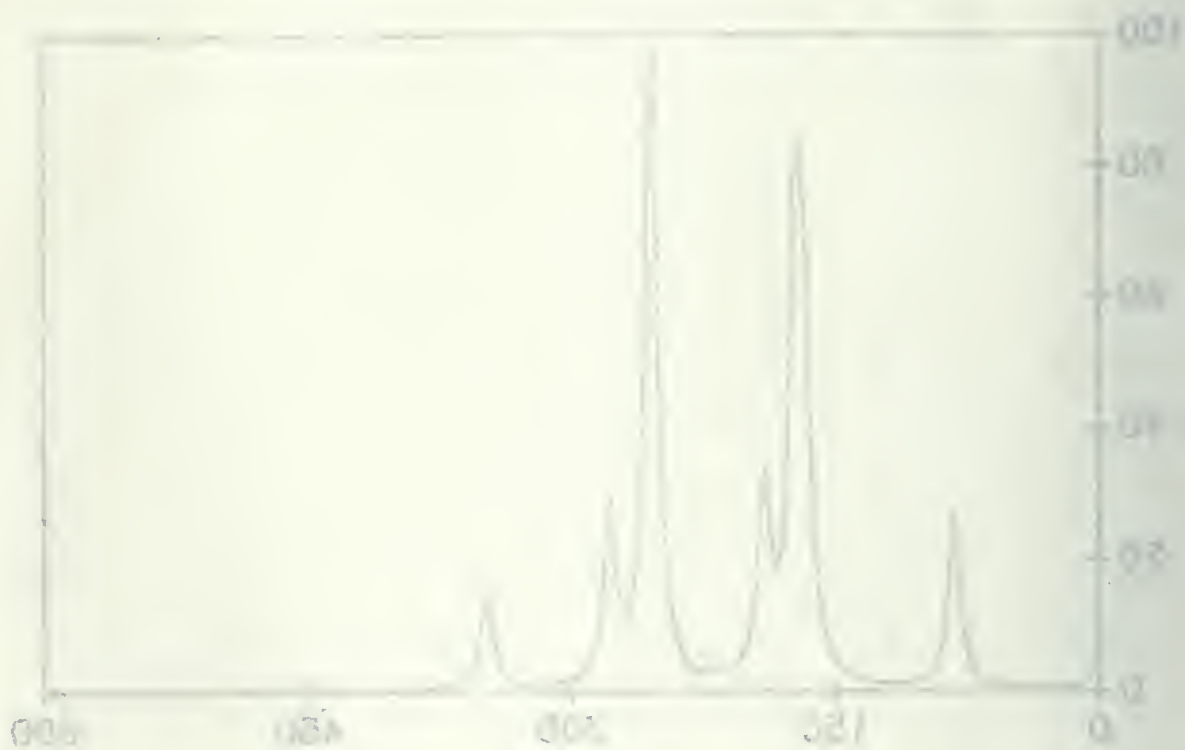

Figure(4.11) The ab initio calculated spectrum of CH_3CDS^a.

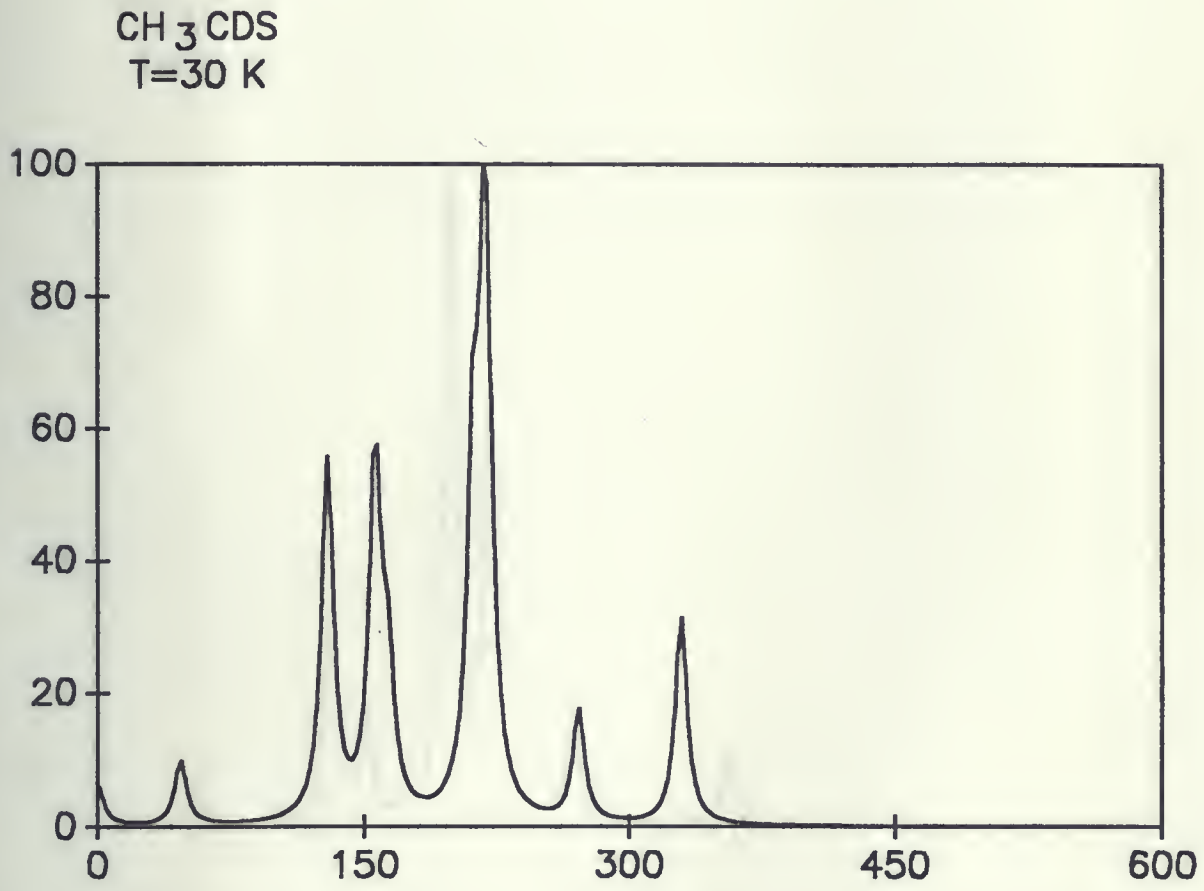

a) T= 30.0 K

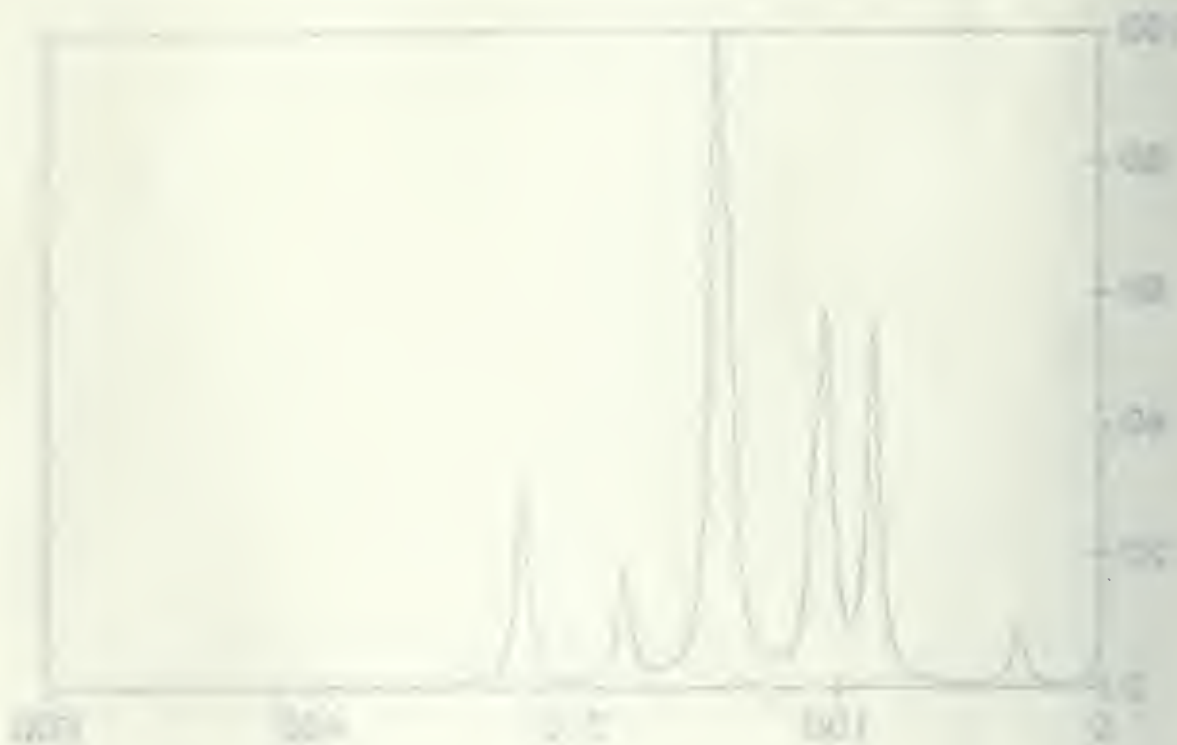

Figure(4.12) The ab initio calculated spectrum of CD_3CHS[a].

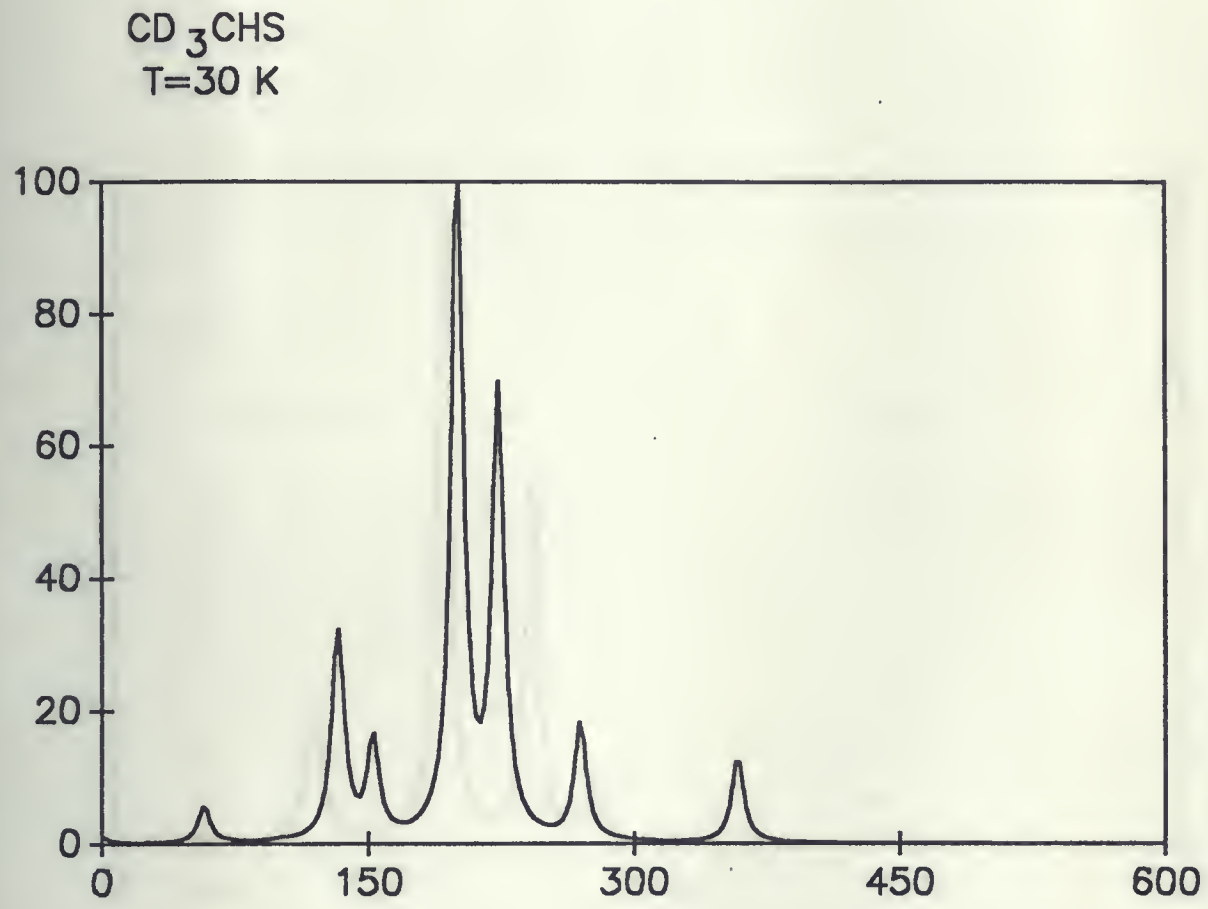

a) T= 30.0 K

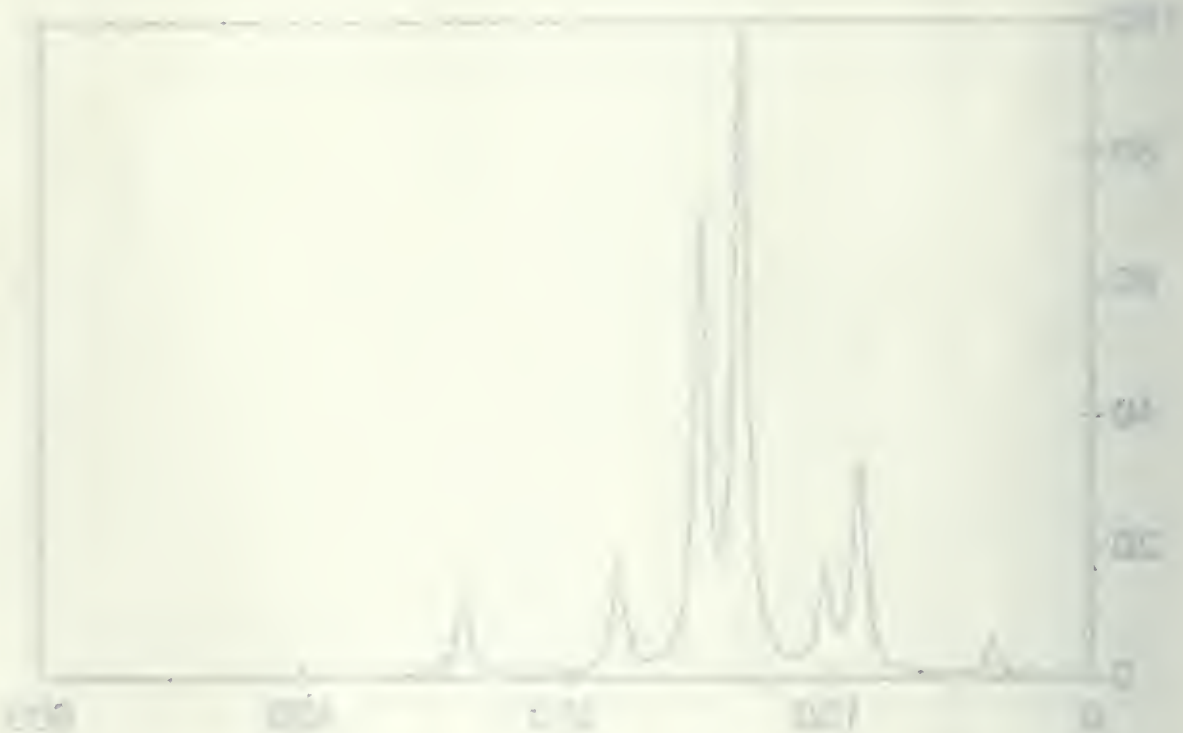

Figure(4.13) The ab initio calculated spectrum of CD_3CDS[a].

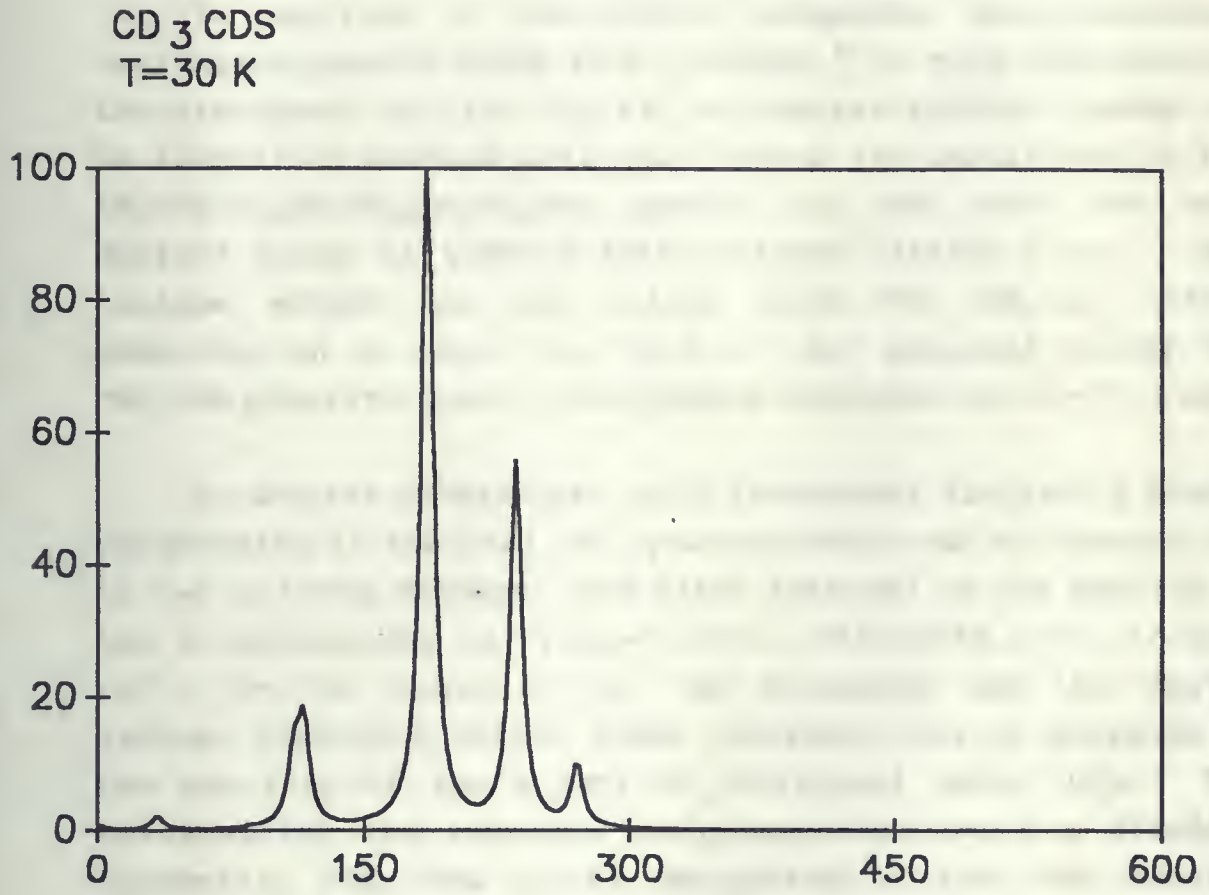

a) T= 30.0 K

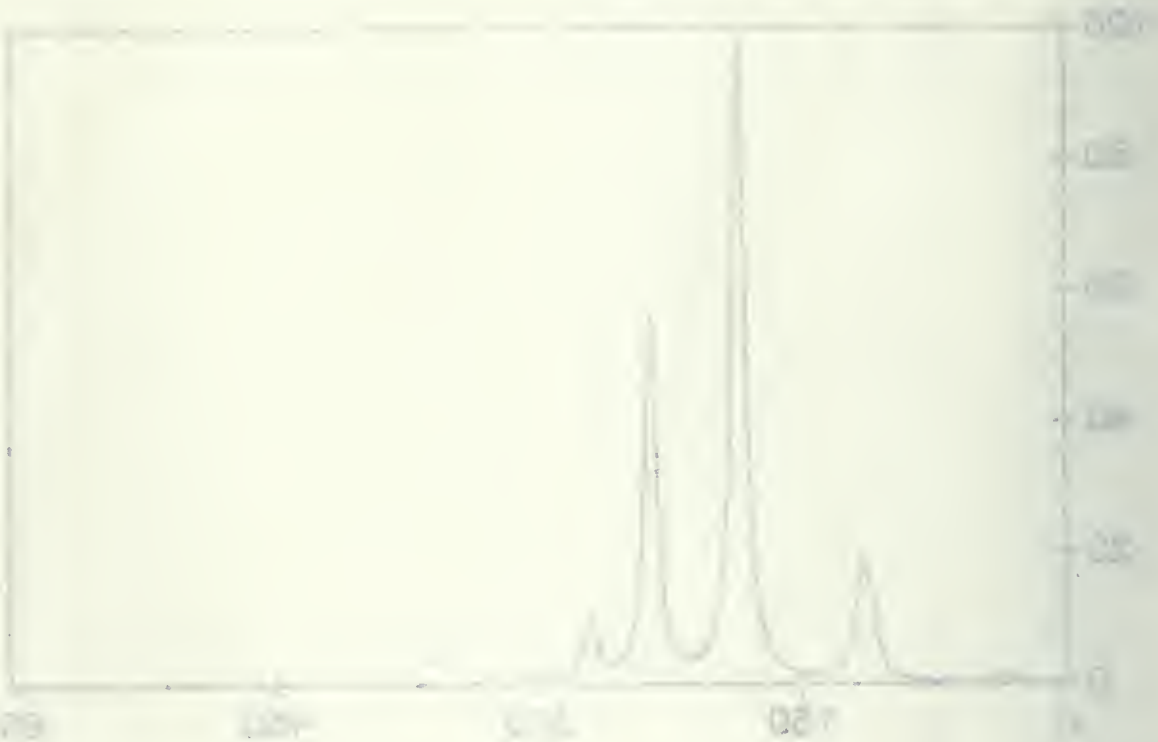

4.5) The Supersonic-Jet Specra

The supersonic-jet spectra over the range 15800-17800 cm^{-1} are given in figures(4.14) and (4.15). Figures (4.16) and (4.17) show the phosphorescence excitation spectra of thioacetaldehyde and its deuterated isotopomers recorded under jet cooled conditions. Listings of the band heads in the excitation spectrum are given in Tables(4.23) to (4.26).

In contrast to the highly congested phosphorescence excitation spectra which were recorded [12] at room temperature, the electronic origins $0_0^0a_1$ of the singlet-triplet system can be identified without difficulty under jet conditions in the $CH_3CHS/CH_3CDS/CD_3CHS/CD_3CDS$ spectra as the onset of well defined bands at 16294.9/16360.9/16299.7/16367.2 cm^{-1}. The isotope effect on the origin band for CH_3/CD_3 methyl substitution is small +4.8/+6.3 cm^{-1} but somewhat larger for CHS/CDS substitution at the aldehyde hydrogen +66.0/+67.5 cm^{-1}.

To shorter wavelengths each isotopomer displays a simple progression in the cold jet spectrum which can be tracked out to two or three members. The first interval in the spectra of the 4 isotopomers is, respectively: +52.0/+39.0/+40.9/+29.6 cm^{-1}. On the basis of the low frequency and the CH_3/CD_3 isotope frequency shifts these intervals can be assigned to the activity of the $\upsilon_{15}(a")$ CH_3 torsional mode, 15_0^1e. The notation for the vibronic assignments follows the standard convention with the quanta designated by the high barrier description. The symmetry species of the torsional sub-levels is given by the representations of the G_6 nonrigid group. The third band in the spectra of the isotopomers can be grouped into the progression at +110.9/+101.3/+93.4/+81.8 cm^{-1} and bears the assignment $15_0^2a_1$. The corresponding intervals, 15_1^0e in the warm jet spectra which extend to longer wavelengths from the origin band are observed at -163.0/-160.1/-161.4/-122.6 in the $CH_3CHS/CH_3CDS/CD_3CHS/CD_3CDS$ spectra.

In the S_0/T_1 states, the C=S bond length was calculated to be 1.6064/1.7449 Å. An increase in C=S bond length of 0.1385 Å is greater than would be expected for a 2.0 to 1.5 change in bond order. It does however demonstrate that the C=S valence vibration should be strongly active in the spectrum. The vibrational frequencies for υ_9(C=S) stretching mode are calculated to be 673.30/654.85/624.74/619.58 cm^{-1} for the 4 isotopomers. The major intervals between the torsional band clusters observed in the spectra at +747.2/+721.3/+681.5/+677.2 cm^{-1} are given this assignment. The other interval which can be observed to form characteristic band clusters is found at 394.8 in the spectrum of CH_3CHS. The structural and frequency data is of help here. In the S_0 state the CCS group is calculated to have an angle of 126.61^0 which falls to 120.00^0 in the excited state. The vibrational mode which most closely corresponds to CCS motion, υ_{10}(CCS), is calculated to be 377.73 cm^{-1} in the S_0 state and 279.06 cm^{-1} in the T_1 state. Thus the cluster at +394.8 cm^{-1} is assigned to $10_0^1 15_0^2 a_1$. Within the υ_9(C=S) group of torsional bands in CH_3CDS a set of bands is observed which is not found in CH_3CHS. The effect of D/H substitution allows the assignment to be made to the in-plane υ_8(CCD) aldehyde hydrogen bend. Thus, the band at +889.0 cm^{-1} in CDS is assigned to $8_0^1 15_0^2 a_1$. The final and perhaps most interesting assignment is that of the out - of - plane mode, υ_{14}(a"). On the basis of a rigid molecule of C_s symmetry the vibronic-spin-orbit selection rules only allow for a' -- a' and a" -- a" levels to combine. The moderately intense band at +249.4 cm^{-1} in CH_3CHS that shifts to +215.8 cm^{-1} in CH_3CDS is assigned to the υ_{14} wagging mode.

TABLE (4.24) Observed Band Heads in the Excitation Spectrum of CH_3CHS[a]

obs.	diff.	assign.[b]	obs.	diff.	assign.
warm jet spectrum			16503.5	+208.3	|
			16516.3	+221.4	⌟
15987.2	-307.7	$15_2^0a_1$	16544.3	+249.4	14_0^1e
16035.3	-259.6	15_2^1e	16628.1	+333.2	
16131.9	-163.0	15_1^0e	16689.7	+394.8	$10_0^1 15_0^2a_1$
16188.7	-106.2	$15_1^1a_2$	17021.5	+726.6	
			17042.1	+747.2	$9_0^1a_1$
cold jet spectra			17094.7	+799.8	$9_0^1 15_0^1e$
			17153.8	+858.9	$9_0^1 15_0^2a_1$
16294.9	0.0	$0_0^0a_1$	17160.3	+865.4	⌜
16346.9	+52.0	15_0^1e	17165.7	+870.8	|
16405.8	+110.9	$15_0^2a_1$	17173.0	+878.1	|
16417.5	+122.6	⌜	17182.9	+888.0	$9_0^1 15_0^2e$
16426.1	+131.2	|	17210.8	+915.9	|
16435.5	+140.6	|	17222.6	+927.7	|
16459.1	+164.2	15_0^2e	17235.3	+940.4	|
16463.6	+168.6	|	17246.1	+951.2	⌟
16475.5	+180.6	|	17290.6	+995.7	$9_0^1 14_0^1e$
16487.8	+192.9	|	17429.9	+1135.0	
16499.6	+204.7	|	17513.1	+1218.2	

a) in cm^{-1}.

b) see text for notation.

TABLE (4.25) Observed Band Heads in the Excitation Spectrum of CH_3CDS[a]

obs.	diff.	assign.	obs.	diff.	assign.
warm jet spectrum					
15847.1	-511.6		16527.7	+166.8	|
15943.6	-415.1	15_3^0e	16546.7	+185.8	⌟
16057.6	-303.3	$15_2^0a_1$	16576.7	+215.8	14_0^1e
16072.4	-286.3		16662.1	+301.2	
16200.8	-160.1	15_1^0e	16741.2	+380.3	$10_0^1 15_0^2 a_1$
16249.8	-111.1	$15_1^1a_2$	17082.2	+721.3	$9_0^1a_1$
16292.6	-68.3	15_1^2e	17123.6	+762.7	$9_0^1 15_0^1 e$
			17153.7	+792.8	$8_0^1a_1$
cold jet spectra			17186.6	+825.7	$9_0^1 15_0^2 a_1$
			17196.9	+836.0	⌜
16360.9	0.0	$0_0^0a_1$	17201.2	+840.2	|
16399.9	+39.0	15_0^1e	17208.0	+847.1	$9_0^1 15_0^2 e$
16462.2	+101.3	$15_0^2a_1$	17234.8	+873.9	|
16468.3	+107.4	⌜	17242.5	+881.6	⌟
16473.6	+112.7	|	17249.9	+889.0	$8_0^1 15_0^2 a_1$
16477.9	+117.0	|	17261.5	+900.6	
16484.6	+123.7	15_0^2e	17266.1	+905.2	
16511.8	+150.9	|	17272.3	+911.4	
16519.8	+158.9	|	17299.1	+938.2	$9_0^2 14_0^1 e$
16527.7	+166.8	|	17377.8	+1016.9	
16546.7	+185.8	|	17447.2	+1086.3	

a) in cm^{-1}.

TABLE (4.26) Observed Band Heads in the Excitation Spectrum of CD_3CHS[a]

obs.	diff.	assign.	obs.	diff.	assign.
warm jet spectrum			16484.5	+184.8	⎢
			16496.7	+197.0	⎢
15955.7	-344.0	15_3^0e	16650.1	+350.4	⎣
15046.0	-253.7		16691.9	+392.2	$10_0^1 15_0^2 a_1$
16058.4	-241.3	$15_2^0 a_1$	16981.2	+681.5	$9_0^1 a_1$
16086.2	-213.5	$15_2^1 e$	17020.3	+720.6	$9_0^1 15_0^1 e$
16213.4	-86.3	$15_1^1 a_2$	17072.0	+772.3	$9_0^1 15_0^2 a_1$
16248.3	-51.4	$15_1^2 e$	17111.7	+812.0	
			17122.8	+823.1	
cold jet spectra			17131.8	+832.1	
			17133.9	+834.2	⎡
16299.7	0.0	$0_0^0 a_1$	17151.3	+851.6	⎢
16340.6	+40.9	$15_0^1 e$	17162.4	+862.7	$9_0^1 15_0^2 e$
16393.1	+93.4	$15_0^2 a_1$	17173.8	+874.1	⎢
16432.7	+133.0	⎡	17203.5	+903.8	⎣
16440.7	+141.0	⎢	17243.3	+943.6	
16443.8	+144.1	⎢			
16453.7	+154.0	$15_0^2 e$			
16473.2	+173.5	⎣			

a) in cm^{-1}.

TABLE (4.27) Observed Band Heads in the Excitation Spectrum of CD_3CDS[a]

obs.	diff.	assign.	obs.	diff.	assign.
warm jet spectrum			16492.5	+125.3	|
			16500.8	+133.6	15_0^2e
15867.2	-500.0	14_1^0e	16503.5	+136.3	|
15887.1	-480.1	$14_1^0 15\ a_2$	16528.4	+161.2	|
16030.4	-336.8	15_3^0e	16541.5	+174.3	⌟
16051.2	-316.2	$15_3^1a_2$	16551.2	+184.0	14_0^1e
16107.4	-259.8	15_3^2e	16557.1	+189.9	
16132.6	-234.6	$15_2^0a_1$	16703.3	+336.1	
16157.4	-209.8	15_2^1e	16964.3	+597.1	
16211.2	-156.0	$15_2^2a_1$	17044.4	+677.2	$9_0^1a_1$
16244.6	-122.6	15_1^0e	17073.7	+706.5	$9_0^1 15_0^1e$
16274.0	-93.2	$15_1^1a_2$	17125.3	+758.1	$8_0^1a_1$
16303.2	-65.0	15_1^2e	17156.3	+789.1	
			17160.1	+792.9	
cold jet spectra			17166.7	+799.5	$9_0^1 15_0^2a_1$
			17175.55	+808.3	⌜
16367.2	0.0	$0_0^0a_1$	17178.8	+811.6	|
16396.8	+29.6	15_0^1e	17202.5	+835.3	$9_0^1 14_0^2e$
16449.0	+81.8	$15_0^2a_1$	17226.6	+859.4	|
16481.6	+114.4	⌜	17231.7	+864.5	⌟
16484.8	+117.6	|			

a) in cm^{-1}.

Figure(4.14) **The Supersonic-Jet spectrum of CH_3CHS and CH_3CDS in the range (15800-17700 cm^{-1})**

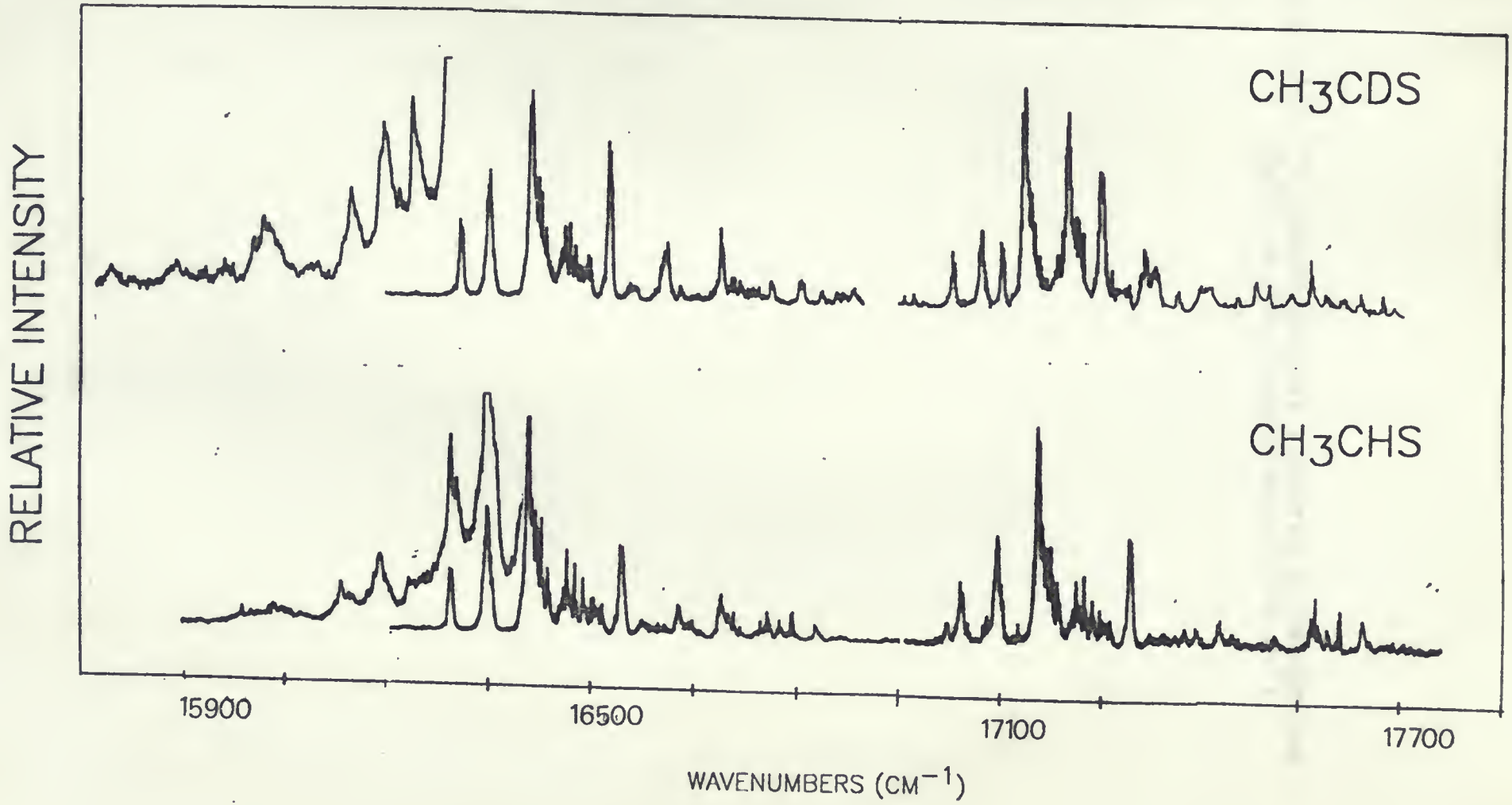
CH3CDS
CH3CHS
RELATIVE INTENSITY
15900
16500
17100
17700
WAVENUMBERS (CM−1)

Figure(4.15) The Supersonic-Jet spectrum of CD_3CHS and CD_3CDS in the range (15800-17700 cm^{-1})

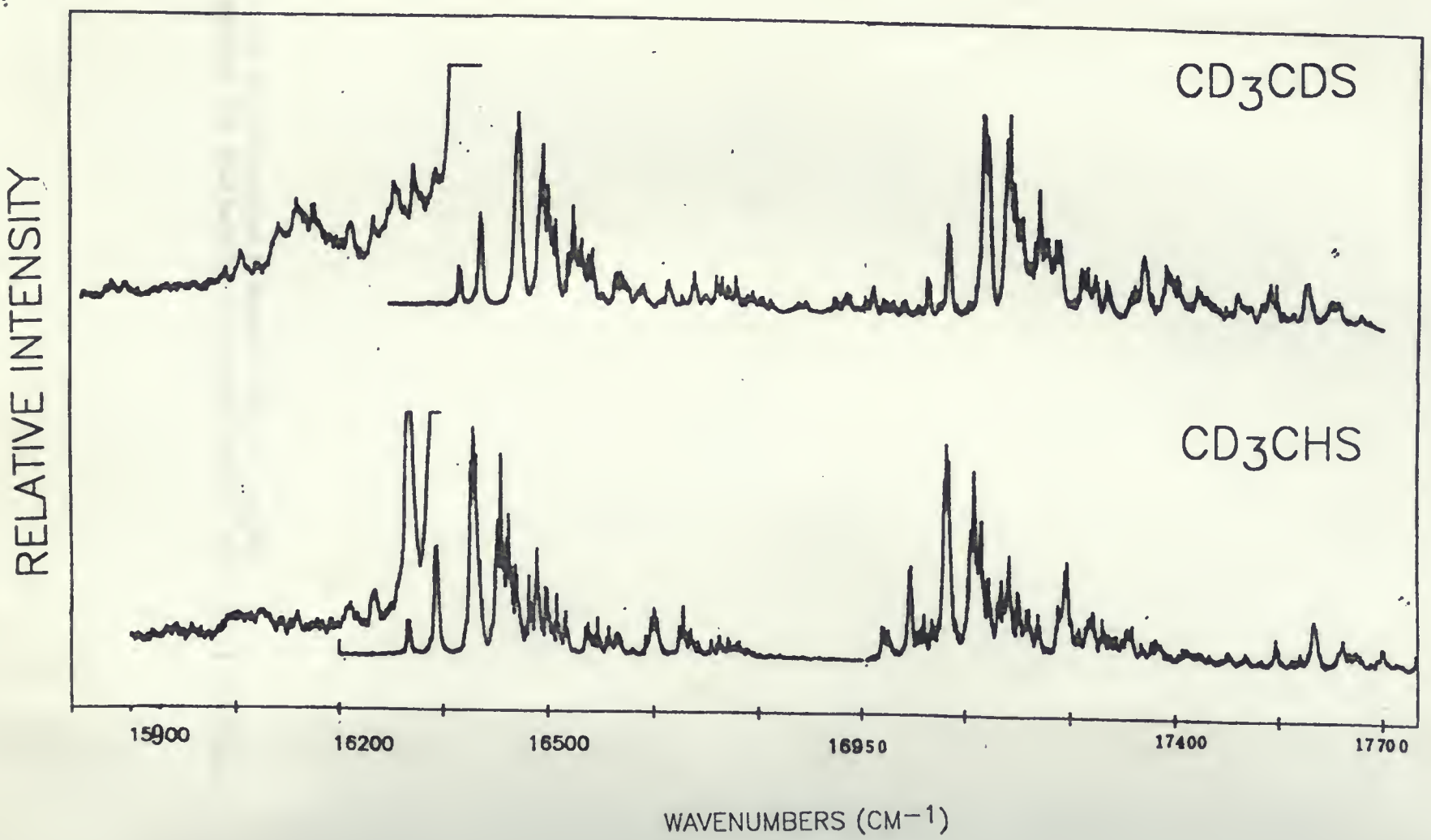
CD3CDS
CD3CHS
RELATIVE INTENSITY
15900
16200
16500
16950
17400
17700
WAVENUMBERS (CM−1)

CO-CO2
CO-CO2

Figure(4.16) The Supersonic-Jet spectrum of CH_3CHS and CH_3CDS in the range (16200-16800 cm^{-1})

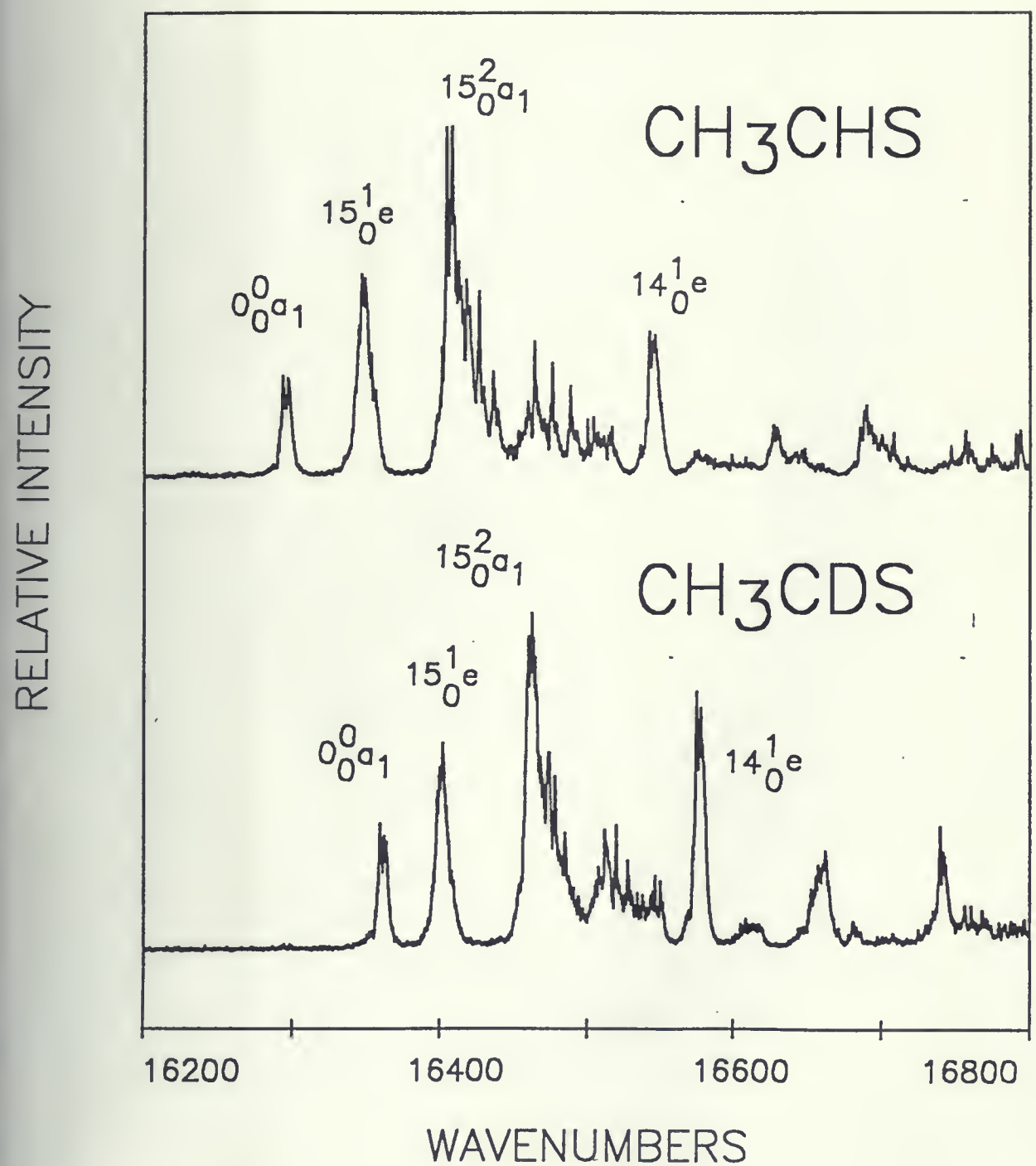
RELATIVE INTENSITY
$15^2_0a_1$
CH_3CHS
15^1_0e
$0^0_0a_1$
14^1_0e
$15^2_0a_1$
CH_3CDS
15^1_0e
$0^0_0a_1$
14^1_0e
16200
16400
16600
16800
WAVENUMBERS

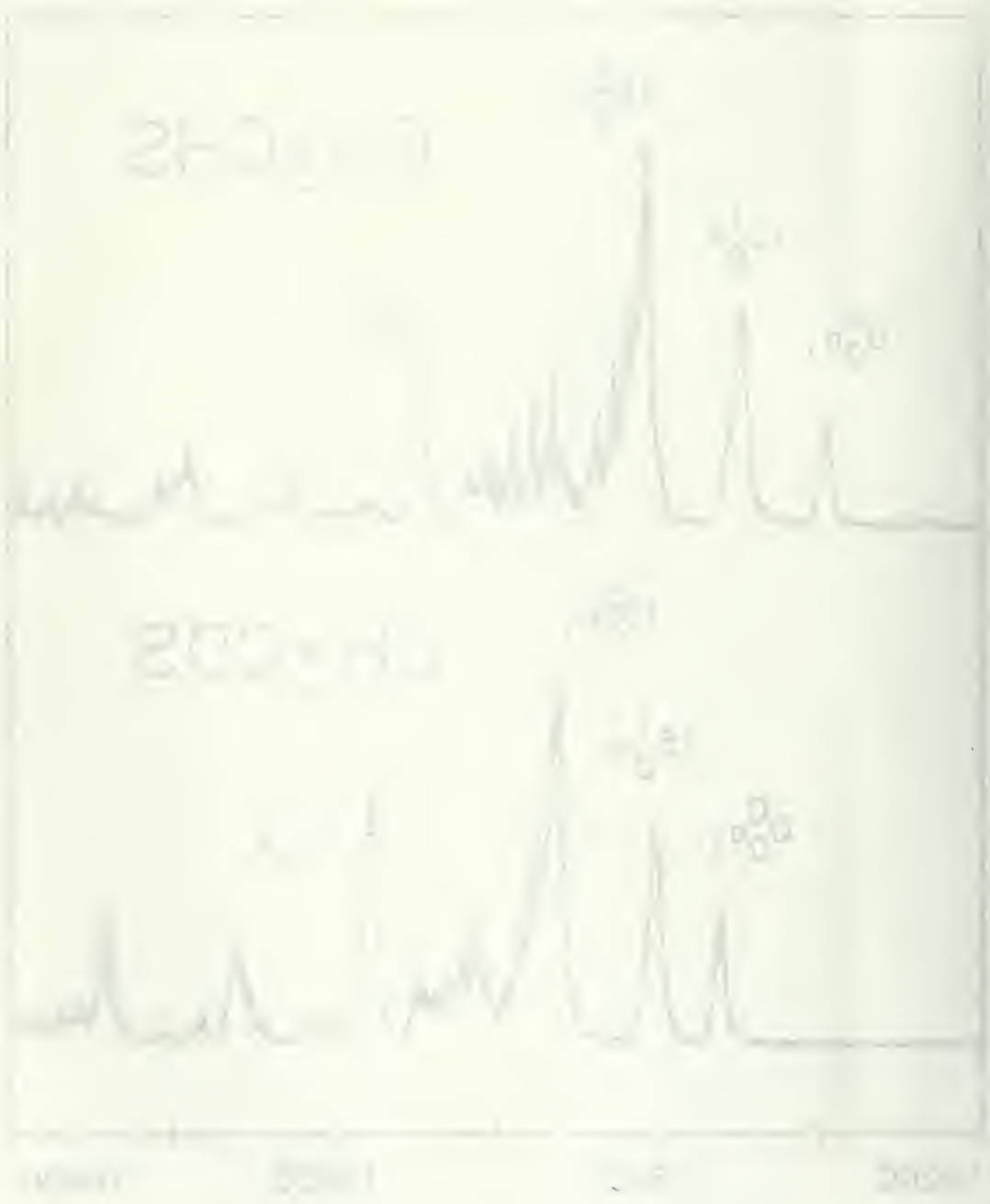

Figure(4.17) The Supersonic-Jet spectrum of CD_3CHS and CD_3CDS in the range (16200-16800 cm^{-1})

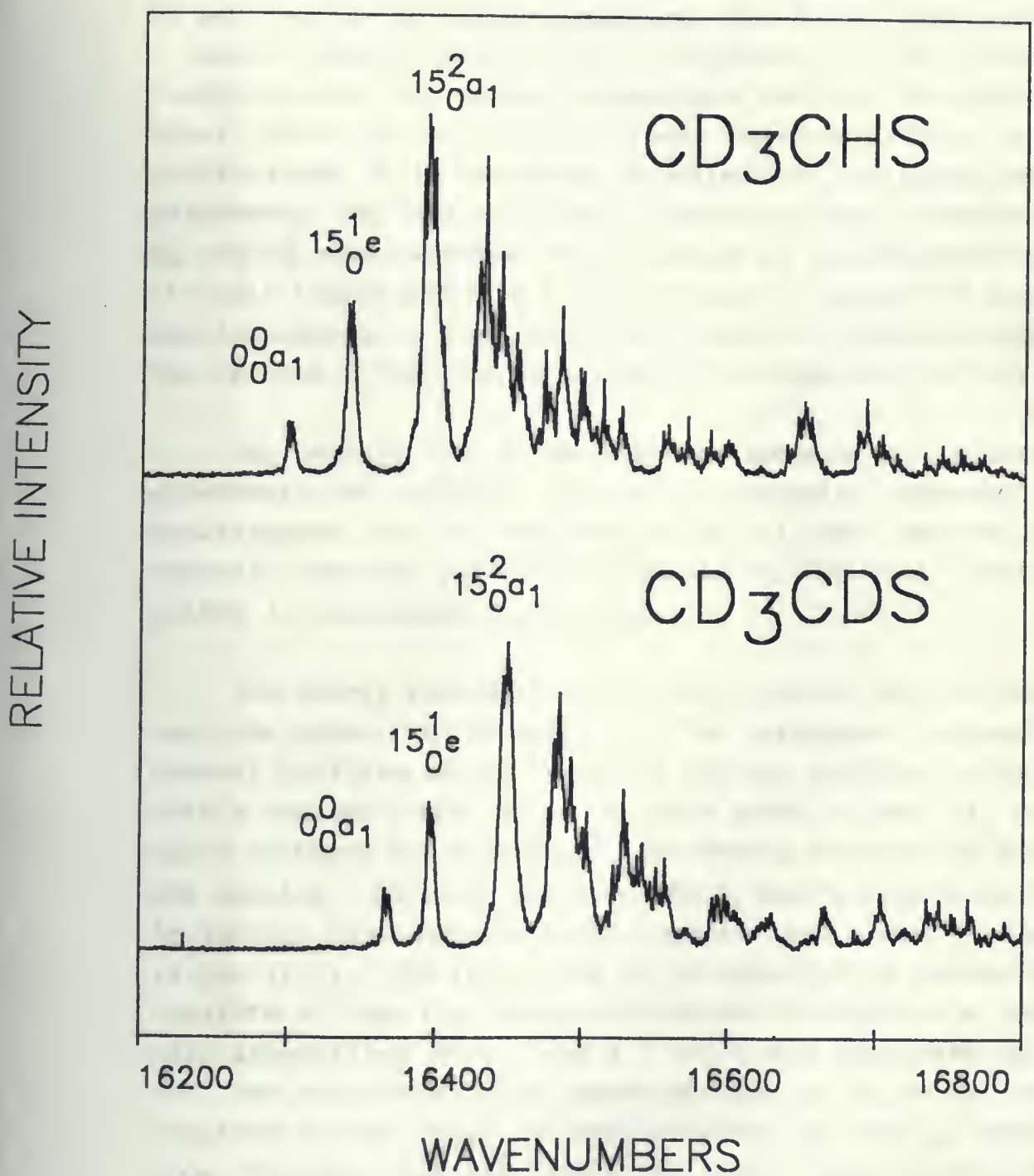
RELATIVE INTENSITY
$15_0^2a_1$
CD_3CHS
15_0^1e
$0_0^0a_1$
$15_0^2a_1$
CD_3CDS
15_0^1e
$0_0^0a_1$
16200
16400
16600
16800
WAVENUMBERS

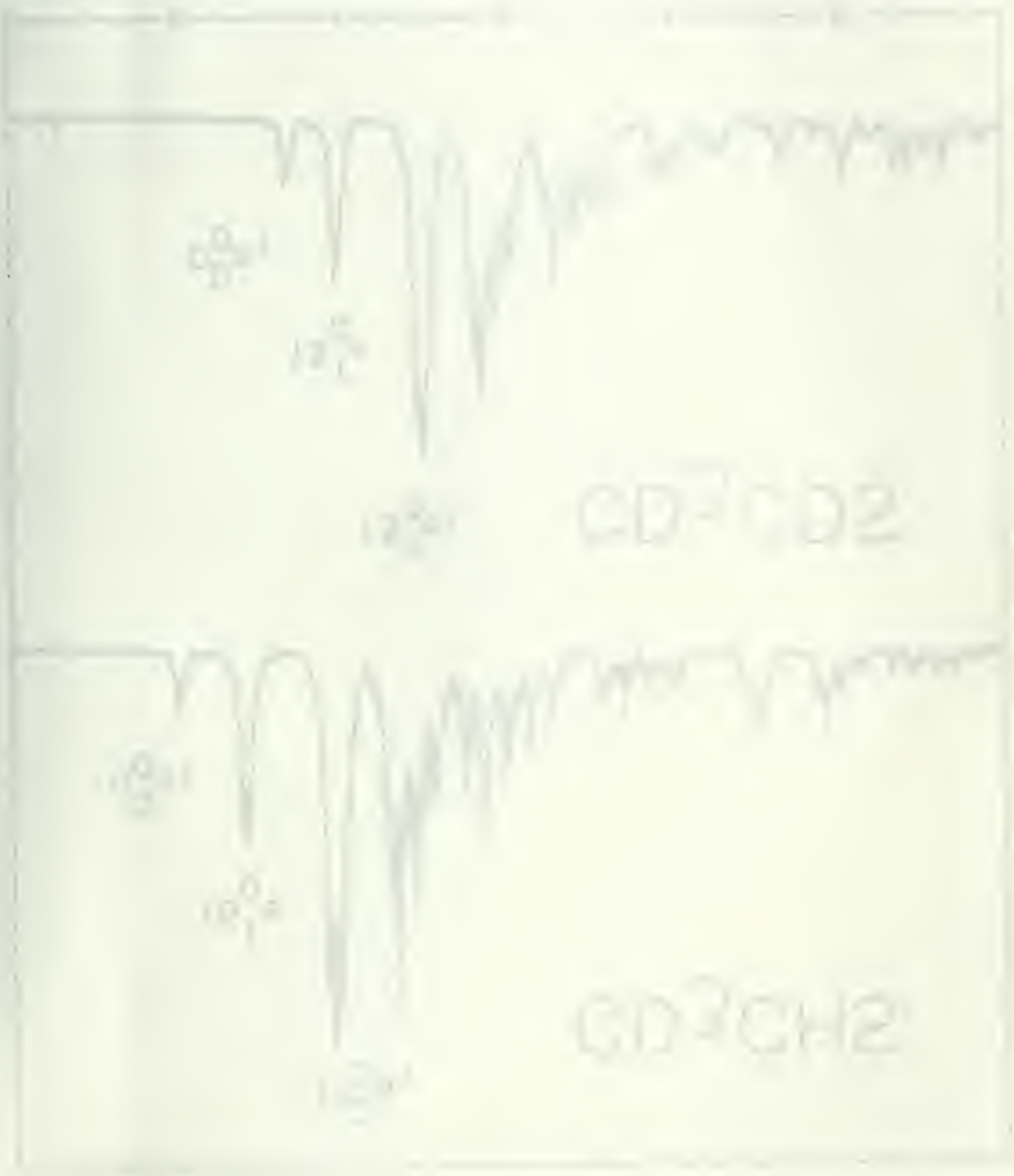
CD3CD2
CD3CH2

4.6) The scaled spectra

A model describing a fit to the jet spectra was derived by scaling the ab initio potential. The 6-31G* data provides a good starting point for a refinement of the potential functions. As the Fourier expansions contain too many high order terms for a complete least squares fitting of the coefficients it is necessary to select an arbitrary set for adjustment. For both electronic states the three constants A_{13}^{CC}, A_{23}^{CC} and A_{13}^{SS} were selected. The constant A_{00}^{CC} was adjusted to set the equilibrium position to zero energy. A global fit was made simultaneously to the four isotopomers of thioacetaldehyde. The results of the fitting procedure are shown in Table(4.28).

The overall fit of the modelled spectra to the observed supersonic-jet spectra is only adequate, however, the simultaneous fit of the data from all four species to a uniquely defined potential surfaces in the two electronic states is considered to be good.

The energy levels of the S_0 and T_1 states were calculated and are shown in Table(4.29). The agreement between the overall profiles of the observed and the spectrum calculated with a scaled 6-31G* basis is quite good in that all of the major features are reproduced. The energy transitions between the wagging - torsion levels of the S_0 and T_1 states are shown in Table(4.30), and the scaled spectra are shown in Figures (4.18)-(4.21). The first band in the spectrum is composite and consists of the two internal rotation doublets 0^0a_1 and 0^0e with intensities of 8.2 and 4.3 which are separated by 0.75 cm^{-1}. The next band in the spectrum 15_0^1e at +58.00 cm^{-1} can be regarded as the first quantum addition of the υ_{15} torsional mode. The next band $15_0^2a_1$ forms the third member of the methyl torsion Its component band, $15_1^1a_2$, does not appear in the spectrum since the low temperature of the supersonic jet

allows for only the population of the two lowest levels: $v=0a_1$ and $v=0e$. The next band $15_0^2a_1$ at +110.9 cm^{-1} forms the third member of the progression. The length and the strength of this progesssion in methyl torsion provides a measure of the displacement of the equilibrium structure which occurs on $S_0 \rightarrow T_1$ excitation. On the basis of Franck Condon arguments it may be concluded that the calculated length and strength of the torsional progression in the purely ab initio procedure is too great and the calculated changes in the θ structural coordinate are too large.

The potential surface of Figure (4.2) shows that the ab initio calculated minima in the triplet state is found along the $(-45.66^0,+24.68^0)$ $(+45.66^0,-24.68^0)$ negative sloping diagonal. The result of fitting the simulated, (6-31G* scaled) to the observed spectra generates a potential which has a corresponding minimum at $(-41.08^0, 22.38^0)$. In this case the minimum in the scaled potential is closer to the ground state origin by $\Delta\theta= 45.66^0-41.08^0=4.58^0$ and $\Delta\alpha=24.68^0-22.38^0=2.30^0$. This smaller value of the θ displacement then accounts for the observed reduced Franck Condon activity in the torsional progression in the middle trace of Figure(5.1) and the better description of the band intensities. The other major difference is that the barrier to torsion = 54.07 cm^{-1} is smaller than in the ab initio 146.24 cm^{-1} case. The flatter potential in the scaled model is then directly responsible for the better agreement between the observed and calculated frequency intervals.

While this procedure seems to be satisfactory for the lower bands in the spectrum, the contour of the 15_0^2e band appears to be quite different and extends over a 50 cm^{-1} range in a series of weak subbands. The upper level for this particular transition, $v_{15}=2e$, lies above the top of the barrier and as a result the methyl group breaks into free rotation. Above the barrier the molecule acquires an

additional degree of rotational freedom and an extra free rotation quantum number which has the effect of spreading the rotational fine structure over a wide range. As our model does not treat the case of free rotation we have simulated the profile of these bands with a contour of 50 cm^{-1} width at half height.

The equilibrium position falls from the ab initio position of $\alpha=24.68^0$ to 22.38^0 when the potential is scaled. This shift is accompanied by a reduction in the barrier to molecular inversion from 321.79 to 246.58 cm^{-1}. As would be expected from a one dimensional Franck - Condon consideration, the net result is that the intensity of the 14^1_0e band falls from being the strongest band in the spectrum to a value which is close to the observed intensity.

The coupling between the υ_{15} torsion and υ_{14} wagging modes can be clearly observed in the CH_3CHS/CH_3CDS band patterns. The calculations of Table(4.16) show that in the T_1 state the υ_{15} harmonic frequencies for CH_3CHS/CH_3CDS vary as 148.60/145.80 cm^{-1}, yet the v_{15}=1e intervals in the spectrum vary as +52.0/+39.0 cm^{-1}. This sizeable isotope shift is not observed for the S_0 hot band intervals -163.0/-160.1 cm^{-1} and therefore must be a result of a coupling between the two large amplitude modes. It is possible to view this coupling as an interaction between the υ_{14} and υ_{15} stacks of levels of the same nonrigid symmetry species. As an example, the single quantum addition of aldehyde wagging consists of two sublevels $v_{14}=1a_2$ and $v_{14}=1e$. A coupling between these two wagging levels would drive the lower $v_{15}=1a_2$, $v_{15}=1e$ and $v_{15}=2a_1$ torsional levels downwards and the $v_{14}=1a_2$ and $v_{14}=1e$ levels upwards. As the υ_{14} mode undergoes an appreciable downward shift on aldehyde isotope substitution, the perturbations would be stronger in the case of the CH_3CDS isotopomer than they are for CH_3CHS. Thus the υ_{15} frequencies would shift to lower

values and generate anomalous isotope patterns. This effect is reproduced in the 6-31G* scaled calculations, 58.00/35.96 cm^{-1}. If anything, the calculations tend to overestimate the effects of coupling. The effect of coupling can also be seen in the combination band $14_0^1 15_0^1 a_1$ of CH_3CDS. Here the combination level $v_{14}=1, v_{15}=1a_1$ would be pushed upwards by $v_{15}=2a_1$ which would lead to an increased torsional frequency. The calculated value of 73.72 cm^{-1} for torsional quanta attached to a quantum of wagging compares well to the observed value of 85.4 cm^{-1}. It should be clear from the above discussion that the lower S_0 state is well behaved and the two modes can be regarded as completely separable. In the excited state all of the levels of the υ_{14} and υ_{15} manifolds interact with each other with the strength of the coupling changing with the extent of the isotopic substitution. Further experimental studies which are capable of resolving the rotational fine structure will be necessary before a more accurate picture can be given of the intermode coupling in the excited T_1 state.

TABLE (4.28) The scaled ab initio Coefficients[a] for the S_0 and T_1 Potential Energy Surfaces of Thioacetaldehyde.

Potential Energy $V(\alpha,\theta)$			
S_0 State		T_1 State	
A_{00}^{CC}	20033.310	A_{00}^{CC}	9731.188
A_{10}^{CC}	-19713.575	A_{10}^{CC}	-10835.322
A_{13}^{CC}	200.860	A_{13}^{CC}	495.771
A_{23}^{CC}	-520.595	A_{23}^{CC}	-474.227
A_{13}^{SS}	700.397	A_{13}^{SS}	36.425
		A_{30}^{CC}	1323.175
		A_{33}^{CC}	5.992
		A_{33}^{SS}	190.008

a) values in cm^{-1}.

TABLE (4.29). Calculated and Observed Torsion - Wagging Energy Levels for the S_0 and T_1 Electronic States of Thioacetaldhyde[a] (in cm^{-1}).

			CH_3CHS		CH_3CDS	
υ_{14}	υ_{15}	sym.	S_0[b]	T_1[b]	S_0[b]	T_1[b]
0	0	a_1	0.00	0.00	0.00	0.00
0	0	e	0.00	0.75	0.00	0.62
0	1	e	170.66(163.0)	58.00(52.0)	167.01(160.1)	35.96(39.0)
0	1	a_2	170.99	62.90	167.21	37.87
0	2	a_1	321.45(307.7)	129.99(110.9)	317.01(303.3)	121.03(101.3)
0	2	e	325.75	148.81	319.76	127.08
0	3	e	444.06	184.89	441.83	144.89
0	3	a_2	473.10	201.04	462.65	147.17
1	0	a_2	863.64	288.80	626.19	252.21
1	0	e	863.66	237.83(249.4)	626.19	204.12(215.8)
B_α			17.1836	16.6484	8.63403	8.45328
$B_{\alpha,\theta}$			-2.46940	-1.79673	-1.25475	-0.98516
B_θ			7.54545	6.99067	6.86259	6.30203

			CD_3CHS		CD_3CDS	
υ_{14}	υ_{15}	sym.	S_0[b]	T_1[b]	S_0[b]	T_1[b]
0	0	a_1	0.00	0.00	0.00	0.00
0	0	e	0.00	0.08	0.00	0.08
0	1	e	126.49	37.02(40.9)	121.85(122.6)	22.13(29.6)
0	1	a_2	126.50	37.62	121.85	22.37
0	2	a_1	245.12(241.3)	98.03(93.4)	236.78(234.6)	90.77(81.8)
0	2	e	245.19	102.91	236.82	93.63
0	3	e	353.99(344.0)	138.87	343.32(336.8)	114.45
0	3	a_2	354.94	155.12	343.76	119.51
1	0	a_2	820.01	213.66	603.89	180.62
1	0	e	820.03	196.13	603.89	162.58(184.0)
B_α			15.5988	15.6035	8.01629	8.00446
$B_{\alpha,\theta}$			-1.13304	-0.96459	-0.75148	-0.64420
B_θ			3.71869	3.58986	3.38002	3.31126

a) Observed values are given in brackets.

b) Potential energy data from table (4.28).

TABLE (4.30) Calculated energy levels for the Torsion - Wagging modes in the S_0 and T_1 electronic states of Thioacetaldehyde isotopomers.[a,b]

CH_3CHS			CH_3CDS		
	cm^{-1}.	int.		cm^{-1}.	int.
15_0^2e	148.81	100.0	15_0^2e	127.08	100.0
$15_0^2a_1$	129.99	79.8	14_0^1e	204.12	70.0
15_0^1e	58.00	48.9	$15_0^2a_1$	121.02	58.7
14_0^1e	237.83	41.0	$15_0^4a_1$	204.12	31.0
15_0^3e	184.89	36.1	15_0^1e	35.95	21.2
$15_0^4a_1$	259.65	31.9	$14_0^1 15_0^1 a_1$	277.84	10.8
$0_0^0a_1$	0.00	8.2	$0_0^0a_1$	0.00	6.3
0_0^0e	0.75	4.3	0_0^0e	0.62	3.3

CD_3CHS			CD_3CDS		
	cm^{-1}.	int.		cm^{-1}.	int.
15_0^3e	138.87	100.0	15_0^4e	162.59	100.0
15_0^4e	196.13	49.9	15_0^3e	114.46	53.8
$15_0^4a_1$	178.81	44.1	$15_0^4a_1$	161.57	47.5
15_0^2e	102.91	25.4	15_0^2e	93.63	18.7
15_0^2e	98.03	24.2	$15_0^2a_1$	90.76	18.2
15_0^1e	37.02	11.3	Xa_1	220.72	11.3
Xa_1	332.06	4.3	Xa_1	284.30	9.3
Xa_1	281.61	3.7	15_0^1e	22.31	6.4
$0_0^0a_1$	0.00	1.1	$0_0^0a_1$	0.00	1.2
0_0^0e	0.08	0.9	0_0^0e	0.08	0.9

a) units in cm^{-1}.

b) Employing Potential and Kinetic energy data used in table (4.29).

Figure(4.18) The scaled 6-31G* spectrum of CH_3CHS

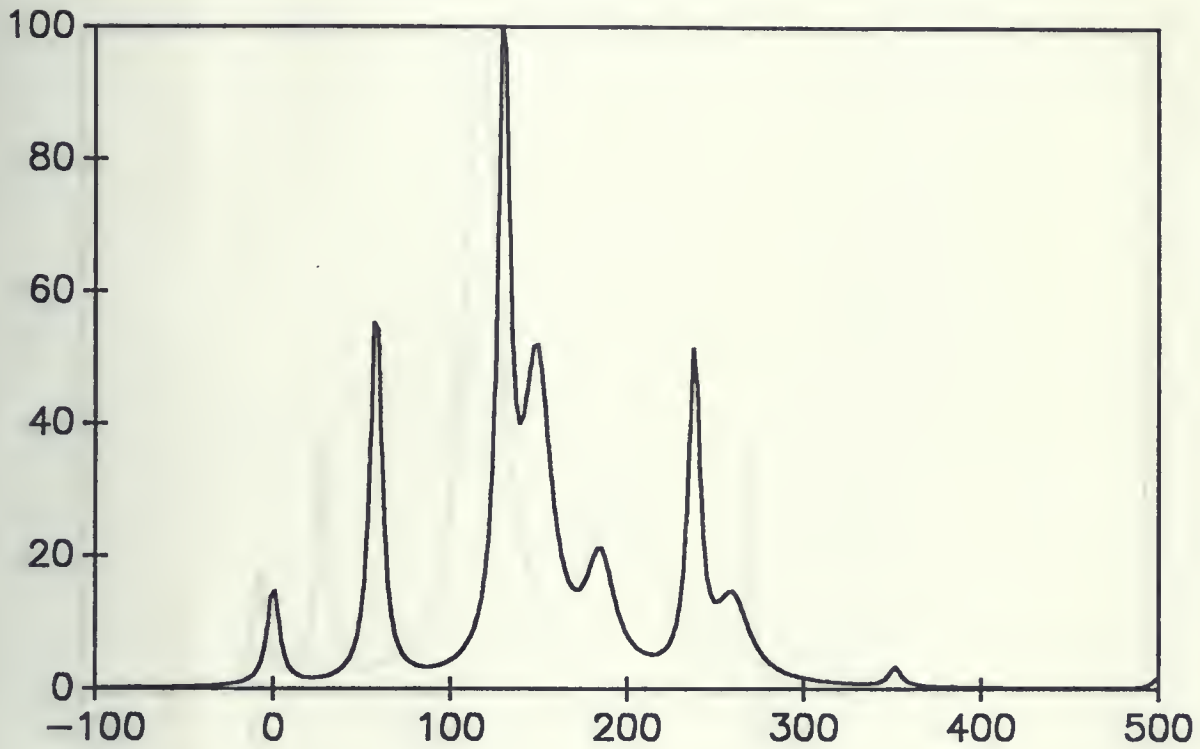

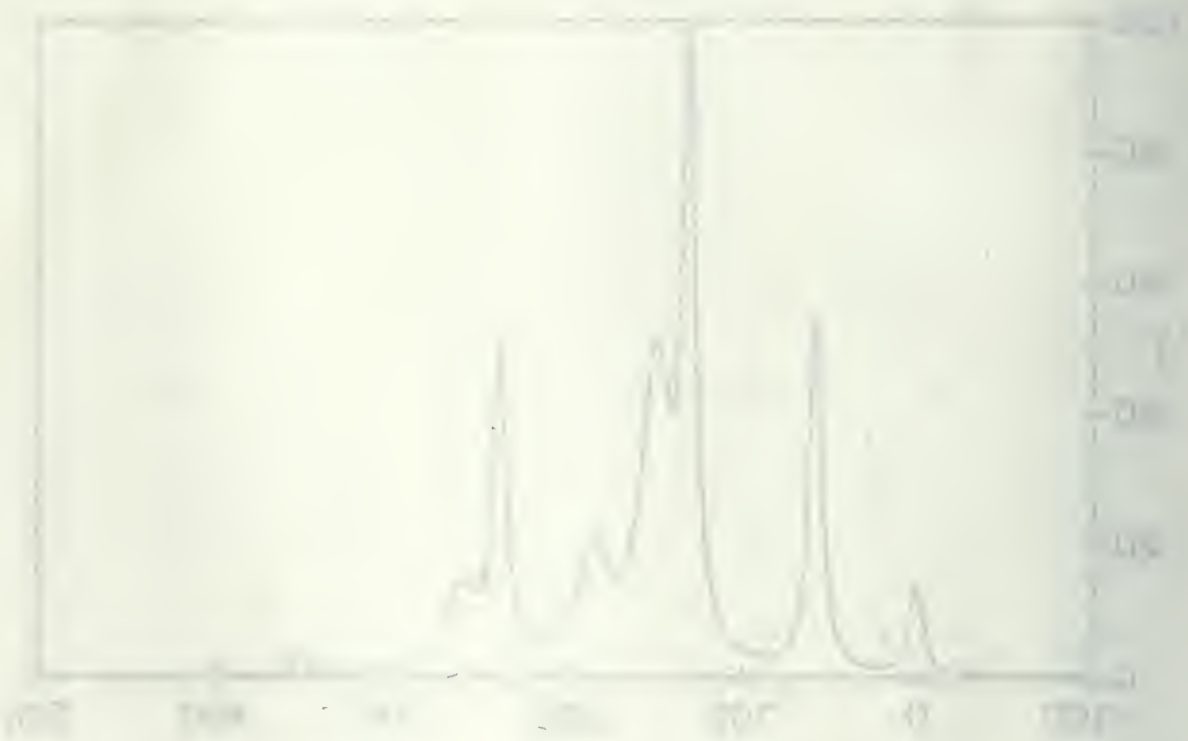

Figure(4.19) The scaled 6-31G* spectrum of CH_3CDS

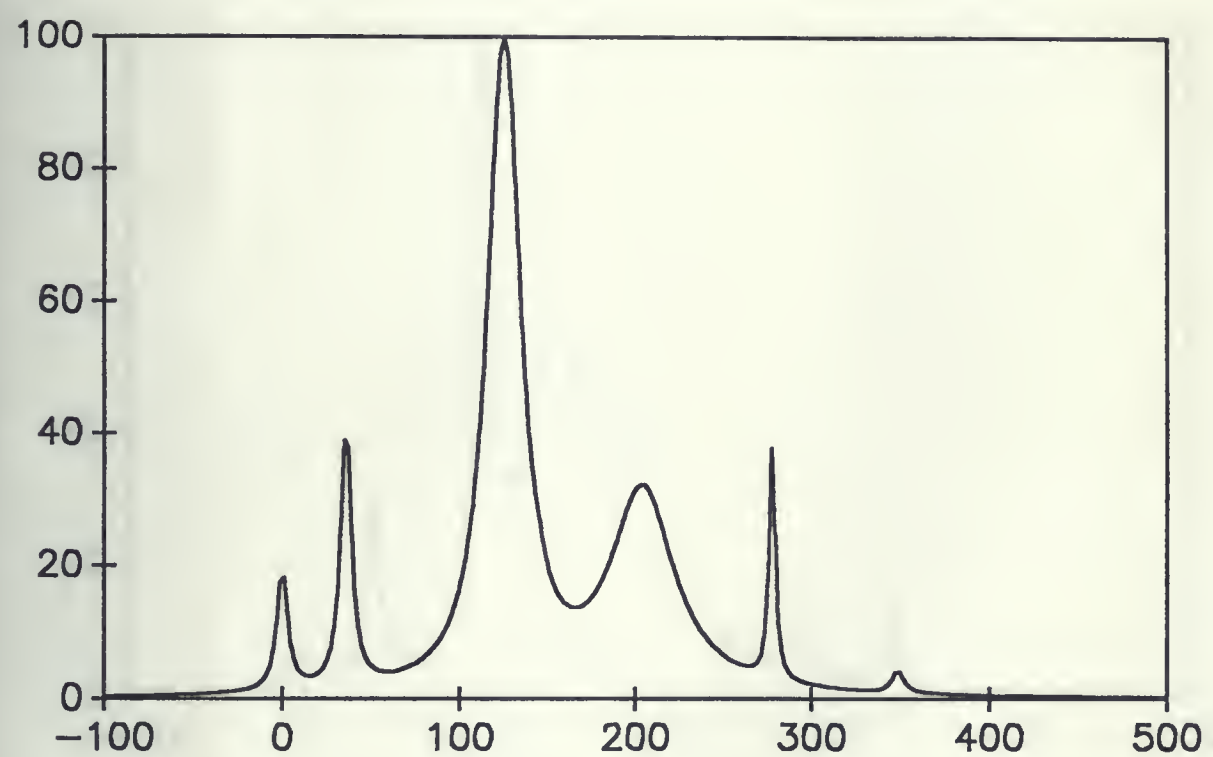

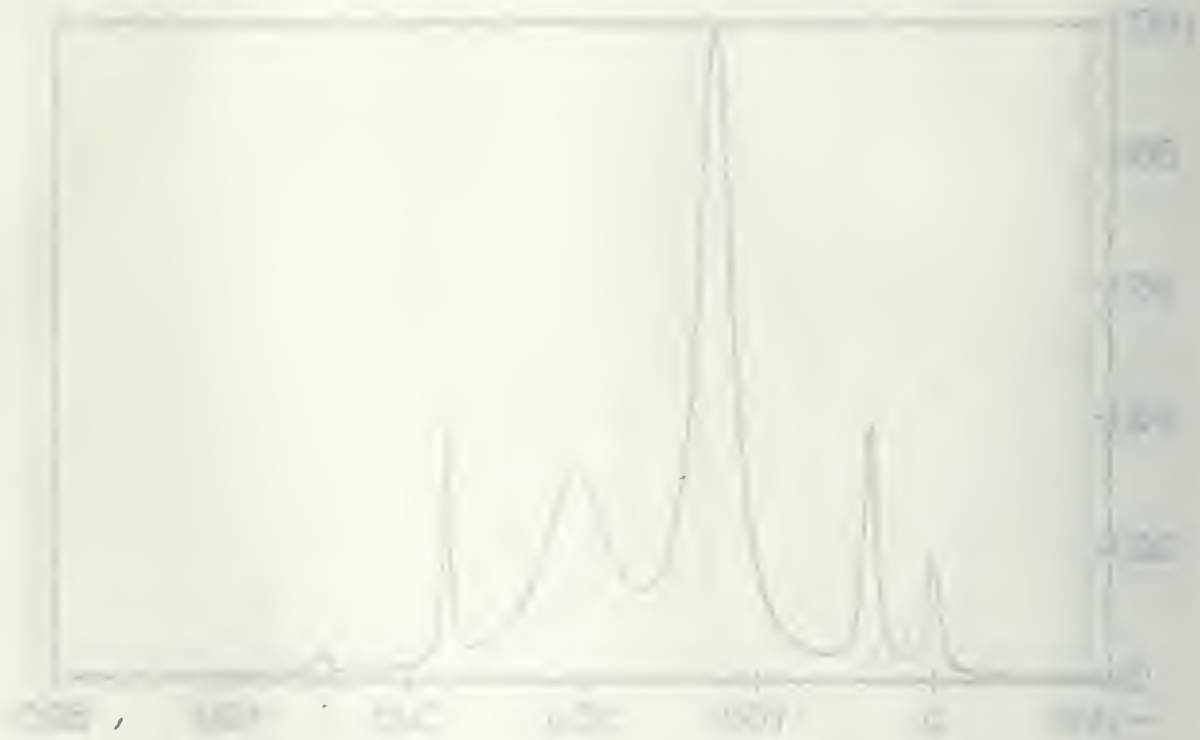

Figure(4.20) The scaled 6-31G* spectrum of CD_3CHS

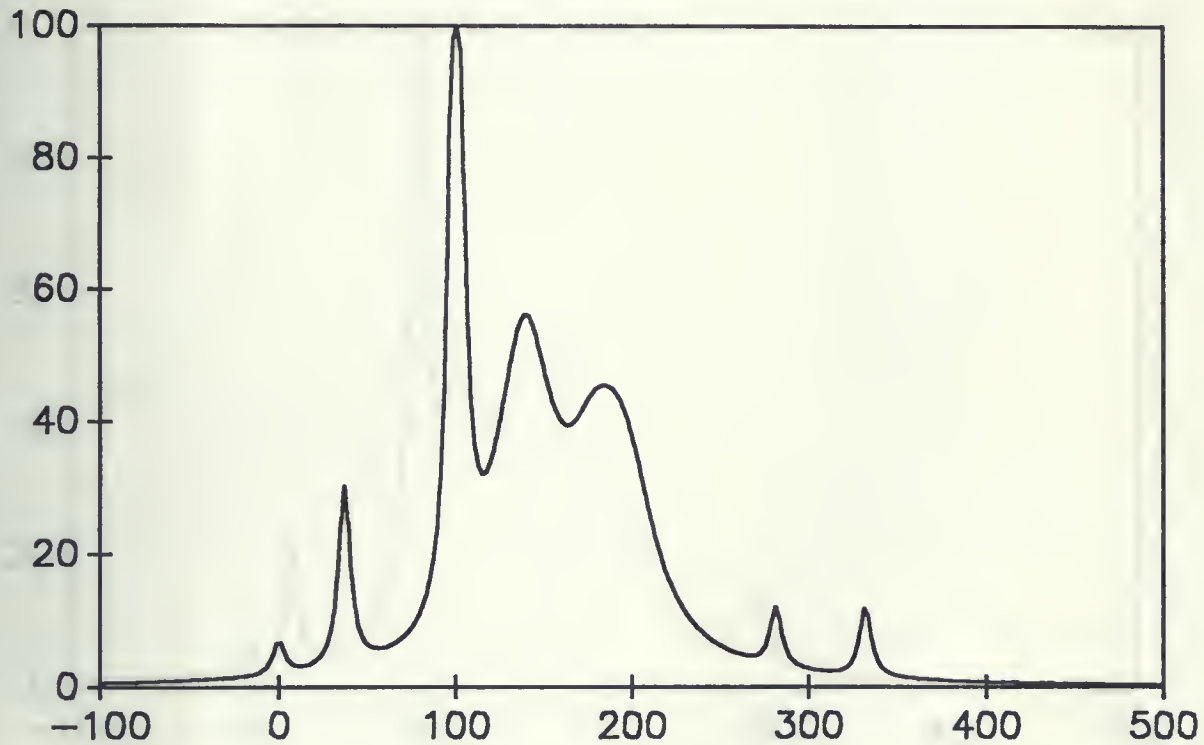

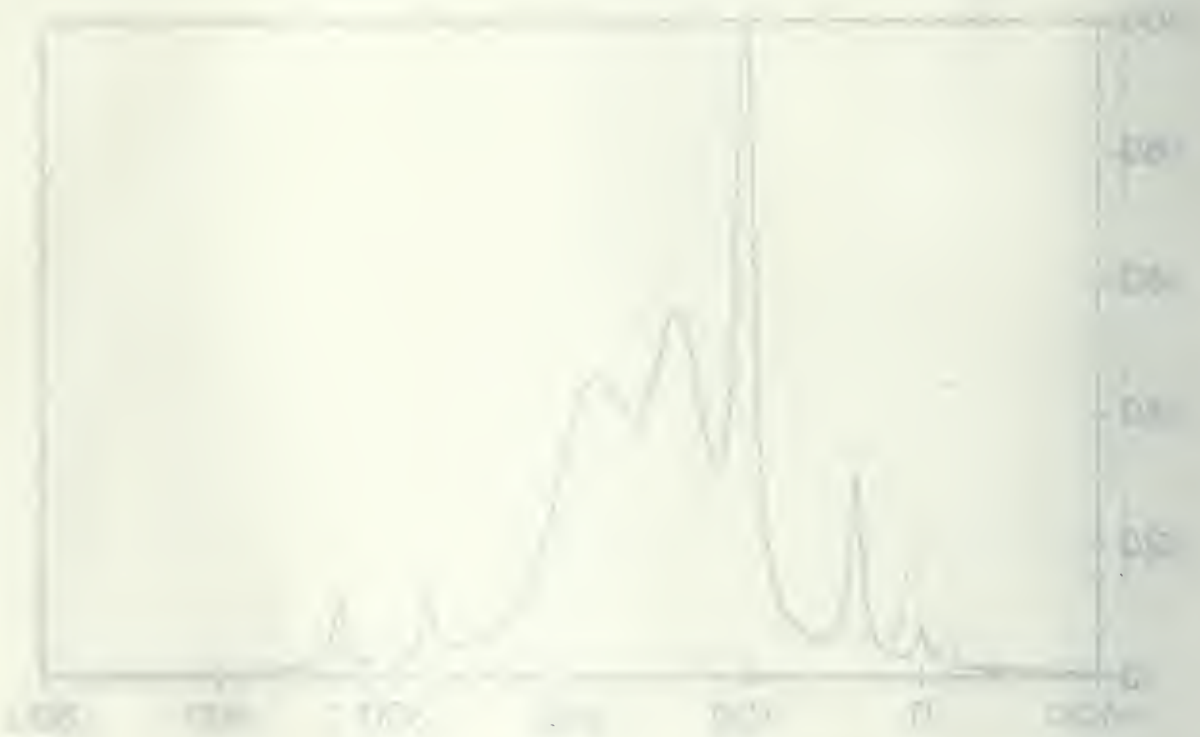

Figure(4.21) The scaled 6-31G* spectrum of CD_3CDS

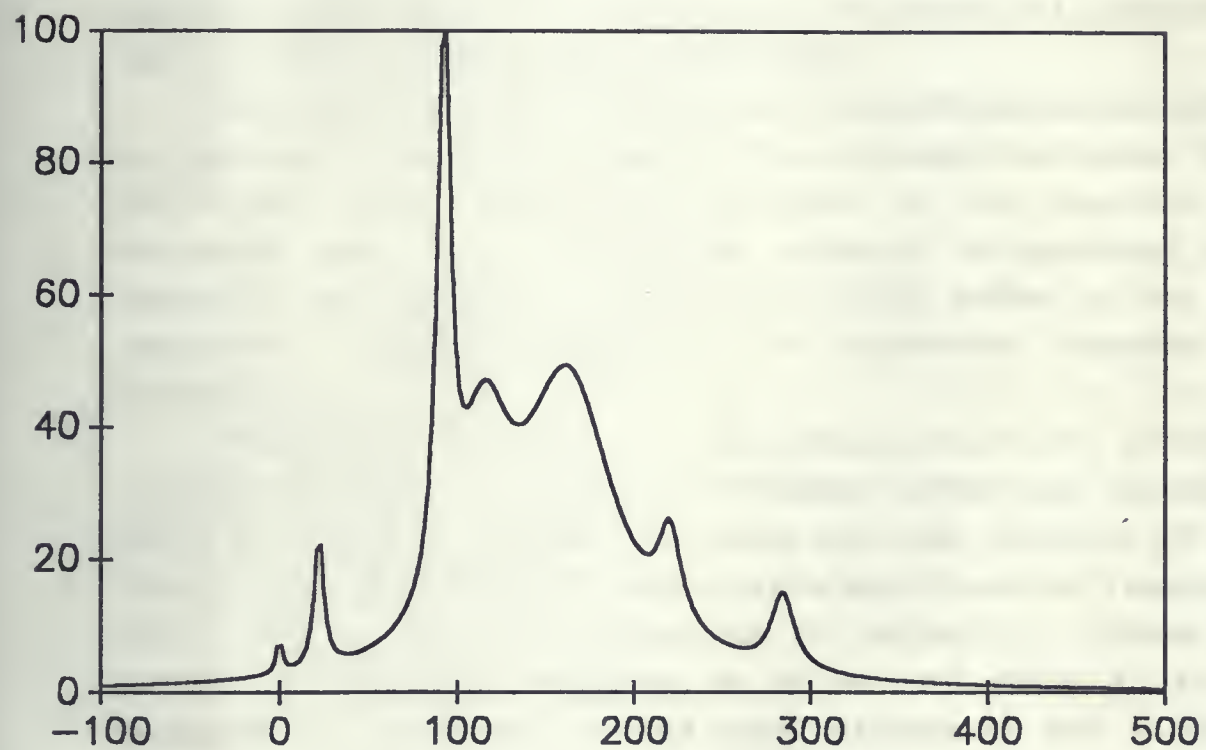

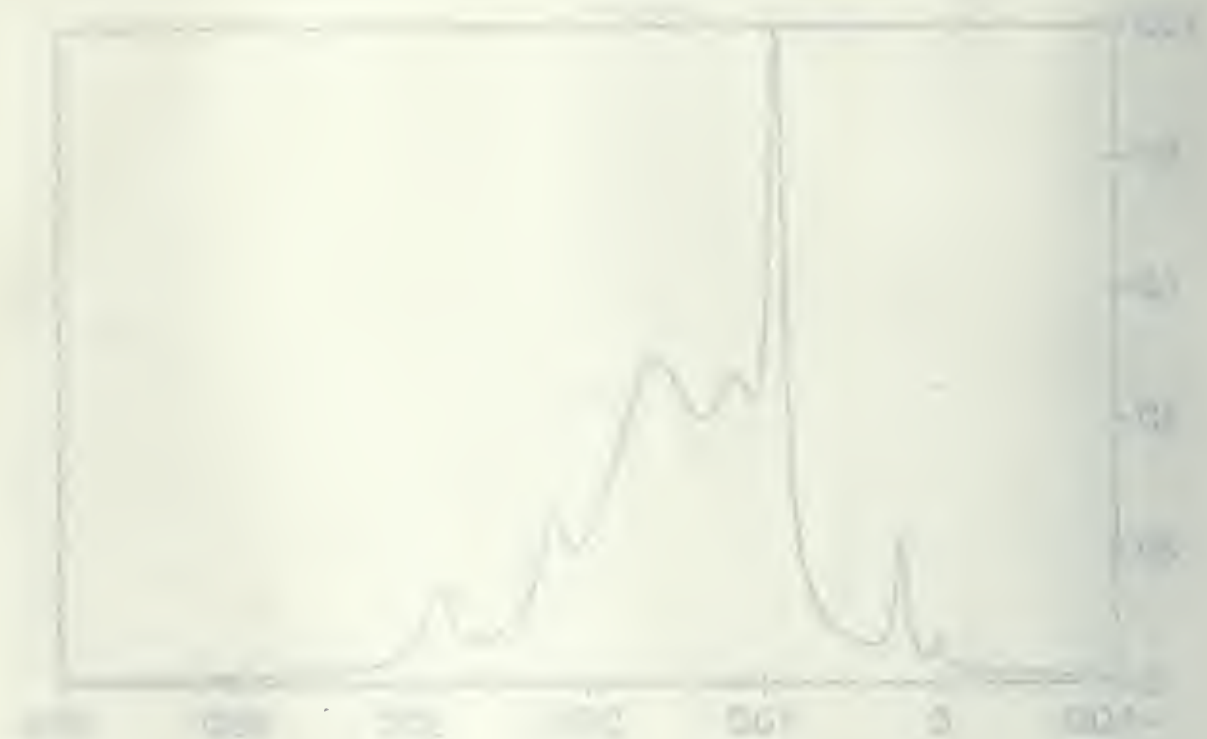

CONCLUSIONS

The visible system of thioacetaldehyde which was detected as an excitation spectrum is assigned to a spin forbidden electronic transition between the $\tilde{a}^3A''$ and $\tilde{A}^1A'$ states. Under room temperature conditions the vibrational structure was observed to be highly congested and the electronic band origin could not be identified. The same spectrum recorded by the pyrolysis jet method was found to be very open and individual bands could be identified and assigned.

The analysis of the vibrational fine structure was aided by molecular orbital ab initio calculations performed at a RHF/6-31G* level. With this technique it was possible to calculate the small amplitude harmonic frequencies and identify the $\upsilon_8(CCH_a)$, $\upsilon_9(C{=}S)$ and $\upsilon_{10}(CCS)$ modes in the jet spectrum. These assignments are collected together in Table(5.1).

Of greater interest is the large amplitude torsion-wagging dynamics. In the S_0 electronic state the molecular frame of thioacetaldehyde is planar and the rotation of the methyl group provides the single large amplitude low frequency mode. The ab initio calculations of Table(4.1) place the barrier to internal rotation at 541.44 cm^{-1} which is to be compared to the data derived from microwave[7] and visible[9] spectra of 549.8 and 534.3 cm^{-1}. The microwave analysis[7] yields a moment of inertia for the methyl group I_T=3.123 amu $Å^2$ which is in excellent agreement with the calculated value of 3.134 amu $Å^2$. The RHF/6-31G* procedure appears to give a satisfactory agreement to the experimental data as the energy levels calculated from the two - dimensional torsion - wagging Hamiltonian agree relatively well with the ground state combination differences. For example, the levels v_{15}=1e/v_{15}=2a_1

calculated at 151.806/283.172 cm^{-1} compare favourably with the observed hot band intervals at -163.0/-307.7 cm^{-1} . In the present model, the torsion and wagging motions are treated as a pair of coupled one-fold and three-fold symmetric tops. In this picture, the three CH bonds of the methyl group may be regarded as a finely balanced propeller which does not vibrate the centre of mass of the molecule as the three hydrogens rotate about the C-C bond. The corrections introduced by the variable kinetic energy terms in the Hamiltonian are small and the calculated frequency for v_{15}=1e shifts from 151.806 to 152.012 cm^{-1}. Thus, in the present model the variation in the kinetic energy with respect to the two large amplitude coordinates is not a major contributor to the torsion wagging frequencies and is not able to account for the discrepancy between the observed and calculated frequencies.

The UHF/6-31G* calculations show that the molecular conformation changes on $n \rightarrow \pi^*$ electron promotion. The equilibrium position of the T_1 upper state is found to be α=+24.68^0 and θ=+74.34^0 or -45.66^0 with respect to the S_0 state, α=0.0^0,θ=0.0^0. The net result is that strong activity is induced into spectrum from the two modes which most closely correspond to the molecular distortions, namely, aldehyde wagging Q_{14} and methyl torsion Q_{15}. The calculated potential surface is of interest. When the aldehyde group is clamped into the planar configuration, the antieclipsed form, α=0.00^0, θ=60.00^0, is more stable than the eclipsed form, α=0.0^0,θ=0.0^0 by 146.24 cm^{-1}. This eclipsed - antieclipsed displacement in conformation on electronic excitation has been attributed to a hyperconjugation between the out of plane π type orbitals of sulphur and the p type s orbitals of the methyl hydrogens[9].

The potential functions derived from the ab initio procedure were found to be a good starting point for a refinement of the simulated spectrum. Selected expansion

coefficients were adjusted until a global fit was similutaneously achieved with all four isotopomers. By this process it was possible to reproduce most of the features in the observed jet spectrum, as illustrated in Figure(5.1). The υ_{14}, υ_{15} intermode coupling is of special interest. In the lower S_0 state, the two modes are well behaved and there appears to be very little coupling. In the upper T_1 state, all of the levels are found to be perturbed to some extent. As an example, the first quantum of torsion, v_{15}=1e, should not be greatly influenced by deuteration of the aldehyde hydrogen, yet the intervals in the spectra of CH_3CHS/CH_3CDS vary as +52.0/+39.0 cm^{-1}. While the rigid harmonic model gives a very poor representation of the υ_{15} frequencies 148.60/145.80 cm^{-1},the nonrigid scaled calculation appears to reproduce the perturbations quite well. This secondary isotope effect can be attributed to an repulsive interaction between the v_{14}=1e and v_{15}=1e states.

The parameters of the modelled T_1 surface are shown in Table(5.1). Of importance is that heights of the barriers to torsion and wagging of 54.07 and 246.58 cm^{-1}, are considerably less than the <u>ab initio</u> values of 146.58 and 321.79 cm^{-1}. Likewise the scaled equilibrium positions of $\alpha=22.38^0$ and $\theta=-41.08^0$ are somewhat lower than those derived directly from molecular orbital theory.

It is possible to summarize the results by concluding that the structure and dynamics which are derived from 6-31G* <u>ab initio</u> theory provide a good starting point for both the assignment of the observed spectrum and the refinement of the simulated spectrum. While the RHF procedure gives a good description of the ground state structure and dynamics, the triplet potential surface generated by the UHF method is too bumpy and undulating. The UHF calculations also generate minima in the potential surface which are found to be greater than those observed at the T_1 position of equilibrium.

Higher level molecular orbital calculations which include corrections for electron correlation and extended basis functions could possibly improve the quality of spectrum synthesized by the molecular orbital technique.

TABLE(5.1) Spectroscopic Parameters for Thioacetaldehyde (in cm^{-1}).

	CH_3CHS		CH_3CDS	
	obs.	calc.	obs.	calc.
		S_0 State		
υ_{15}(tor.)	163.0	170.66	160.1	167.01
$2\upsilon_{15}$(tor.)	307.7	321.45	303.3	317.01
		T_1 State[a]		
υ_{15}(tor.)	52.0	58.00	39.0	35.96
$2\upsilon_{15}$(tor.)	110.9	129.99	101.3	121.03
υ_{14}(wag.)	249.4	237.83	215.8	204.12
υ_9(C=S)	747.2	673.30	721.3	654.85
υ_{10}(CCS)	283.9	279.06	279.0	275.08
	CD_3CHS		CD_3CDS	
	obs.	calc.	obs.	calc.
		S_0 State		
υ_{15}(tor.)	?	126.49	122.6	121.85
$2\upsilon_{15}$(tor.)	241.3	245.12	234.6	236.78
		T_1 State[a]		
υ_{15}(tor.)	40.9	37.02	29.6	22.13
$2\upsilon_{15}$(tor.)	93.4	98.03	81.8	90.77
υ_9(C=S)	681.5	624.74	677.2	619.58
$\upsilon_8(CCH_a)$	?	832.51	751.8	781.49

a) V(22.38°,-41.08°)=V(22.38°,78.92°)=0.0 ; V(0.0°,0.0°)=246.58 ; V(0.0°,60.0°)=192.50 ; V(22.38°,18.92°)=452.06 ; (V in cm^{-1}).

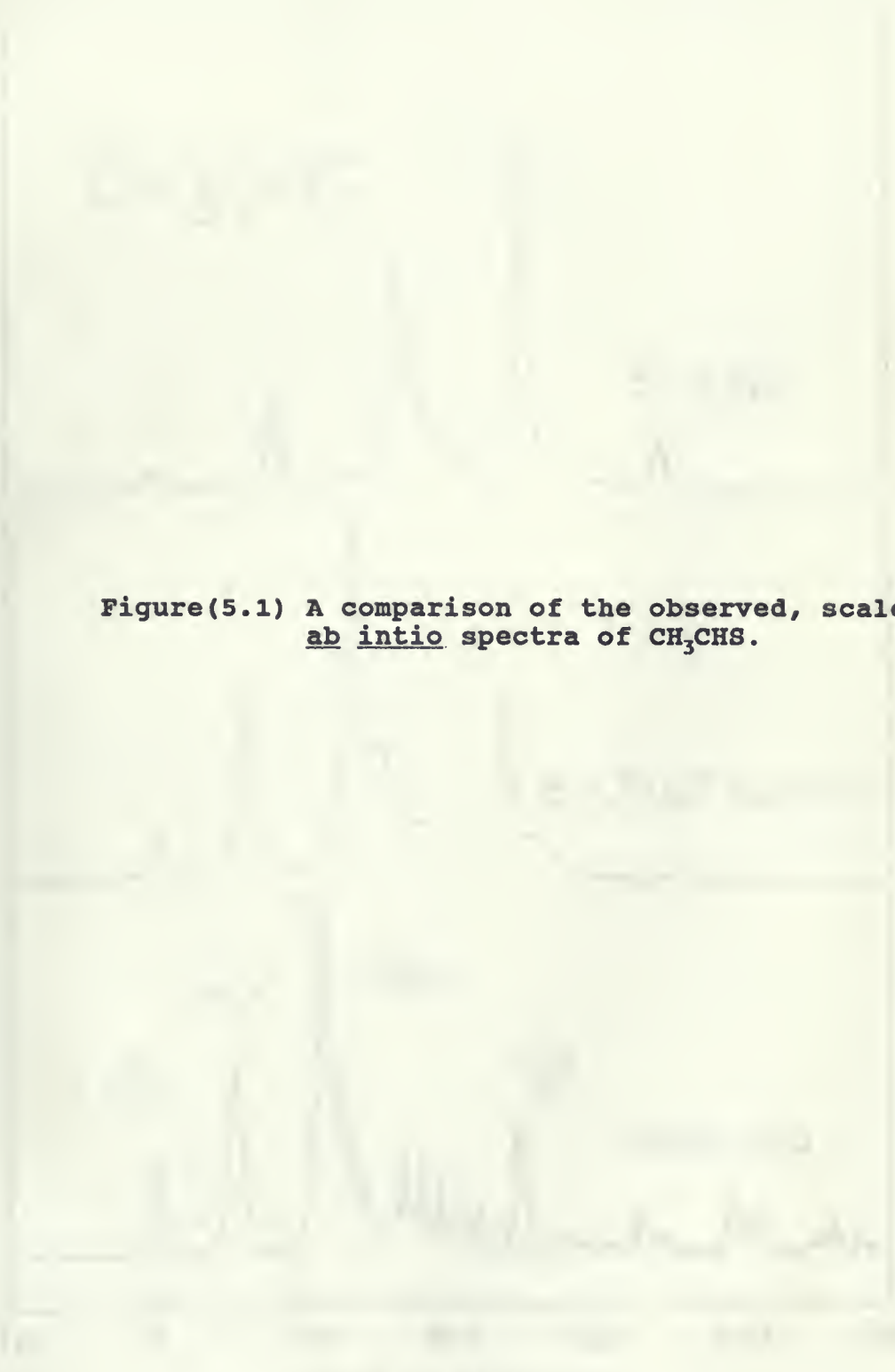

Figure(5.1) A comparison of the observed, scaled, and *ab intio* spectra of CH_3CHS.

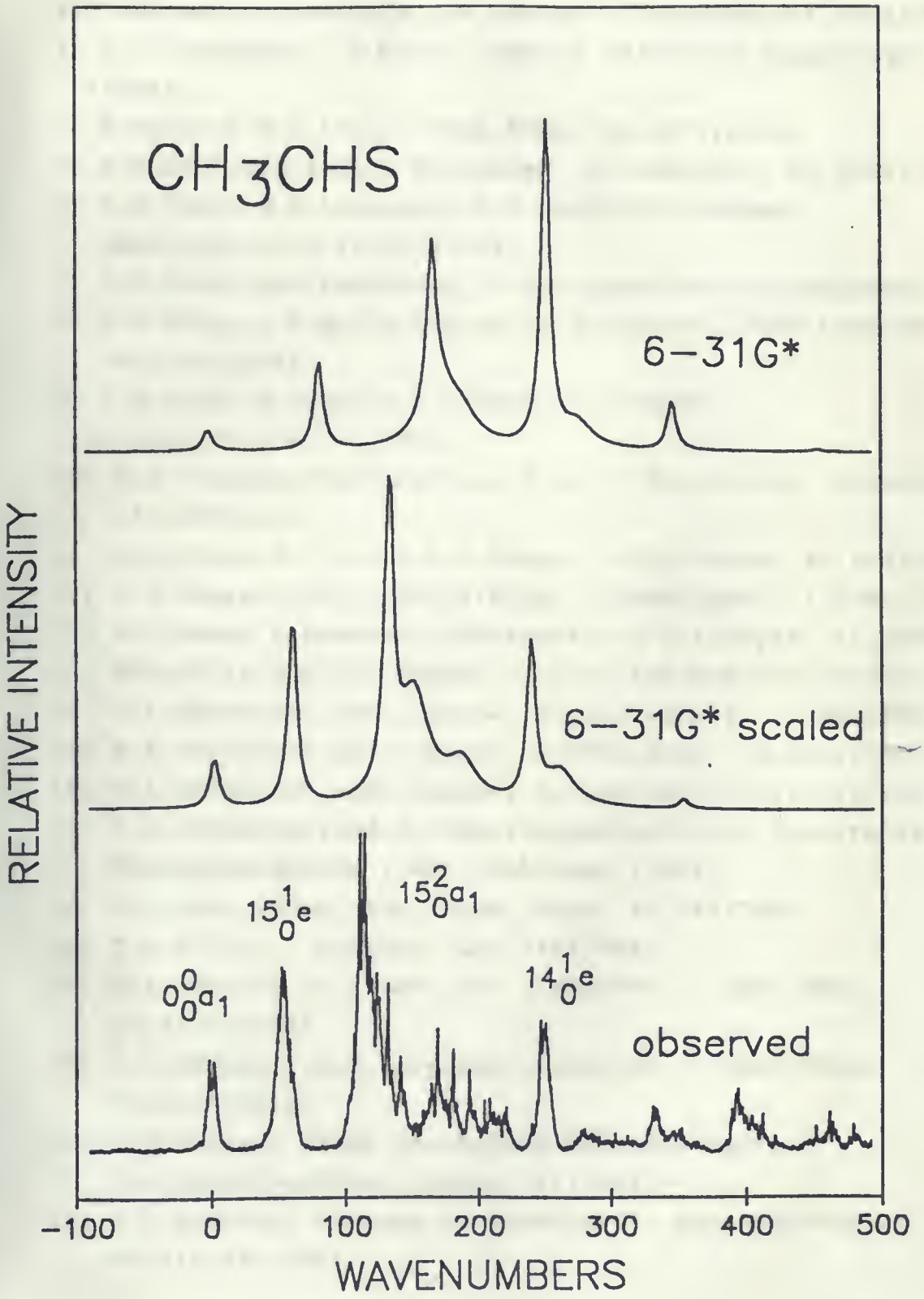
CH3CHS
6-31G*
6-31G* scaled
observed
RELATIVE INTENSITY
$0_0^0 a_1$
$15_0^1 e$
$15_0^2 a_1$
$14_0^1 e$
-100
0
100
200
300
400
500
WAVENUMBERS

REFERENCES

1) J.S.Crighton,S.Bell, J.Molec.Spectrosc.112,315,(1985)

2) P.Groner,G.A.Guirgis,J.R.Durig, J.Chem.Phys.45,1904(1986)

3) D.J.Clouthier,D.C.Moule, "Topics in Current Chemistry" 150, (1988)

4) M.Noble,E.D.C.Lee, J.Chem.Phys. 81,1632(1984)

5) M.Baba,I.Hanazaki,U.Nagashima, J.Chem.phys. 82,3938(1985)

6) H.W.Kroto,B.M.Landsberg,R.J.Suffolk,A.Vodden. Chem.Phys.Lett.29,265(1974)

7) H.W.Kroto,B.M.Landsberg, J.Mol.Spectrosc.62,346(1976)

8) R.H.Judge,D.C.Moule,A.E.Bruno,R.P.Steer, Chem.Phys.Lett. 102,385(1983)

9) R.H.Judge,D.C.Moule,A.E.Bruno,R.P.Steer, J.Chem.Phys.87,60(1987)

10) Y.G.Smeyers,M.N.Bellido,A.Nino, J.Mol.Struct.(Therochem) 166,259(1988)

11) A.E.Bruno,D.C.Moule,R.P.Steer, J.Photochem. 46,169(1989)

12) Y.G.Smeyers,D.C.Moule,A.Nino, J.Chem.Phys. 93,5786(1990)

13) W.J.Hehre,L.Radom,P.R.Schleyer,and J.A.Pople, AB INITIO MOLECULAR ORBITAL THEORY.93,JW&S,Inc.New York,(1986)

14) M.A.Harthcock,and J.Laane, J.Molec.Spect. ,300(1982)

15) M.A.Harthcock,and J.Laane, J.Chem.Phys. 79,2103(1983)

16) M.A.Harthcock,and J.Laane, J.Chem.Phys. 89,4231(1985)

17) D.J.Clouthier,and D.C.Moule,SperSonic-Jet Spectra of Thioacetaldehyde , not published (1988)

18) D.H.Levy ,Anuu. Rev. Phys. Chem. 31,197(1980)

19) T.A.Miller , Science ,223,545(1984)

20) R.E.Smelley ,D.H.Levy,and L.Wharton ,J.Chem.Phys. 63,4977(1975)

21) R.E.Smelley ,D.H.Levy,and L.Wharton ,J.Chem.Phys. 64,3266(1976)

22) J.M.Hollas, "High Resolution Spectroscopy", Butterworths&CoLtd.London,541(1982)

23) D.L.Andrews, "Lasers in Chemistry", Springer-Verlag, Berlin,83(1986)

24) J.R.Dunlop,J.Karoczak,and D.J.Clouthier, Chem.Phys.Lett. 151,362(1988)
25) M.L.Rutherford,D.J.Clouthier,and F.J.Holler, Appl.Spectrosc.43,532(1989)
26) J.Simons , J.Phys.Chem.,95,10179,(1991)
27) A.Hinchliffe "COMPUTIONAL QUANTUM CHEMISTRY" ,John Wiely&Sons,Chichester ,(1989)
28) A.Hinchliffe "AB initio DETERMINATION OF MOLECULAR PROPERTIES",Adam Hilger , Bristol (1987)
29) A.Szabo and N.S.Ostluad "MODERN QUANTUM CHEMISTRY: INTRODUCTION TO ADVANCED ELECTRONIC STRUCTUER THEORY" Macmillan Publishing Co.Inc. , New York , (1982)
30) J.P.Lowe "QUANTUM CHEMISTRY" Academic Press ,Inc., Orlando (1987)
31) W.J.Hehre ,L.Radom ,P.V.R.Schleyer ,and J.A.Pople "AB INITIO MOLECULAR ORBITAL THEORY" John Wiely&Sons ,NewYork, (1986)
32) T.Clark "A HAND BOOK OF COMPUTATIONAL THEORY" John Wiely&Sons,New York , (1985)
33) S.M.Blinder ,A.J.Phys. 33,431 ,(1965)
34) R.L.Hilderbrandt ,J.Chem.Phys.,51,1654, (1969)
35) M.W.Schmidt, J.A.Boatz, K.K.Baldridge, S.Koseki, M.S.Gordon, S.T. Elbert, B.Lam, GAMESS,(1987)
36) S.L.Altman ,Proc.R.Soc.Ser.A298,184 ,(1967)
37) C.M.WOODMAN , Molec.Phys. 19,753 ,(1970)
38) C.Longnet-Higgins , Molec.Phys. 6,445(1963)
39) J.Maruani ,A.Hernandez-Laguac,and Y.G.Smeyers J.Chem.Phys.63,4515(1975)
40) C.R.Quade and C.L.Lin ,J.Chem.Phys. 38,540 (1963)
41) Y.G.Smeyers and A.Hernandez-Laguna ,Int.J.Quantum Chem. 22,68, (1982)
42) Y.G.Smeyers and A.Hernandez-Laguna J.Molec.Struc.(Theochem.)149,127 (1987)
43) Y.G.Smeyers ,J.Molec.Struc.(Theochem.)107,3 (1985)

44) Y.G.Smeyers ,A.Nino ,M.N.Bellido ,Theoret.Chim.Acta 74,259,(1985)
45) Y.G.Smeyers ,A.Nino ,M.N.Bellido J.Molec.Struct.(Theochem),166,1 (1988)
46) D.C.Moule ,Inertia Program ,Brock University, St.Catharines,(1991)
47) W.A.Guillory , "Introduction to Molecular Structure and Spectroscopy" ,Allan and Bacon,Inc.,Boston , (1977)
48) D.C.Harris and M.D.Bertolucci ,"Symmetry and Spectroscopy" Oxford Press ,New York , (1978)
49) E.B.Wilson ,Jr., J.Chem.Phys. ,3,276 ,(1935)
50) D.C.Moule ,A.Nino , Etanal Program , (1991)